This document is downloaded from DR-NTU (https://dr.ntu.edu.sg)
Nanyang Technological University, Singapore.

Mechanism investigation and process monitoring of electrical discharge machining

Xiao, Zhiyun

2005

Ling S. F. (2005). Mechanism investigation and process monitoring of electrical discharge machining. Doctoral thesis, Nanyang Technological University, Singapore.

https://hdl.handle.net/10356/5417

https://doi.org/10.32657/10356/5417

Nanyang Technological University

Downloaded on 18 Apr 2025 14:43:33 SGT

ATTENTION: The Singapore Copyright Act applies to the use of this document. Nanyang Technological University Library

Mechanism Investigation and Process Monitoring of Electrical Discharge Machining

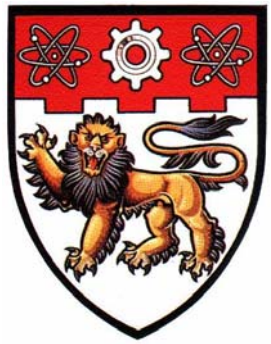

XIAO ZHIYUN

School of Mechanical and Aerospace Engineering

A Thesis Submitted to Nanyang Technological University

In full fulfillment for the requirement of the degree of

Doctor of Philosophy

October 2005

ATTENTION: The Singapore Copyright Act applies to the use of this document. Nanyang Technological University Library

ABSTRACT

Although been widely used and accepted as the standard material removal process in many manufacturing applications, electrical discharge machining (EDM) today remains to a certain extent an experience-oriented processing technique without thorough understanding its mechanism. To improve process performance, better understanding of the discharge mechanism and the relationships among process performance, discharging conditions, and working parameters is aimed in this research. Studies started by investigating discharge mechanism to understand what is happening during an individual discharge. Supported by the obtained information, a new monitoring method to precisely monitor discharge conditions was developed. After that, the influences of working parameters on process performance and discharge conditions were investigated, and models used to predict process performance were established. The contributions or the main contents of this report can be summarized as following:

- The mechanisms of spark and arc were well interpreted by analyzing input electrical impedance. To investigate the discharge mechanism, EDM process was viewed as a time-varying electrical system because the occurring of discharging is resulted from the applied electrical power. Input electrical impedance inherently reflects the characteristics of this process whose variation is due to the changes of deionization status of the dielectric media inside discharge gap, thus it provides abundant information of discharge mechanism. In addition, the identification of working parameters using input electrical impedance was also achieved.

- An on-line monitoring system was realized and quantified monitoring results were obtained, which reliably represents the discharge conditions. Discharge conditions are commonly denoted as series of discharge pulses, including opens, offs, short-

ATTENTION: The Singapore Copyright Act applies to the use of this document. Nanyang Technological University Library

circuits, sparks and arcs. Monitoring of discharge conditions mainly focus on classifying sparks and arcs correctly because these two types of pulse are the dominant ones and exhibit quite similar characteristics. Based on the understanding of discharge mechanism, several features of input electrical impedance were extracted and a fuzzy classifier was developed to distinguish sparks and arcs.

- The crucial factors of EDM performance were identified after the monitoring results of discharge conditions were quantitatively obtained. The influences of working parameters on discharge conditions and process performance were investigated through conducting detailed screening experiments. It was proved that input power and discharge conditions are the crucial factors of EDM performance. The material removal rate is influenced significantly by input power and the time percentage of spark, while surface roughness is mainly determined by input power and the time percentage of arc.

- An on-line performance predictor was realized, which can be readily used in the control system that will be developed in the future. Since input power and discharge conditions were proved to be the crucial factors of EDM process, its performance could be determined as a function of these factors. Neural Network and empirical models for predicting material removal rate and surface roughness were developed in this research. These models can predict EDM performance with acceptable errors, while empirical models are easier to be achieved than Neural Network model because less experiment needs to be carried out. The empirical models also proved that arcs decrease machining efficiency of EDM process and should be avoided effectively.

ATTENTION: The Singapore Copyright Act applies to the use of this document. Nanyang Technological University Library

ACKNOWLEDGEMENT

First and foremost, I would like to express my sincerest gratitude to my supervising professor, Ling Shih-Fu and my advisor Dr. Huang Han for their guidance, encouragement and support throughout my research work at NTU. From them, I have learned a lot of invaluable things more than doing research only. Theirs sincerity and generosity in giving me personal help will be bore in my mind forever.

I also like to acknowledge the assistance from Dr. Liang Fengguang, Dr. Fu Lianyu and Dr. Wen Guilin for their valuable suggestions in doing my research. At the same time, I would like to give my thanks to my research colleague, Ms. Hou Xiaoyan, Mr. Li Xiangchao, Ms. Ying Yanling, Dr. Luan Jingeng, Dr. Zhang Dong, Dr. Li Weihua, etc. for their kind help. In addition, the help from the technicians of Mechanics of Machines Lab and SIMTech is indispensable in conducting all my experiments.

I would like to express my sincerest thanks to my wife for her support and encouragement through all the difficult time. Special thanks give to my parents and brother for their love and support for these years.

I am also grateful to Nanyang Technological University, School of Mechanical and Aerospace Engineering for the financial support and all the necessary facilities and resources.

ATTENTION: The Singapore Copyright Act applies to the use of this document. Nanyang Technological University Library

TABLE OF CONTENTS

ABSTRACT ..... ***i***

ACKNOWLEDGEMENTS ..... ***iii***

TABLE OF CONTENTS ..... ***iv***

LIST OF FIGURES ..... ***vi***

LIST OF TABLES ..... ***x***

LIST OF SYMBOLS ..... ***xi***

CHAPTER 1. INTRODUCTION **1**

1.1 Background and Motivation 1

1.2 Objective and Scope 3

1.3 Outline of Thesis 7

CHAPTER 2. ELECTRICAL DISCHARGE MACHINING **8**

2.1 Basic Knowledge of EDM 9

2.2 State-of-the-art of EDM 18

CHAPTER 3. INPUT ELECTRICAL IMPEDANCE OF EDM **30**

3.1 Electrical Impedance Method 31

3.2 Measurement of Input Electrical Impedance 36

CHAPTER 4. MECHANISM OF ELECTRICAL DISCHARGE MACHINING **48**

4.1 Discharge Mechanism of Spark 50

4.2 Discharge Mechanism of Arc 56

4.3 Effects of Working Parameters on Input Electrical Impedance 60

4.4 Summary 73

ATTENTION: The Singapore Copyright Act applies to the use of this document. Nanyang Technological University Library

TABLE OF CONTENTS

CHAPTER 5. MONITORING OF DISCHARGE CONDITIONS.....74

5.1 Wavelet Analysis for Signal De-noise and Segmentation.....76

5.2 Detection of Opens, Offs, Short-Circuits.....84

5.3 Classification of Sparks and Arcs.....84

5.4 Monitoring Results of Discharge Conditions.....96

5.5 Verification of Monitoring Results.....98

5.6 Summary.....100

CHAPTER 6. INFLUENCES OF WORKING PARAMETERS ON DISCHARGE CONDITIONS AND PROCESS PERFORMANCE.....101

6.1 Repeatability study of EDM Process.....103

6.2 Determination of Electrode Polarity.....108

6.3 Taguchi Method for Experimental Design.....111

6.4 Influences of Working Parameters on Discharge Conditions and Process Performance.....128

6.5 Summary.....129

CHAPTER 7. DEVELOPMENT OF PERFORMANCE PREDICTOR FOR EDM PROCESS.....130

7.1 ANN Model of EDM Performance.....131

7.2 Empirical Models of EDM Performance.....144

7.3 Summary.....153

CHAPTER 8. CONCLUSIONS AND RECOMMENDATIONS.....154

8.1 Conclusions.....154

8.2 Recommendations.....157

REFERENCES.....161

ATTENTION: The Singapore Copyright Act applies to the use of this document. Nanyang Technological University Library

LIST OF FIGURES

Figure 1-1 Affiliations among working parameters, discharge conditions, process performance and monitoring results 5

Figure 2-1 Ideal discharge pulses 15

Figure 3-1 Input and output of black system 31
Figure 3-2 Simplified EDM system 32
Figure 3-3 CHARMILLES ROBOFORM 200 EDM Machine 37
Figure 3-4 Electrode and workpiece with their fixtures 38
Figure 3-5 Schematic diagram of data acquisition system 39
Figure 3-6 Voltage and current after de-noising 40
Figure 3-7 Magnitude and phase of input electrical impedance of pulse 1 41
Figure 3-8 Real part and imaginary part of input electrical impedance of pulse 1 41
Figure 3-9 Magnitude and phase of input electrical impedance of pulse 2 42
Figure 3-10 Real part and imaginary part of input electrical impedance of pulse 2 42
Figure 3-11 Magnitude and phase of input electrical impedance of pulse 3 43
Figure 3-12 Real part and imaginary part of input electrical impedance of pulse 3 43
Figure 3-13 Magnitude and phase of input electrical impedance of pulse 4 44
Figure 3-14 Real part and imaginary part of input electrical impedance of pulse 4 44
Figure 3-15 Magnitude and phase of input electrical impedance of pulse 5 45
Figure 3-16 Real part and imaginary part of input electrical impedance of pulse 5 45
Figure 3-17 Magnitude and phase of input electrical impedance of pulse 6 46
Figure 3-18 Real part and imaginary part of input electrical impedance of pulse 6 46
Figure 3-19 Magnitude and phase of input electrical impedance of pulse 7 47
Figure 3-20 Real part and imaginary part of input electrical impedance of pulse 7 47

Figure 4-1 Voltage and current of a typical spark 50

ATTENTION: The Singapore Copyright Act applies to the use of this document. Nanyang Technological University Library

LIST OF FIGURES

Figure 4-2 Magnitude and phase of input electrical impedance of a typical spark 51

Figure 4-3 Real part and imaginary part of input electrical impedance of a typical spark 51

Figure 4-4 Schematic representation of discharging phases..... 56

Figure 4-5 Voltage and current of a typical arc 57

Figure 4-6 Magnitude and phase of input electrical impedance of a typical arc 57

Figure 4-7 Real part and imaginary part of input electrical impedance of a typical arc. 58

Figure 4-8 Voltage and current for different polarities..... 62

Figure 4-9 Magnitude and phase of input electrical impedance for different polarities. 62

Figure 4-10 Real part and imaginary part of input electrical impedance for different polarities..... 63

Figure 4-11 Voltage and current for different electrodes 64

Figure 4-12 Magnitude and phase of input electrical impedance for different electrodes..... 65

Figure 4-13 Real part and imaginary part of input electrical impedance for different electrodes..... 65

Figure 4-14 Voltage and current for different workpieces 67

Figure 4-15 Magnitude and phase of input electrical impedance for different workpieces..... 67

Figure 4-16 Real part and imaginary part of input electrical impedance for different workpieces..... 68

Figure 4-17 Voltage and current for different dielectrics 69

Figure 4-18 Magnitude and phase of input electrical impedance for different dielectrics..... 70

Figure 4-19 Real part and imaginary part of input electrical impedance for different dielectrics..... 70

Figure 4-20 Voltage and current for different gap sizes 72

ATTENTION: The Singapore Copyright Act applies to the use of this document. Nanyang Technological University Library

LIST OF FIGURES

Figure 4-21 Magnitude and phase of input electrical impedance for different gap sizes72

Figure 4-22 Real part and imaginary part of input electrical impedance for different gap sizes 73

Figure 5-1 Structure of on-line monitoring system 76

Figure 5-2 Single level wavelet decomposition 80

Figure 5-3 Original voltage and current trains 80

Figure 5-4 Voltage and current after de-noising 81

Figure 5-5 Coefficients of CWT at scale 10 83

Figure 5-6 Structure of a fuzzy logic system 90

Figure 5-7 Example of singleton and non-singleton fuzzifiers 91

Figure 5-8 Schematic representation of the fuzzy classifier 95

Figure 5-9 Voltage and current trains collected from experiment 97

Figure 5-10 Material removal rate and time percentage of spark vs gap size 99

Figure 5-11 Surface roughness and time percentage of arc vs gap size 99

Figure 6-1 Material removal rate 104

Figure 6-2 Relative wear ratio 104

Figure 6-3 Surface roughness 105

Figure 6-4 Monitoring results of discharge conditions 105

Figure 6-5 Machining depth vs time 106

Figure 6-6 Material removal rate vs time 107

Figure 6-7 Percentage of spark vs time 107

Figure 6-8 Percentage of arc vs time 108

Figure 6-9 Influences of electrode polarity on MRR 110

Figure 6-10 Influences of electrode polarity on SR 110

Figure 6-11 Influences of open voltage on MRR and SR 118

ATTENTION: The Singapore Copyright Act applies to the use of this document. Nanyang Technological University Library

LIST OF FIGURES

Figure 6-12 Influences of open voltage on spark and arc 118

Figure 6-13 Influences of peak current on MRR and SR 120

Figure 6-14 Influences of peak current on spark and arc..... 120

Figure 6-15 Influences of pulse on-time on MRR and SR 122

Figure 6-16 Influences of pulse on-time on spark and arc..... 122

Figure 6-17 Influences of pulse interval on MRR and SR 124

Figure 6-18 Influences of pulse interval on spark and arc..... 124

Figure 6-19 Influences of gap size on MRR and SR 126

Figure 6-20 Influences of gap size on spark and arc 126

Figure 6-21 Influences of ultrasonic vibration on MRR and SR..... 128

Figure 6-22 Influences of ultrasonic vibration on spark and arc 128

Figure 7-1 Architecture of a feed-forward multi-layer NN 134

Figure 7-2 Structure of the developed Neural Network..... 141

Figure 7-3 Errors of process performance between validation experiments and NN... 143

Figure 7-4 Errors of process performance between testing experiments and NN 144

Figure 7-5 Errors of process performance between experiments and empirical models150

Figure 7-6 Errors of process performance between experiments and empirical models151

Figure 7-7 Errors of process performance between experiments and empirical models152

Figure 7-8 On-line performance predictor of EDM process..... 152

Figure 8-1 Flowchart of the on-line monitoring system 158

Figure 8-2 Interface of the software of the monitoring and control system 158

Figure 8-3 On-line monitoring and control system of EDM 160

Figure 8-4 On-line monitoring and control system of EDM 160

ATTENTION: The Singapore Copyright Act applies to the use of this document. Nanyang Technological University Library

LIST OF TABLES

Table 4-1 Resistivity of workpiece materials 66

Table 5-1 Features extracted for pulse 1 to pulse 7 88

Table 5-2 Fuzzy reasoning results for pulse 1 to pulse 7 95

Table 5-3 Monitoring results of discharge conditions 96

Table 5-4 Monitoring results of discharge conditions 97

Table 6-1 Process parameters and their levels 113

Table 6-2 Experimental layout using an L_{18} orthogonal array 114

Table 6-3 Experimental results base on Taguchi procedure 115

Table 6-4 Signal-to-noise response table for material removal rate 116

Table 6-5 Signal-to-noise response table for surface roughness 116

Table 6-6 Results of the confirmation experiments 116

Table 7-1 Numbers of the records for NN model 139

Table 7-2 Errors of process performance between validation experiments and NN 142

Table 7-3 Errors of process performance between testing experiments and NN 143

Table 7-4 Errors of process performance between experiments and empirical models 149

Table 7-5 Errors of process performance between experiments and empirical models 150

Table 7-6 Errors of process performance between experiments and empirical models 151

ATTENTION: The Singapore Copyright Act applies to the use of this document. Nanyang Technological University Library

LIST OF SYMBOLS

V	*Amplitude of voltage*
$v(t)$	*Voltage*
$V(t)$	*Analytical signal of* $v(t)$
I	*Amplitude of current*
$i(t)$	*Current*
$I(t)$	*Analytical signal of* $i(t)$
$Z(t)$	*Electrical Impedance*
$R(t)$	*Real part of electrical impedance*
$X(t)$	*Imaginary part of electrical impedance*
$\varphi(t)$	*Phase of electrical impedance*
$z(t)$	*Complex signal*
$s_r(t)$	*Real part of complex signal*
$s_i(t)$	*Imaginary part of complex signal*
$A(t)$	*Amplitude of complex signal*
$S(\omega)$	*Spectrum*
$\lvert S(\omega)\rvert^2$	*Energy density spectrum*
$\Phi(t,s)$	*Kernel of transform*
$\Psi(t,s)$	*Conjugate kernel*
$x(t)$	*Signal*
$x(s)$	*Transformation of* $x(t)$
f	*Frequency*
$sgn(f)$	*Signum function*
$X(f)$	*Fourier transform of* $x(t)$
A	*Area*
ε	*Permittivity of dielectric*

ATTENTION: The Singapore Copyright Act applies to the use of this document. Nanyang Technological University Library

LIST OF SYMBOLS

k	*Amount of reduction of effective electrical field*
d	*Distance*
Q	*Charges*
$\psi_i(x)$	*Basic function*
$h(\frac{t-a}{b})$	*Wavelet mother function*
a	*Dilation factor*
b	*Translation factor*
c_i	*Coefficient of Wavelet transform*
$c_{m,n}$	*Discrete coefficient*
$W(j,k)$	*Discrete Wavelet transform*
$h_{m,n}$	*Discrete basic function*
$y[k]$	*Output of filter*
$W_f(a,b)$	*Continuous Wavelet transform*
$\theta_s(x)$	*Smoothing operator*
y_d	*Output of defuzzifier*
$\mu_A(x)$	*Degree of membership*
B^{l*}	*Output of the l-th rule*
δ_l	*Center of gravity of fuzzy set*
L_{ij}	*Lose function*
η_{ij}	*S/N ratio*
X_i	*Input of neural network*
O	*Output of neural network*
Y	*Target output*
$E(w)$	*Error function*

ATTENTION: The Singapore Copyright Act applies to the use of this document. Nanyang Technological University Library

LIST OF SYMBOLS

H_{ij}	*Output of hidden node*
$f(x)$	*Transfer function*
W_{ij}	*Weight of neural network*
β_i	*Bias of node*
TP_s	*Time percentage of spark*
TP_a	*Time percentage of arc*
MR_s	*Material removal of a single spark*
MR_a	*Material removal of a single arc*
T_s	*Effective machining duration of spark*
T_a	*Effective machining duration of arc*
c_m	*Machining coefficient*
c_v	*Contribution coefficient of voltage to material removal rate*
c_i	*Contribution coefficient of current to material removal rate*
c_a	*Contribution coefficient of arc to material removal rate*
R_a	*Surface roughness*
D_s	*Depth of crater leaved by a single spark*
D_a	*Depth of crater leaved by a single arc*
k_m	*Machining coefficient*
k_v	*Contribution coefficient of voltage to surface roughness*
k_i	*Contribution coefficient of current to surface roughness*
o_s	*Overlap coefficient of sparks*
o_a	*Overlap coefficient of arcs*
k_a	*Contribution coefficient of arc to surface roughness*

ATTENTION: The Singapore Copyright Act applies to the use of this document. Nanyang Technological University Library

Chapter One

Introduction

1.1 Background and Motivation

Electrical discharge machining has gained more and more applications in manufacturing industries due to its outstanding advantages over conventional material removal processes when used for manufacturing tools, dies, and other difficult-to-cut parts. Although this process has been accepted as the standard machining process in many applications, its discharge mechanism has still not been fully understood as the pre-breakdown and breakdown of the dielectric media inside discharge gap involves unpredictable and ultra-fast events. For this reason, till now, a systematical description of the discharge mechanism has not been obtained, which makes an effective monitoring system difficult to be achieved.

For these years, researchers have tried to investigate the discharge mechanism of this process and expand its application to more industrial fields. At the same time a number of attempts for improving the performance of this process have been developed: optimization of process performance, establishment of process models, development of

ATTENTION: The Singapore Copyright Act applies to the use of this document. Nanyang Technological University Library

monitoring and control systems, etc. Despite the broad range, these attempts share the same objectives of achieving more metal removal coupled with a reduction in electrode wear and improved surface quality. Previous studies have shown that although the performance of EDM process is influenced complicatedly by many electrical and non-electrical parameters, the discharge conditions have overwhelming influences on them. Essentially, the input electrical power and the discharge conditions determine the process performance. Hence to improve the performance of EDM process, the discharge conditions must be correctly monitored. However, due to the complicated and stochastic nature of discharging process, efforts of developing reliable monitoring systems are still in progress. Discharge conditions are conventionally denoted as series of discharge pulses. Therefore the development of a pulse discriminator, which is able to detect deleterious discharge pulses, is very important for improving the performance of EDM process.

Generally, the discharge pulses can be classified into five types: opens, sparks, arcs and short-circuits, plus the intervals between two successive pulses that can be treated as off pulses. Among these pulses, opens, offs and short-circuits can be detected easily due to their distinctive characteristics. However, it is difficult to differentiate sparks and arcs because these two types of pulse exhibit quite similar characteristics. The monitoring systems are often based on the identification of adverse arcing occurring during machining because arcs usually cause surface damage of workpiece and decrease machining efficiency. In order to differentiate sparks and arcs, the discharge mechanisms of sparks and arcs must be well understood. Hence a monitoring signature, which can be used to investigate the discharge mechanism and differentiate sparks and arcs, should be selected carefully. Traditionally, signatures used for mechanism and

ATTENTION: The Singapore Copyright Act applies to the use of this document. Nanyang Technological University Library

monitoring investigations include voltage and current of discharge pulse, high frequency component of discharging process, discharge delay time and emitted radio frequency during machining. Previous studies have shown that although these signatures have been used in various occasions, they cannot interpret the discharge mechanism essentially and are insufficiently effective to differentiate sparks and arcs. To have a deeper understanding of discharge mechanism and realize a more reliable monitoring system, more effective signatures are in demand if possible.

Although EDM process is stochastic, it basically can be viewed as an electrical system because the occurring of discharge is resulted from the applied electrical power source. For electrical system, input electrical impedance is an inherent characteristic that will not vary with the inputs, but its changes do reflect the changes of the system itself. It is believed that arcs occur at the same spot as previous pulses because the dielectric media inside discharge gap is not fully deionized. Provided the distinctions between sparks and arcs are mainly due to different deionization status of the dielectric media, the input electrical impedances of sparks and arcs affirmatively have different characteristics. Thus, input electrical impedance is potentially a good signature for investigating the discharge mechanism and differentiating sparks and arcs.

1.2 Objective and Scope

In order to obtain the expected EDM performance, a possible approach is measuring the process performance on-line and adjusting the controllable working parameters when the measured process performance deviate from the expected one. However during machining, it is quite difficult, if not impossible, to measure the process

ATTENTION: The Singapore Copyright Act applies to the use of this document. Nanyang Technological University Library

performance directly, especially when EDM process is employed to fabricate micro-products. Hence, as an alternatively way, the discharge conditions instead of process performance are directly measured and used to indicate whether a control action is needed. For this purpose, the monitoring system of discharge conditions must be realized and the relationships among controllable working parameters, discharge conditions and process performance must be understood. That is, both working parameters and process performance need to be related to a certain small set of fundamental parameters (monitoring results of discharge conditions), which can be continuously measured on-line. For these purpose, investigations along four directions were carried out systematically in this research. The first one is investigating discharge mechanism. The second is monitoring discharge conditions. The third is studying the influences of controllable working parameters on discharge conditions and process performance, and fourthly, establishing models to predict process performance. The affiliations among the controllable working parameters, discharge conditions, monitoring results and process performance are shown in Figure 1-1.

Mechanism of discharging process: The aim of discharge mechanism study in this research is to investigate what is happening during an individual discharge pulse. As the discharge mechanism of opens, offs and short-circuits are easy to be understood, and because sparks and arcs are the dominant pulses involved in discharging process, the discharge mechanism of sparks and arcs was studied in detail. Through treating discharge gap as a black system and further simplifying it as a time-varying capacitor and resistor, the discharge mechanism of these two types of pulse was well interpreted after introducing the signature of input electrical impedance. As there are many working parameters have influences on input electrical impedance, to verify the

ATTENTION: The Singapore Copyright Act applies to the use of this document. Nanyang Technological University Library

reliability of the obtained discharge mechanism, the influences of working parameters on input electrical impedance were studied. The identification of these working parameters using input electrical impedance was also addressed.

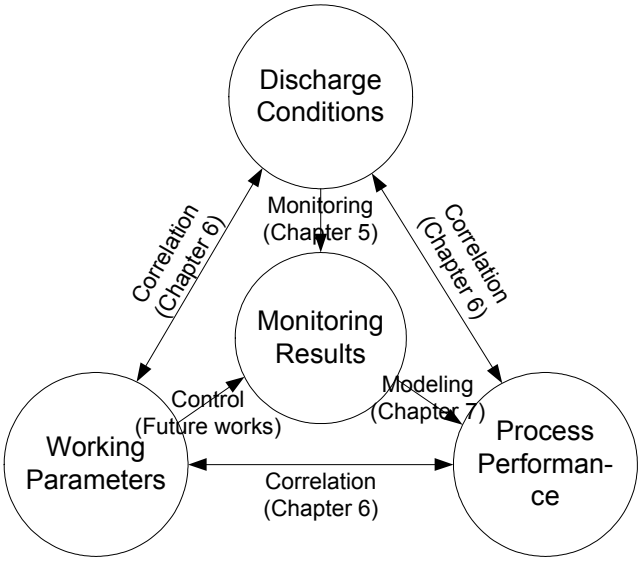

Figure 1-1 Affiliations among working parameters, discharge conditions, process performance and monitoring results

Monitoring of discharge conditions: The objective of monitoring study in this research is developing a monitoring system to correctly classify all the five types discharge pulse. Among these five types of pulse, opens, offs and short-circuits can be detected easily. The most challenging problem is to classify sparks and arcs correctly because these two types of pulse exhibit quite similar characteristics. For this purpose, input electrical impedance is employed as the signature, several features of the waveforms of this signature were extracted and a fuzzy classifier was developed to fulfill this task. The achieved monitoring system can differentiate sparks and arcs effectively and classify all the discharge pulses. Quantified monitoring results can be obtained after segmenting the discharge train into separate pulses and processing them

ATTENTION: The Singapore Copyright Act applies to the use of this document. Nanyang Technological University Library

individually. In addition, the correctness of the monitoring results was also verified through conducting verification experiments.

Influences of working parameters on EDM: Researchers have tried to explain the performance of EDM process using working parameters only, however they encountered lots of difficulties because the performance of EDM process will be influenced greatly not only by the working parameters, but also the discharge conditions. The objective of studying the influence of working parameters in this research is to understand the relationship among working parameters, discharge conditions and process performance, and identify the crucial factors of the performance of EDM process. For this purpose, detailed screening experiments were carried out. The influences of controllable working parameters on discharge conditions and process performance were investigated one by one while keeping the others at their optimum values. To save experimental cost and time, only those factors that have important influences on EDM performance had been taken into account. Those factors that have less important or are difficult to be controlled, were neglected. To ensure these neglects will not influence the research results, a repeatability study was carried out first to see whether EDM is a repeatable and controllable process. In addition, to determine the initial values of the working parameters for screening experiments, Taguchi method was employed to design the experiments.

EDM performance prediction: Conventionally, most of the models of EDM process are established to correlate working parameters with process performance. However, working parameter only cannot describe the process performance essentially, and due to a large number of variables and the stochastic nature of EDM process, these models

ATTENTION: The Singapore Copyright Act applies to the use of this document. Nanyang Technological University Library

are difficult to predict the process performance successfully. The objective of modeling study in this research is establishing models to predict process performance accurately. In this research, neural network and empirical models were developed to predict material removal rate and surface roughness respectively. As the material properties of electrode and workpiece and the electrical polarity have important influences on process performance, they should be taken into consideration for modeling purpose. However, as positive electrode polarity is suitable for machining the selected steel workpiece with copper electrode, they were neglected in this research.

1.3 Outline of Thesis

The basic knowledge and a detail literature review of EDM process are given in chapter two. A brief outline and the state-of-the-art of research works on EDM process were given in this chapter. The calculation and measurement of input electrical impedance are introduced in chapter three. In chapter four, the study of discharge mechanism using input electrical impedance and the study of the influences of working parameters on input electrical impedance are elaborated. In chapter five, a complete on-line monitoring system is developed to classify all discharge pulses. To find the crucial factors and give an essential explanation of process performance, the influences of working parameters on discharge conditions and process performance are studied and illuminated in chapter six. In chapter seven, the development of performance predictor for EDM process is discussed, empirical and Neural Network models are established. A summary of this research work is provided in chapter eight along with some recommendations and future works. The exploratory development of the control system is briefly introduced in this chapter too.

ATTENTION: The Singapore Copyright Act applies to the use of this document. Nanyang Technological University Library

Chapter Two

Electrical Discharge Machining

EDM is among the earliest nontraditional manufacturing processes. Its basis can be traced as far back as 1770 when English chemist Joseph priestly discovered the erosive effective of electrical discharges or sparks. In earlier days, very few saw the benefits of EDM process and the popularity of this primitive technology was scarce because as much electrode material was removed as the workpiece was, and the manual feed mechanism leads to more arcing than sparking. It was only in 1943 at the Moscow University where Lazarenko and Lazarenko [1] exploited the destructive properties of electrical discharges for constructive use. The Lazarenko EDM system made EDM machining more profitable and was widely used at the EDM machine in 1950s and later served as the model for successive developments in EDM. Their works were the turning point in the history of the EDM process. In the 1980s with the advent of computer numerical control in EDM that brought about tremendous advances in improving the efficiency of the machining process [2]. These growing merits of EDM have since then been intensely sought by the manufacturing industries yielding enormous economic benefits and generating keen research interests.

ATTENTION: The Singapore Copyright Act applies to the use of this document. Nanyang Technological University Library

2.1 Basic Knowledge of EDM

2.1.1 Material Removal Mechanism

The removal of material in electrical discharge machining is based upon the erosion effect of electrical discharge occurring between two electrodes immersed in a dielectric media. The underlying material removal mechanism in the EDM process is very complex and stochastic. It is a combination of electrodynamic, electromagnetic, thermodynamic, and hydrodynamic action [3]. Several theories have been forwarded in attempts to explain the complex phenomenon of "erosive discharging" [4-5].

1. Electro-mechanical theory:

This theory suggests that abrasion of material particles takes place as a result of the concentrated electric field. It proposes that the electric field separates the material particles of the workpiece as it exceeds the forces of cohesion in the lattice of the material. This theory neglects any thermal effects and experimental evidence lacks supports for it.

2. Thermo-mechanical theory:

This theory suggests that material removal in EDM operations is attributed to the melting of material caused by "flame jets". These so-called flame jets are formed as a result of various electrical effects of discharge. However, this theory does not agree with experiments data and fails to give a reasonable explanation of the effect of spark erosion.

3. Thermo-electric theory:

This theory, best supported by experimental evidence, suggests that metal removal in EDM operations takes place as a result of the generation of extremely high temperature

ATTENTION: The Singapore Copyright Act applies to the use of this document. Nanyang Technological University Library

generated by the high intensity of the discharge current. Although well supported, the theory cannot be considered as definite and complete because of difficulties in interpretation.

While several theories of how EDM works have been advanced over the years, most of the evidence supports the thermo-electric model. The following nine steps show what is believed to happen during an EDM cycle [6].

1) A charged electrode is brought near the workplace. Between them is insulating oil, known in EDM as dielectric fluid. Even though a dielectric fluid is a good insulator, a large enough electrical potential can cause the fluid to break down into ionic (charged) fragments, allowing an electrical current to pass from electrode to workpiece.
2) As the number of ionic (charged) particles increases, the insulating properties of the dielectric fluid begin to decrease along a narrow channel centered in the strongest part of the field. Voltage has reached its peak, but current is still zero.
3) A current is established as the fluid becomes less of an insulator. Voltage begins to decrease.
4) Heat builds up rapidly as current increases, and the voltage continues to drop. The heat vaporizes some of the fluid, workpiece, and electrode, and a discharge channel begins to form between the electrode and workpiece.
5) A vapor bubble tries to expand outward, but a rush of ions towards the discharge channel limits its expansion. The extremely intense electro-magnetic field that has built up attracts these ions. Current continues to rise, voltage drops.
6) Near the end of the on time, current and voltage have stabilized, heat and pressure within the vapor bubble have reached their maximum, and some metal is being

ATTENTION: The Singapore Copyright Act applies to the use of this document. Nanyang Technological University Library

removed. The layer of metal directly under the discharge column is in molten state, but is held in place by the pressure of the vapor bubble. The discharge channel consists now of a superheated plasma made up of vaporized metal, dielectric oil, and carbon with an intense current passing through it.

7) At the beginning of the off time, current and voltage drop to zero. The temperature decreases rapidly, collapsing the vapor bubble and causing the molten metal to be expelled from the workpiece.
8) Fresh dielectric fluid rushes in, flushing the debris away and quenching the surface of the workpiece. Unexpelled molten metal solidifies to form what is known as the recast layer.
9) The expelled metal solidifies into tiny spheres dispersed in the dielectric oil along with bits of carbon from the electrode. The remaining vapor rises to the surface. Without a sufficient off time, debris would collect making the spark unstable. This situation could create a DC arc that can damage the electrode and the surface of workpiece.

This on/off sequence represents one EDM cycle that can repeat up to several hundreds kilo times per second. There can be only one cycle occurring at any given time. Once this cycle is understood we can start to control the duration and intensity of the on/off pulses to make EDM work for us.

2.1.2 Performance of EDM

Three closely interrelated parameters: machining productivity (material removal rate), tool wear ratio, and the integrity of the surface produced, are employed in evaluating

ATTENTION: The Singapore Copyright Act applies to the use of this document. Nanyang Technological University Library

the approximate efficiency of electrical discharge machining. As an evaluation based on several parameters is cumbersome and ambiguous regardless of the kind of process involved, usually it becomes necessary to describe a definite conditional value to each of the parameters and to introduce a substitute parameter permitting a global process evaluation. In order to avoid this situation, the machining productivity obtained while imposing limits on the maximum values of the remaining parameters is employed as the chief criterion evaluating the electrical discharge process.

The definitions of these three process performance are listed below:

- Material removal rate (MRR): the metal removed from the workpiece during a certain machining duration. Since the rate of removal is dependent upon current intensity, the removal rate is directly proportional to an increase in amperage.
- Tool wear ratio (TWR): the ratio of volume of electrode material worn away to the volume of workpiece material removed. It may be corner or end wear.
- Surface integrality (SI): contains several factors, the size of craters leaved on the surface, the depth of the recast layer, and the depth of heat affect zone. Among these factors, the commonly used one to characterize SI is surface roughness (SR).

EDM is a complex and stochastic process. Its performance is affected by many working parameters and a single parameter change will influence the process in a complex way. The key electrical parameters that have important influences on this process are listed below:

- Voltage: the voltage used is usually a DC power supply source of 40 to 400 Volts. An AC power source can also be used but it usually couple with a DC rectifier. The

ATTENTION: The Singapore Copyright Act applies to the use of this document. Nanyang Technological University Library

preset voltage determines the width of the discharge gap between the leading edge of the electrode and the workpiece.

- Current: this is the most important factor. It determines the amount energy that transfer to heat during the process, so it can influence the performances easily. Usually, high current will increase the material removal rate, but it often leads to damage of the surface of workpiece. Furthermore, the depth and size of craters will be large, which will decrease the surface finish. In addition, because of the bigger discharge gap, the overcut will increase which results low accuracy of the product.
- Pulse on-time: all the work is done during pulse on-time. The longer the discharge is sustained, the more the material removed is. Consequently, the craters left on surface will be broader and deeper, resulted a rougher surface finish. Obviously with shorter duration of discharge, the surface finish will be better.
- Pulse interval: during pulse interval, the pulse rests and the deionization of the dielectric takes place. Bigger the pulse interval, greater will be the required machining time. Pulse interval also governs the stability of the process, an insufficient off time can leads to erratic cycling.
- Frequency: frequency is a measure of the number of the current is turned on and off. Low frequency leads to deeper craters, larger material removal rate and thicker recast layer, which cannot be used when surface integrity is concerned. Contrary, high frequency will have better surface finish and thinner recast layer.

2.1.3 Discharge Pulses in EDM Process

Past work on EDM processes has clearly established that the conditions prevailing in the gap have an often, overbearing influence on the quality of the machined surface.

ATTENTION: The Singapore Copyright Act applies to the use of this document. Nanyang Technological University Library

The ability to machine holes with a consistent quality will therefore depend on the ability of the EDM machine to provide optimum conditions for the individual discharges. The metallic debris presented in the dielectric in the machining gap, especially under the poor flushing conditions, make the gap condition complex and subject to variation. As a result, unfavorable machining conditions frequently occur at the gap causing bad localized discharge (arcs) and short circuit. This results in substantial damage to the machined surface and a reduction in the efficiency for the machining cycle. Hence, potentially the single most important characteristic of the EDM process influencing the quality of the drilled holes is the gap condition.

Based on the studies of EDM, Ahmed [7] and Rajurkar [8] have characterized the conditions existing in the machining gap through measurements of the instantaneous gap voltage, gap current and the radio frequency emission from the discharge. Generally, discharge pulses can be classified into several types: open, spark, arc, and short circuit. The gap voltage and current corresponding to these discharge pulses are shown in Figure 2-1.

- Open pulse, occurring when the distance between both electrodes is too large, the voltage is not high enough to breakdown the dielectric fluid, the energy for discharge is continuously accumulated, which obviously do not contribute to any material removal or electrode wear.
- The spark pulse indicates an effective discharge with an ignition delay time that results proper machining of the work surface.
- The arc pulse occurs in the same localized region as the previous discharge. Such localized discharges lead to poor surface finish and poor dimensional control of the machined surface. An arc is classified as a bad-machining discharge.

ATTENTION: The Singapore Copyright Act applies to the use of this document. Nanyang Technological University Library

- A short circuit occurs when metallic contact occurs between the electrode and the workpiece. It also does not contribute to material removal and cause damage to tool and workpiece. Short circuits are frequently caused by the presence of excessive debris in the gap or when the servo feed rate exceeds the rate at which the workpiece is being machined.

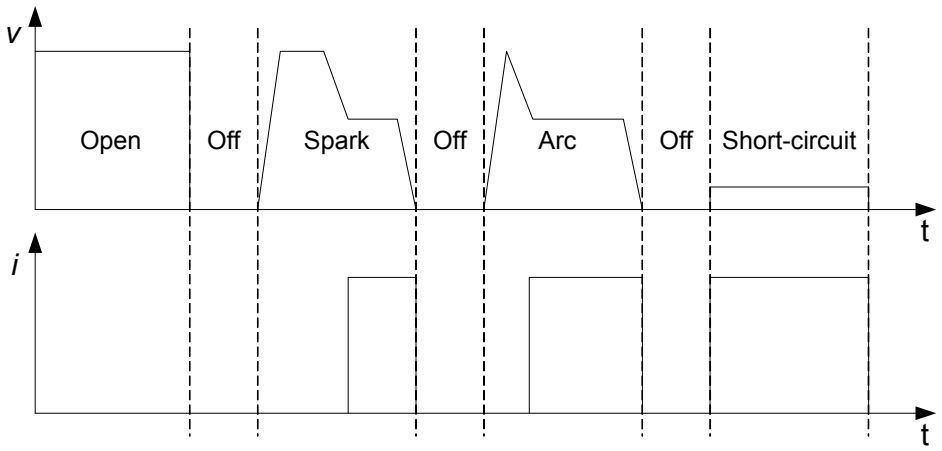

Figure 2-1 Ideal discharge pulses

The occurrence of frequent short circuit, open conditions, and arc discharges drastically reduces the efficiency of the machining cycle. When a voltage is applied across the machining gap, electrical breakdown occurs at the point when the field strength exceeds the breakdown value. In a configuration wherein the electrode surfaces are smooth and there is a uniform distribution of the dielectric fluid, breakdown will occur at that point where the gap between the electrodes is the smallest. However, in the EDM process the electrode surfaces are not smooth and the dielectric is usually not free of debris. Hence electrical breakdown can occur at points other than the minimum distance. The metallic debris suspended in the dielectric tends to concentrate the field in its neighborhood so that breakdown will occur in the vicinity of

ATTENTION: The Singapore Copyright Act applies to the use of this document. Nanyang Technological University Library

these particles. Also, residual ionization from a previous discharge promotes the subsequent discharges to occur at the same discharge column location, with the result of that, relatively deep craters are formed in the workpiece before the discharge transfers to another region. The latter type of discharge is classified as "arcs". The gap voltage corresponding to an arc usually does not have an appreciable ignition delay. Arcs are detrimental to the quality of the machined surface because they lead to non-uniform machining. If complete deionization of the dielectric takes place between consecutive discharges, then machining occurs more uniformly resulting in the surface quality of the machined surface being good. Under such conditions, the discharge is similar to the signal classified as "spark". In an ideal EDM process, all of the discharge pulses should be spark.

2.1.4 Variations of EDM

A number of EDM variations based on the basic configuration of EDM have emerged in the industry to cope with the machining of exotic materials or super hard metal alloys used exclusively in the manufacturing of aeronautical and aerospace parts. Wire-EDM is one of the most favorable variants owing to its ability to machine conductive, exotic and high strength and temperature resistive materials with the scope of generating intricate shapes and profiles [9]. It uses a thin continuously traveling wire feed through the workpiece by a microprocessor eliminating the need for elaborate pre-shaped electrodes, which are required in the EDM.

The recent trend in reducing the size of products has given micro-EDM a significant amount of research attention. Micro-EDM is capable of machining not only micro-

ATTENTION: The Singapore Copyright Act applies to the use of this document. Nanyang Technological University Library

holes and micro-shafts as small as 5μm in diameter but also complex three-dimensional micro-cavities [10]. Masuzawa et al. [11] made several successful attempts producing micro-parts such as micro-pins, micro-nozzles and micro-cavities using micro-EDM. In addition, a feasibility study of applying micro-EDM as an alternative method for producing photo-masks used in the integrated circuit industry has been conducted [12]. The manufacturing of electrodes used for micro-EDM encounters a lot of problems because the required electrode size is so small and the required precision is very high. Masuzawa [13] developed a new technique called wire electrical discharge grinding to alleviate these problems. The principle of the wire electrical discharge grinding process is similar to Wire-EDM. The tool electrode is machined by feeding downwards against a traveling sacrificial wire.

In addition, there is widespread academic and industrial interest in the development and use of hybrid machining process involving high-speed machining, laser beam machining and electrical chemical machining, etc. It utilized both conventional and unconventional material removal process making use of the combined advantages and limiting the adverse effects when applied individually. Several studies on the combined machining technology of ultrasonic machining and EDM, electrical chemical machining and EDM, EDM and laser beam machining have been carried out [14-15]. Other more specialized variations including electrical discharge texturing used for the texturing of cold rolled steel and aluminum sheets and electrical discharge grinding used for the manufacture of polycrystalline diamond cutting tools have also been reported [16].

ATTENTION: The Singapore Copyright Act applies to the use of this document. Nanyang Technological University Library

2.2 State-of-the-art of EDM

2.2.1 Applications

EDM has gained more and more application in manufacturing industries, and in some applications, EDM has replaced traditional machining processes. Such as in the milling of heat-treated tool steels, milled material has to be within an acceptable hardness range of less than 30-35HRC with ordinary tools [17]. However, EDM allows tool steels to be treated to full hardness before machining, avoiding the problems of dimensional variability, which are characteristic of post-treatment [18]. Since EDM does not induce mechanical stresses during machining, it provides an additional advantage in the manufacture of intricate products. Weng and Her [19] carried out several successful experiments involving an electrode of 50μm diameter and a multi-electrode for the bath production of micro-parts. This proposed method significantly reduces the production time and costs of fabricating both the electrodes and parts.

In recent years, the use of EDM for ceramics has overcome the technological limitation of the process requiring the electrical resistance of material with threshold values of approximately 100 or 300Ω/cm [20]. Mohri et al. [21] brought a new perspective to this traditional EDM phenomenon by using an assisting electrode facilitating the sparking of insulating ceramics. Both EDM and wire-EDM have been successfully tested for diffusing conductive particles from assisting electrode onto the surface of Sialon ceramics or silicon nitride. Other types of insulating ceramics materials including oxide ceramics such as zirconia and alumina, which have very limiting electrical conductive properties have also been examined based on the same technique [22]. On the other hand, Matsuo and Oshima [23] investigated the EDM of

ATTENTION: The Singapore Copyright Act applies to the use of this document. Nanyang Technological University Library

ZrO_2 and Al_2O_3 by doping with carbide, thereby increasing the electrical conductivity of the materials.

The development of different modern composite materials in the last decade has led to an expansion of EDM application. Yan et al. [24] surveyed the various machining processes performed on metal matrix composites and experimented with the machining of Al_2O_3/6061 Al composite using rotary EDM coupled with a disc-like electrode. The feasibility of machining ceramic-metal composite steel plate coated with WC-Co using plasma spraying was also examined [25]. Muller and Monaghan [26] compared the EDM of particle reinforced metal matrix composite with other non-conventional machining process such as laser beam machining and abrasive water jet. It was found that EDM was suitable for machining particle reinforced metal matrix composite with a relatively small amount of sub-surface damage but the MRR was very slow.

2.2.2 Methods for Improving Process Performance

Although electrical discharge machining is becoming more and more popular in many manufacturing field due to its outstanding advantages, it inevitably has some drawbacks that need to be improved in order to make this process more useful, such as increase productivity, decrease electrode wear, improve surface integrity, etc. Various approaches have been proposed for this purpose and will be introduced in this section.

***Polarity setting*:** The polarity of an EDM operation is normally quoted as the polarity of the electrode. In EDM, the choice of electrode polarity is an important factor. In most situations, using negative electrode polarity will decrease the tool wear rate and

ATTENTION: The Singapore Copyright Act applies to the use of this document. Nanyang Technological University Library

increase the material removal rate. The choice of polarity depends on the required removal rates and electrode wear in addition to the materials of the electrode and the workpiece. Electrode polarity guidance covers a range of electrode-workpiece combinations and types of EDM operations is usually provided by the machine manufacturers. When machine carbide and many exotic metals, the polarity is usually negative, however when machine steel, the polarity is positive. Her and Weng [27] found that in machining tungsten carbide, the use of negative electrode polarity is more desirable because negative polarity will give a higher material removal rate, lower electrode wear and better surface finish. Yoshiyuki and Akira [28] found that the material removal rate takes a maximum when the reversed polarity discharge is a little mixed into the normal polarity EDM due to the removal of the carbonized layer and/or heat resolved carbon of the machining fluid from the workpiece surface. The removal rate, electrode wear and surface finish depend on the ratio of the normal polarity discharge to the reversed one regardless of the number of each polarity discharge, and the electrode wear and the surface finish increase with increasing the ratio of the normal polarity EDM. Heng and Masanori [29] proposed a polarity-change pulse to obtain a greater material removal rate and a smaller tool wear.

***Flushing of dielectric fluid*:** There are also many methods for improving EDM performances through using different dielectric media, different powder additive or different flushing methods. The flushing of the dielectric has an adverse effect on the EDM performances. Lonardo and Bruzzone [30] revealed that flushing during the roughing operation affects the MRR and TWR, while in the finish operation, it influences the SR. The flushing rate also influences the crack density and recast layer, which can be minimized by obtaining an optimal flushing rate. In addition, the

ATTENTION: The Singapore Copyright Act applies to the use of this document. Nanyang Technological University Library

different properties of the dielectric media also play a vital role in flushing away the debris from the machining gap. Instead of using the commonly used kerosene, the possibility of using water as the dielectric media for micro-EDM has been experimented [31]. The results revealed a high MRR and low TWR without any metal carbides forming on the workpiece surface. Jung and Park [32] showed that better shape accuracy and surface integrity are obtained by using of kerosene oil than de-ionized water when machining WO-Co composite. They also proved that using spray method obtains better surface integrity than stream method because the dispersion effect of electrical discharge energy, but the MRR is lower. Some researchers have proved that some debris into the dielectric fluid can improve the performances of the EDM process [33]. The powder particles facilitate the ignition process by creating a higher discharge probability and lowering the breakdown strength of the insulating dielectric fluid [34]. As a result, it increases the MRR, reduces the TWR and produces a strong corrosion resistant surface [35]. Tzeng and Lee [36] proved that proper addition of powders to the dielectric fluid increase the MRR and decrease the TWR.

***Rotating the electrodes*:** Besides flushing of dielectric media, the techniques of applying rotational motion to the electrodes also affect EDM performance. Guu and Hocheng [37] provided a workpiece rotary motion to improve the circulation of the dielectric media in the gap and temperature distribution of the workpiece to yielding better MRR and SR. On the other hand, Kunieda and Masuzawa [38] proposed a horizontal EDM process in which the main machining axis is horizontal instead of the conventional vertical axis. The change of the basic construction in addition to the rotary motion of the workpiece offered an accessible evacuation of debris improving the erosion efficiency and accuracy of this process. Similarly, the rotary motion of

ATTENTION: The Singapore Copyright Act applies to the use of this document. Nanyang Technological University Library

electrode serves as an effective gap flushing technique, which significantly improves the MRR and SR [39]. Soni and Chakraverti [40] compared the various performances of rotating electrode with the stationary electrode. The results showed an improvement in MRR due to better flushing action and sparking efficiency with little SR, but the SR was high.

***Forced vibration of electrode*:** Forced vibration is a common and effective method to improve the performance of EDM. If the tool electrode is made to vibrate so that the gap between the tool and work opens and closes regularly, discharge is no longer entirely dependent upon the gap conditions. Sparking will occur when the electrodes are closest, and deionization of the dielectric fluid can take place when the gap is large enough to prevent sparking. S. H. Yeo [41] and Kremer [42, 43] applied ultrasonic vibrations, at 20000 Hz, to the electrode of EDM and obtained various improvements. Removal of the molten metal from every crater was faster, lowering the machining time. The heat affect layer was reduced, fewer micro-cracks resulted and fatigue resistance was improved six fold. However, electrode wear and surface roughness were higher. Enache et al. [44] studied the effects of the controlled force vibration introduced to the electrode on the various EDM performances. It was found that the vibratory motion yields comparable effects as the rotary motion of electrode, improving the MRR, enhancing the surface quality and increasing the stability of machining process.

***Waveform of power supply*:** In order to improve the accuracy of the products machined by EDM, many specialist and researcher have done lots of experiments to study how to reduce the electrode wear. In the second half of 1960's, a power supply

ATTENTION: The Singapore Copyright Act applies to the use of this document. Nanyang Technological University Library

using switching devices to provide a rectangular waveform current was introduced to enable less than 1% low wear machining. Thereafter, with the addition of a high voltage superposing circuit, the low electrode wear machining range further increased. Meanwhile, for further improvement of machining accuracy, no electrode wear machining had been studied. De Bruyn [45] presented a super low electrode wear machining process, which used a sloped waveform current generated by combining inductances, capacitances and resistances as appropriate in an electrical discharge circuit. This method showed the probability of less than 0.1% low wear machining. In addition, Kobayashi and Oizumi [46] proposed a machining method that employs a slope-controllable pulse power supply generated by switching devices. The electrode wear ratio could be less than 0.1%.

Except for the methods introduced above, there are lots of ways that have been explored to increase MRR. For example, Kunieda and Muto [47] experimented a multi-electrode discharging system delivering additional discharges simultaneously from a corresponding electrode connected serially. The TWR and energy efficiency were claimed to be better than the conventional EDM without any significant difference in the SR. In addition, an oxygen assisted EDM system, which greatly improves the MRR, was tested also by supplying oxygen into the discharge gap [48].

There are also some approaches that have been studied recently for improving the surface quality. For instance, the surface alloying method using the composite electrode to improve the surface properties of the workpiece has been reported by a number of authors [49]. In addition, ball burnish machining with EDM (BEDM) has been experimented to improve the workpiece surface integrity. It uses hard smooth

ATTENTION: The Singapore Copyright Act applies to the use of this document. Nanyang Technological University Library

balls attached to the electrode to form a plastic deformation layer on the workpiece surface during sparking, yielding a hardened and modified surface micro-structure [50]. It also improves the corrosion resistance, fatigue strength and SR of the workpeice surface [51]. Yan et al. [52] applied rotary motion to BEDM to further improve the MRR and SR when compared to conventional EDM.

2.2.3 Optimization and Modeling of EDM Process

The EDM process has a very strong stochastic nature, which makes it difficult to be optimized. The optimization of this process often involves relating the various process variables with the process performances, maximizing the MRR while minimizing the TWR and yielding the desired SR. The process variables include not only the electrical but also non-electrical parameters, which have received quite a substantial amount of research interest.

Traditionally, the selection of the most favorable process parameters was based on experience or handbook values, which produced inconsistent machining performance. Now, the optimization of parameters relies on process analysis to identify the effect of operating variables on achieving the desired machining characteristics. Lin et al. [53] employed grey relational analysis for solving the complicated interrelationships between process parameters and the multiple performance of the EDM process. Other works have applied the Taguchi approach to analyze and design the ideal EDM process. Marafona and Wykes [54] used the Taguchi method to improve the TWR by introducing high carbon content to the electrode prior to the normal sparking process. Lin et al. [55] employed it with a set of fuzzy logic to optimize the process parameters

ATTENTION: The Singapore Copyright Act applies to the use of this document. Nanyang Technological University Library

taking the various performances into consideration. Tzeng and Chen [56] optimized the high-speed EDM process by making use of dynamic signal-to-noise (S/N) ratio to classify the process variables into input signal, control and noise factors generating a dynamic range of output responses. In several cases, S/N ratio together with the analysis of variance (ANOVA) techniques is used to measure the amount of deviation from the desired performances and identify the crucial process variables affecting the process responses [57].

Although it is difficult to model EDM process for its complicated and stochastic nature, there are still some researchers endeavored on the modeling of this process and many different models had been proposed. Pandit and Rajurkar [58] presented a thermal model for EDM material removal rate based on data dependent system, this model is mathematically much simpler and its predictions are much closer to the experimental results compare with complicated model proposed in [59]. Spedding and Wang [60] presented an attempt at modeling EDM through response surface methodology and artificial neural network. Experiments showed that both of the models are able to predict the process performances, such as material removal rate, surface roughness within a reasonable range of input factors. Tsai and Wang [61] established several models for material removal rate, tool wear and surface finish respectively based on various neural-networks taking the effects of electrode polarity into account. They subsequently developed several semi-empirical models for different performances, which are dependent on the thermal, physical and electrical properties of the workpiece and electrode together with pertinent process parameters. It was noted that the semi-empirical models produce a more reliable performances prediction for a given work under different process conditions [62]. Wang et al. [63] developed a hybrid artificial

ATTENTION: The Singapore Copyright Act applies to the use of this document. Nanyang Technological University Library

neural network and genetic algorism methodology to modeling and optimization of EDM. Based on experimental results, the model was tested with satisfactory. Jeswani et al. [4] studied the effects of workpiece and electrode materials on SR and suggested an empirical model, which focused solely on pulse energy, whereas Zhang et al. [64] proposed an empirical model, built on both peak current and pulse duration, for the machining ceramics. It was realized that the discharge current has a greater effect on the MRR while the pulse on time has more influence on the SR and the white layer.

2.2.4 Monitoring of EDM Process

Today, most EDM machines are required to provide certain safe and adaptive control function for improving productivity and finishing quality. Hence real-time monitoring and evaluation of EDM process must be established. Usually, EDM pulse, i.e. the voltage and current of the tool-workpiece gap, are often used for monitoring the EDM process [65], because the metal removal rate, the surface finish and accuracy of the component are characterized strongly by the EDM pulses [66]. Variations in discharge pulses affect the removal rate, size accuracy and surface quality of the workpiece. The establishment of a set of technology conditions for determining the EDM discharge pulses has become a crucial issue in on-line control. Several monitoring technologies, including a four pulses type analyzer [67], emitted radio frequency analyzer [68] and a data dependent system modeling analyzer [69] have been reported in EDM literature. However, the EDM process is of a very strong stochastic nature due to its complicated discharge mechanism, noisy tool-workpiece gap voltage and gap current signal with some degree of unavoidable uncertainty and vagueness. So, it is still not easy to classify the EDM pulses property using previously developed technologies. Now, with

ATTENTION: The Singapore Copyright Act applies to the use of this document. Nanyang Technological University Library

the advance of theories and experimental technology of EDM process, especially with the rising of some other advanced technologies, many other monitoring and control methods based on different monitoring signals had been brought forward.

The instantaneous voltage across the machining gap and its variation with time during each discharge has been found to be a valuable signature of the discharge efficiency. It has been used as a primary measurement variable by a number of researchers to characterize the gap condition. Snoeys et al. [70] used a special instrument called "EDM-process analyzer" built by Philips Eindhoven to study the gap voltage in EDM. The EDM-process analyzer classified EDM pulses into open, spark, arc and short-circuits based on a measurement of the gap voltage. Using the instantaneous gap voltage measurements, Dauw, Snoeys and Dekeyser [71] have developed an "EDM Pulse Discriminator" for the detailed analysis of discharges. The voltage waveforms were classified into fifteen distinct pulse types by the discriminator based on specific features of the pulse shape. In addition, there have also been several attempts to obtain similar classifications through the measurement of the gap current. Rajurkar et al. [72] analyzed the pulse-current signal and developed criteria that detected the transition from sparking to an arcing condition.

Most of the monitoring system of traditional EDM detect only the average gap voltage, and adjust the distance of discharge gap to keep average voltage at reference voltage that is manually preset. However, several authors [71, 73] argued that the gap voltage is not a good indicator of the dynamic responses taking place at the sparking gap due to the high frequency noise component. These authors instead suggested monitoring the time ratio of transient arc measured by the pulse-on time, which shows the trend

ATTENTION: The Singapore Copyright Act applies to the use of this document. Nanyang Technological University Library

towards undesirable arcing. Recently, many monitoring and control systems employ delay time as the monitoring parameters and achieved better results. M. Weck [74] studied the relationship between the pulse type and material removal rate and tool wear by taking the ignition delay time as a process identification parameter and developed an adaptive gap controller, which reduces the number of undesirable pulses.

It has been experimentally found that the harmful arcs also take place with certain delay time during many machining conditions [75], so it is difficult to differentiate them from sparks correctly only using delay time as monitoring parameter. It has been found that the discharge voltage of sparks has a high frequency noise component whereas the arc has no observable high frequency ripple signal. The unstable transient arc is a special discharge state between normal spark and harmful stable arc. The corresponding magnitude and frequency of high frequency component of the discharge voltage is much lower than that of normal spark. Therefore, the time ratio of the transient arc indicates the trend towards arcing has been used to predict the occurrence of harmful stable arc. K. P. Rajurker and W. M. Wang [73] take gap voltage, current and the frequency of discharge to monitor EDM process. This monitoring system is able to identify the five basic EDM discharge pulses and precisely measure their average time radio.

In addition, the emitted radio frequency (RF) has been used to monitor and control EDM process. Hhattacharyya and El-Menshawy [76, 77] developed an RF monitoring system providing a pulse control to the machine power generator by examining the RF signal created from the spark gap. The RF monitoring system detects any drop in the

ATTENTION: The Singapore Copyright Act applies to the use of this document. Nanyang Technological University Library

intensity of signals to a threshold value whenever the discharge changes from sparking to arcing.

The conditions at the gap in EDM are time-variant and substantial changes in the process performance occur over time. Hence, efforts have been made to develop adaptive control for controlling the EDM process [78-87]. Most of the commercially available EDM systems, as well as the systems developed at the research laboratories, attempt to maximize the machining rate with minimum electrode wear at a given surface finish. These systems, having almost similar goal functions and control parameters, differ basically in their identification functions.

The development of industrial application of EDM demands it is able not only to produce parts with good performance, but also to be intelligent to adjust the machining process according to the working conditions and performance requirements. As EDM is complex and stochastic, it is difficult for conventional control systems to achieve this objective. However, the development of intelligent control method offers us a new approach. It is reasonable for us to employ intelligent control system for EDM process. Knowledge-based systems [88] were developed for control purpose, fuzzy controller and neural network also have been used more and more widely [89-98].

ATTENTION: The Singapore Copyright Act applies to the use of this document. Nanyang Technological University Library

Chapter Three

Input Electrical Impedance of EDM

Though EDM is a complicated process, it can still be viewed as a basic electrical system because the occurrences of electrical discharge are resulted from the applied electrical power source. For any electrical system, input electrical impedance is an inherent parameter that will not vary with the inputs, but its changes do reflect the characteristic changes of the system. In fact, input electrical impedance has been successfully used to study some electrical systems, such as spot welding, ultrasonic welding, ultrasonic wire bonding, micro drilling and inertial actuator [99-103]. These works demonstrate that it is possible to use input electrical impedance to explore the discharging mechanism and monitor the discharge conditions of EDM process.

This chapter discussed the impedance method used for discharge mechanism and monitoring studies, including the simplification of EDM system, derivation and calculation of input electrical impedance, etc. In addition, to calculate input electrical impedance, the voltage across and the current flows through the discharge gap need to be collected. The experimental setup was also illustrated in this chapter.

ATTENTION: The Singapore Copyright Act applies to the use of this document. Nanyang Technological University Library

3.1 Electrical Impedance Method

3.1.1 Simplification of EDM System

An EDM system can be modeled as a black box as shown in Figure 3-1. For this black box, its input is the voltage across discharge gap and the output is the current flowing through this gap. This system can be studied using input electrical impedance provided the input voltage and the output current are known, no matter how complicated the box is. In EDM processes, input voltage and output current can be readily measured, and the input electrical impedance can thus be computed. The input electrical impedance will not change with input voltage if this box is constant as output current will change with the input voltage accordingly. If the black box is a time-varying system, the input electrical impedance can reflect its dynamic characteristics as it in fact represents the relationship between the input voltage and the output current.

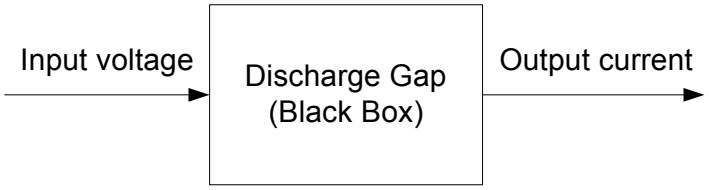

Figure 3-1 Input and output of black box

Based on the knowledge of electrical circuit, the discharge gap between the electrode and the workpiece with dielectric media inside can be viewed as a capacitor. However this capacitor is imperfect due to leakage current, thus it can be simplified as an ideal capacitor and a resistor in parallel, whose values vary with time. In fact, how to simplify the discharge gap is not important because we are not going inside this system.

ATTENTION: The Singapore Copyright Act applies to the use of this document. Nanyang Technological University Library

The simplified EDM system is illustrated in Figure 3-2. The capacitance of the capacitor is thus calculated using equation (3-1) or equation (3-2).

$$C(t) = \frac{Ak(t)\varepsilon}{d} \tag{3-1}$$

$$C(t) = \frac{Q(t)}{V} \tag{3-2}$$

where A is the area of the most closed peak of plate surfaces, ε is the permittivity of the dielectric media, k is defined to reflect the amount of reduction of effective electrical field, d is the distant of the most closed peaks, Q is the charges can be stored on the surfaces of the parallel plates and V is the applied voltage.

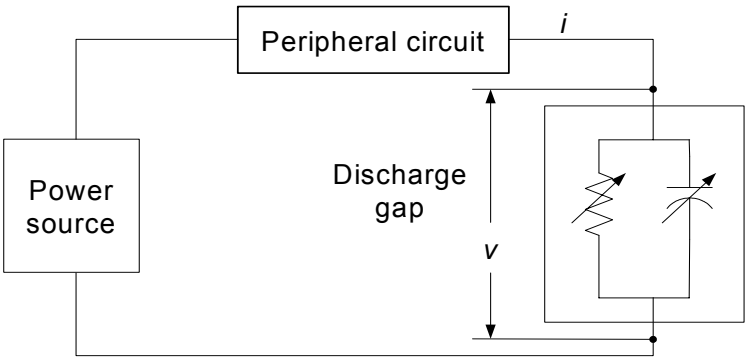

Figure 3-2 Simplified EDM system

3.1.2 Derivations and Calculation of Electrical Impedance

Electrical impedance is a very important property of electrical systems. It is widely used to study stationary process and always appears as a frequency dependent variable. For an electrical system, electrical impedance is always calculated by voltage over current in frequency domain. The ratio of the voltage and current amplitudes gives the absolute value of the electrical impedance at the given frequency, and the phase shift

ATTENTION: The Singapore Copyright Act applies to the use of this document. Nanyang Technological University Library

between the current and the voltage gives the phase of electrical impedance. The electrical impedance of an electrical system at the given frequency is defined as:

$$Z = V / I \tag{3-3}$$

The electrical impedance can also be expressed as the function of frequency as:

$$Z(f) = V(f) / I(f) \tag{3-4}$$

The difficulties in calculating electrical impedance in time domain is the sensed voltage and current are AC signals and they cannot be divided directly. In order to avoid this problem, we first convert the sensed voltage and current in real representations into their corresponding complex representations. The converted signals are called analytic signals [104]. Then impedance can be calculated by dividing the analytic voltage by the analytic current [105]. Electrical impedance can be expressed in complex form as

$$Z(t) = R(t) + jX(t) \tag{3-5}$$

The real part, $R(t)$ represents the resistance, and the imaginary part, $X(t)$ represents the capacitance and inductance.

Electrical impedance also can be expressed in magnitude and phase representation.

$$Z(t) = |Z(t)|e^{j\varphi(t)} \tag{3-6}$$

$$\begin{aligned} |Z(t)| &= \sqrt{R(t)^2 + X(t)^2} \\ \varphi(t) &= \arctan \frac{X(t)}{R(t)} \end{aligned} \tag{3-7}$$

Where $|Z(t)|$ is the magnitude and $\varphi(t)$ is the instantaneous phase of electrical impedance.

ATTENTION: The Singapore Copyright Act applies to the use of this document. Nanyang Technological University Library

Fast Fourier Transformation method (FFT) can be used to transform the signals from time domain into frequency domain, which provides the electrical impedance at a given frequency. However, FFT may neglect important time-dependent characteristics of the electrical impedance. In order to study a transient process, such as a discharging process, it is of great importance to calculate electrical impedance in time domain so as to indicate the time varying of system impedance. To obtain the time domain electrical impedance, in this study, Hilbert transformation method is used.

Hilbert transform of signal $x(t)$ are defined as [105]:

$$x(s) = \hat{x}(t) = H[x(t)] = \frac{1}{\pi}\int_{-\infty}^{\infty}\frac{x(t)}{s-t}dt \tag{3-8}$$

$$x(t) = H^{-1}[x(s)] = \frac{1}{\pi}\int_{-\infty}^{\infty}\frac{x(s)}{t-s}ds \tag{3-9}$$

This shows that Hilbert transform is defined using the kernel $\Phi(t,s) = 1/[\pi(s-t)]$ and the conjugate kernel $\psi(t,s) = 1/[\pi(t-s)]$. That is, the kernels differ only by sign. Here the variable s is a time variable. As a result, the Hilbert transform of a function of time is another function of time of different shape.

Transform (3-8) and (3-9) can also be written in terms of the convolution notation,

$$\hat{x}(t) = \frac{1}{\pi t} * x(t) \tag{3-10}$$

$$x(t) = -\frac{1}{\pi t} * \hat{x}(t) \tag{3-11}$$

Equation (3-10) is a convolution of $x(t)$ with the kernel $\theta(t) = 1/(\pi t)$. The Fourier transform of this kernel is

$$\theta(t) = \frac{1}{\pi t} \overset{F}{\Leftrightarrow} -j\,\mathrm{sgn}(f) \tag{3-12}$$

ATTENTION: The Singapore Copyright Act applies to the use of this document. Nanyang Technological University Library

Where the signum distribution function sgn(f) is defined as:

$$\mathrm{sgn}(f)=\begin{cases}1 & for \quad f>0\\ 0 & for \quad f=0\\ -1 & for \quad f<0\end{cases} \tag{3-13}$$

The theory of Fourier transformations shows that a convolution in the time domain corresponds to the product of Fourier transform. Therefore, the spectrum of $\hat{x}(t)$ is

$$\hat{X}(f)=-j\,\mathrm{sgn}(f)X(f) \tag{3-14}$$

So, the Hilbert transform of $x(t)$ can be calculated using its Fourier transform $\hat{X}(f)$.

$$\hat{x}(t)=F^{-1}(\hat{X}(f)) \tag{3-15}$$

Accordingly, the corresponding analytical signals of $v(t)$ and $i(t)$ are respectively

$$V(t)=v(t)+j\hat{v}(t)=a(t)e^{j\varphi(t)} \tag{3-16}$$

$$I(t)=i(t)+j\hat{i}(t)=b(t)e^{j\phi(t)} \tag{3-17}$$

In the above two equations, $v(t)$ and $i(t)$ is the real signal, $\hat{v}(t)$ and $\hat{i}(t)$ represent the Hilbert transform of $v(t)$ and $i(t)$. $a(t)$ and $b(t)$ are the instantaneous amplitude of $V(t)$ and $I(t)$, which can be calculate using function 3-18. $\varphi(t)$ and $\phi(t)$ are the instantaneous phases which can be evaluated using function 3-19 [106].

$$a(t)=\sqrt{v^2(t)+\hat{v}^2(t)}\;;\; b(t)=\sqrt{i^2(t)+\hat{i}^2(t)} \tag{3-18}$$

$$\varphi(t)=\arctan\left(\frac{\hat{v}(t)}{v(t)}\right);\; \phi(t)=\arctan\left(\frac{\hat{i}(t)}{i(t)}\right) \tag{3-19}$$

After being transformed into complex form, the following calculation becomes possible for evaluating the electrical impedance.

$$Z(t)=\frac{V(t)}{I(t)}=\frac{a(t)}{b(t)}e^{j(\varphi(t)-\phi(t))} \tag{3-20}$$

ATTENTION: The Singapore Copyright Act applies to the use of this document. Nanyang Technological University Library

Where $\frac{a(t)}{b(t)}$ and $\varphi(t)-\phi(t)$ are instantaneous amplitude and phase of $Z(t)$, and the instantaneous frequency of $Z(t)$ can be calculated using function 3-21.

$$\omega(t)=\frac{d\left(\varphi(t)-\phi(t)\right)}{dt} \tag{3-21}$$

3.2 Measurement of Input Electrical Impedance

3.2.1 Data Acquisition System

Figure 3-3 shows the electrical discharge machine used in the experiments, ROBOFORM 200, manufactured by CHARMILLES. The left part is working table, which has the feed control system, electrode fixtures, oil tank, pump system, etc. The right part is control table. The goal of the control system is to yield maximum removal efficiency and minimum electrode wear. However, in this research, in order to find the essential influences of working parameters on discharge conditions and process performance, most of the control functions were disabled during machining.

The dielectric medias to be used in the EDM process basically should satisfy several requirements, such as high dielectric strength, good degree of fluidity and cheap, etc. To investigate the influences of dielectric media on input electrical impedance, several kinds of dielectric media were studied, while for most of the experiments, total EDM 300 mineral oil was used. In addition, to reduce the influences of the temperature of dielectric media, a chill system was used to maintain the dielectric media at a constant temperature. Suitable flushing conditions are important to obtain the highest machining efficiency. Commonly used flushing methods include injection flushing, suction flushing, side flushing and some new developed methods. Several kinds of

ATTENTION: The Singapore Copyright Act applies to the use of this document. Nanyang Technological University Library

flushing methods are available in this EDM machine, however limited by the size of the electrode, only side flushing can be used. The flushing pressure was kept the same for all experiments to avoid the influence of flushing pressure.

Figure 3-3 CHARMILLES ROBOFORM 200 EDM Machine

Four main factors determine the suitability of a material used as an electrode. They are the maximum possible material removal rate, wear ratio, ease with which it can be shaped or fabricated to the desired shape and the cost. For a certain kind of workpiece, using different electrodes will result in quite different process performances and discharge conditions. To investigate the influences of material properties of electrode on input electrical impedance, two types of electrodes were studied. Because the size of the electrode has influences on discharge conditions and process performance too, the electrodes had exact same shape and size in all experiments. At the same time, to study the influences of workpiece's material properties on input electrical impedance, three types of workpieces were investigated, while for the other experiments, copper was employed as electrode and steel was employed as workpiece. Figure 3-4 shows the electrode and workpiece with their fixtures.

ATTENTION: The Singapore Copyright Act applies to the use of this document. Nanyang Technological University Library

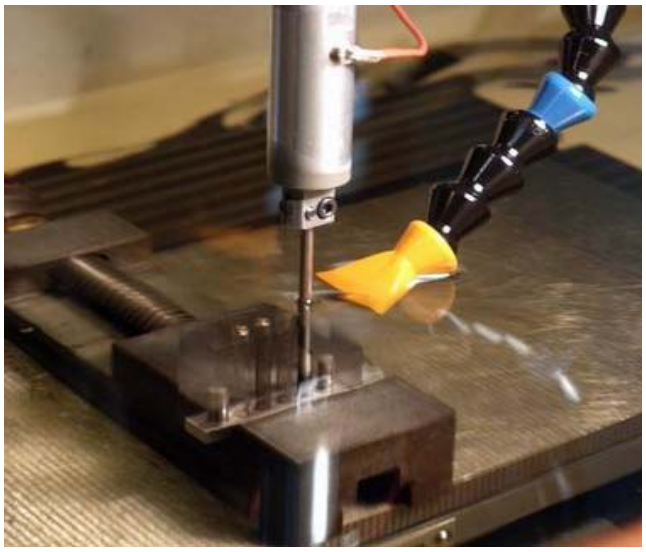

Figure 3-4 Electrode and workpiece with their fixtures

For calculating input electrical impedance, voltage crossing and current flowing through discharge gap need to be collected. The voltage and current are collected using voltage probe and current probe. As open voltage ranges from 80V to 200V and peak current ranges from 0.5A to 128A, suitable voltage and current probes should be selected. In addition, when short pulse on-time and pulse interval are used during machining, the discharge frequency can be very high. Hence to integrallty collect even the shortest discharge pulse, a data acquisition device with high sampling rate, high resolution and large memory is required. To satisfy these requirements, an ACQIRIS data collection board with high to 2G sampling frequency, 128K memories and 12 bits of resolution was used. For the high sampling frequency, it is impossible to collect all the data for a whole machining process, hence only one second's data every minute were collected and stored on computer for off-line analysis. The schematic diagram of the data acquisition system is shown in Figure 3-5, the measurement instruments include:

- Voltage probe (Tektronix P5205)

ATTENTION: The Singapore Copyright Act applies to the use of this document. Nanyang Technological University Library

- Voltage probe power supply (Tektronix 1103)
- Current probe (Tektronix A6302)
- Current amplifier (Tektronix TM502A)
- Acqiris DAQ board
- P4 computer system
- Software for data acquisition

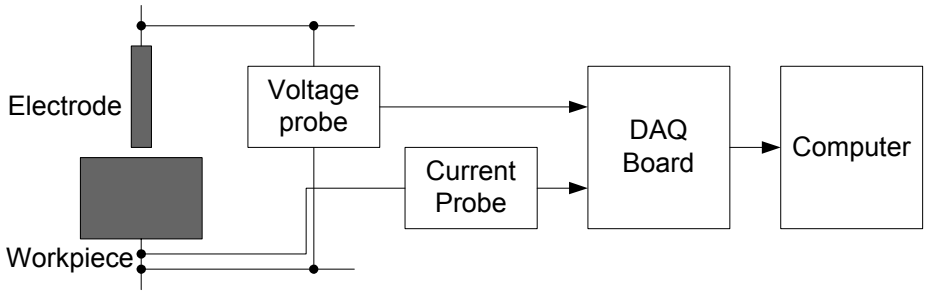

Figure 3-5 Schematic diagram of data acquisition system

3.2.2 Input Electrical Impedance

The application of Hilbert transform requires the transformed signals must be stationary. Otherwise after transformation, frequency deformation will exist. Figure 3-6 shows 200μs de-noised voltage and current collected with 100M sampling frequency. The open voltage, peak current, pulse on-time, pulse interval and gap size in this experiment were set as 120V, 2A, 1.6μs, 1.6μs and 0.02mm, respectively. It can be obviously seen that the collected voltage and current are not stationary, thus Hilbert transform cannot be used to calculate the input electrical impedance for the collected discharge trains directly. However, during a single discharging, as the discharge gap can be simplified as a linear system and the discharge voltage and current can be treated as stationary signals, Hilbert transform can still be applied to evaluate input

ATTENTION: The Singapore Copyright Act applies to the use of this document. Nanyang Technological University Library

electrical impedance for individual discharge pulse. It can be seen from this figure that the discharge trains contain seven discharge pulses. The corresponding input electrical impedances for the seven pulses were calculated and depicted in Figure 3-7 to 3-20.

Take the first pulse for example. Figure 3-7 and 3-8 show the magnitude and phase, real part and imaginary part of input electrical impedance respectively. It can be seen that the resistance, magnitude and phase of input electrical impedance have three obvious phases. In the first phase, magnitude of input electrical impedance and resistance increase, and phase of input electrical impedance is a negative constant. In the second phase, magnitude of input electrical impedance and resistance decrease, and phase of input electrical impedance is a positive constant. In the third phase, magnitude of input electrical impedance and resistance are small constants, while phase of input electrical impedance changes from positive value to negative value linearly. A detailed explanation of the changes of the magnitude and phase, real part and imaginary part of input electrical impedance will be discussed in next chapter.

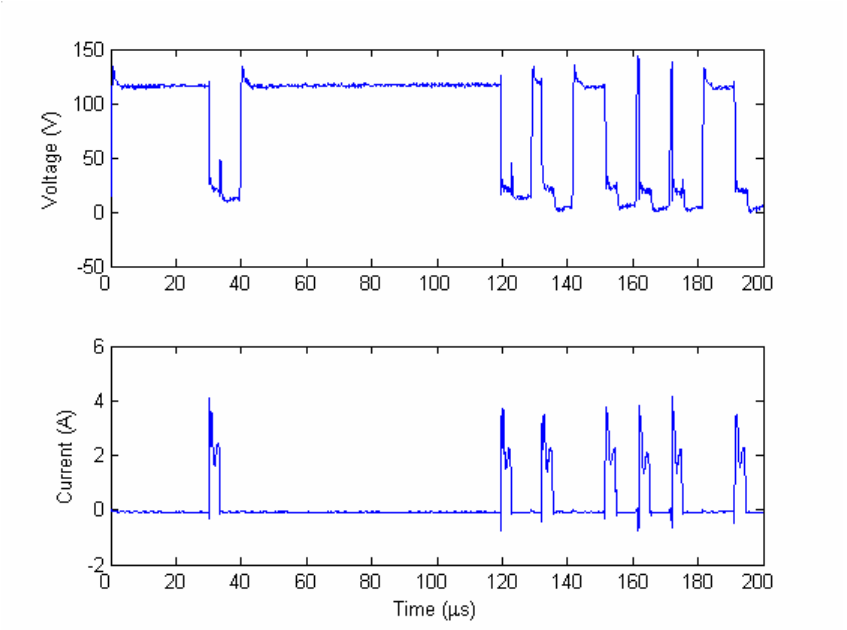

Figure 3-6 Voltage and current after de-noising

ATTENTION: The Singapore Copyright Act applies to the use of this document. Nanyang Technological University Library

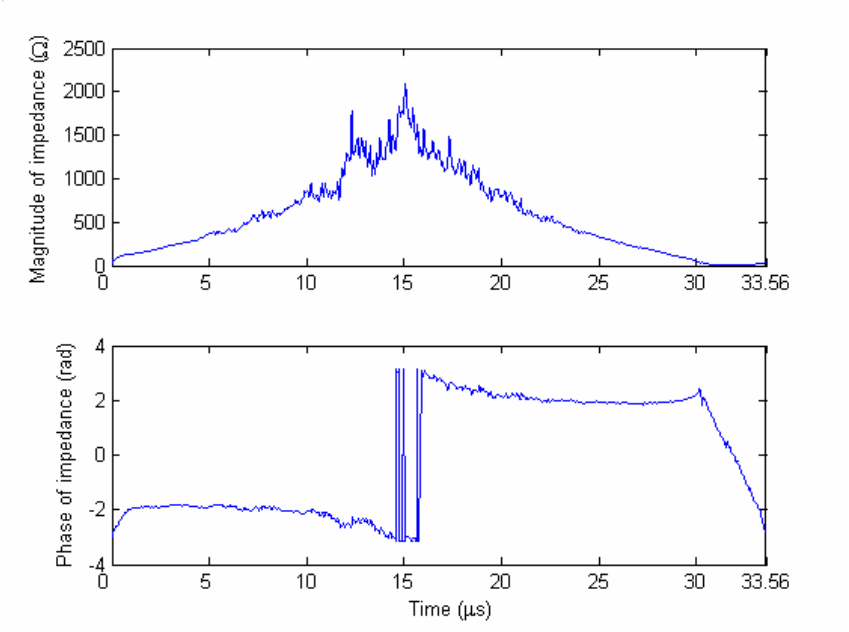

Figure 3-7 Magnitude and phase of input electrical impedance of pulse 1

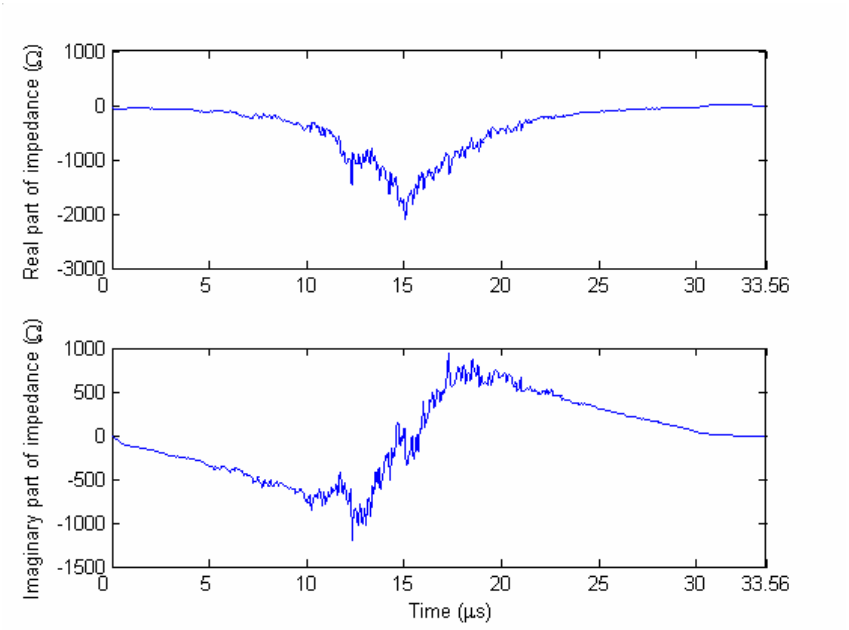

Figure 3-8 Real part and imaginary part of input electrical impedance of pulse 1

ATTENTION: The Singapore Copyright Act applies to the use of this document. Nanyang Technological University Library

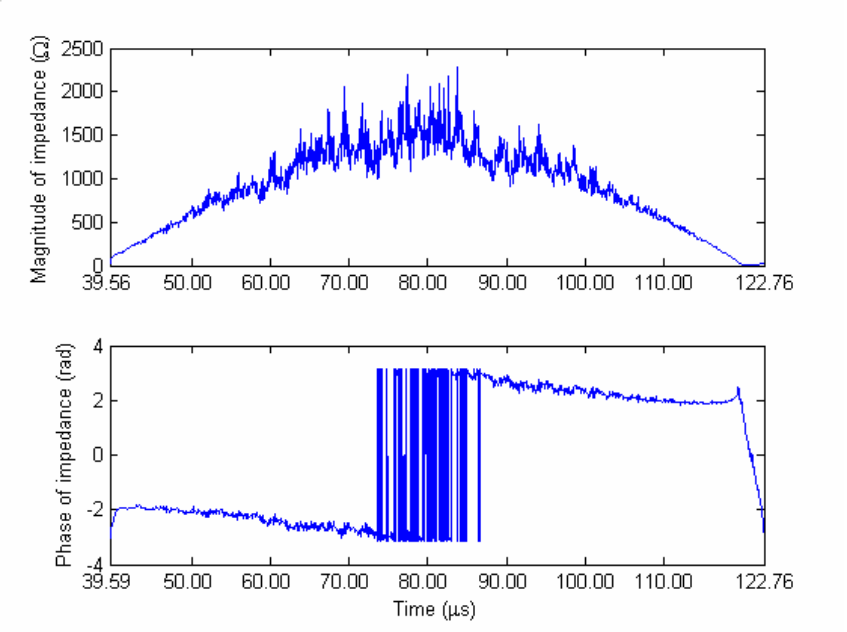

Figure 3-9 Magnitude and phase of input electrical impedance of pulse 2

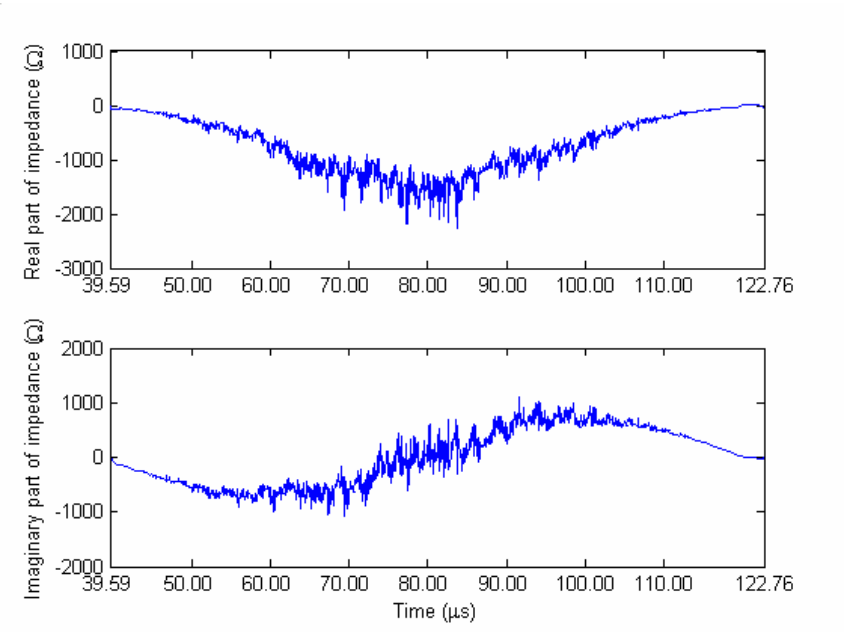

Figure 3-10 Real part and imaginary part of input electrical impedance of pulse 2

ATTENTION: The Singapore Copyright Act applies to the use of this document. Nanyang Technological University Library

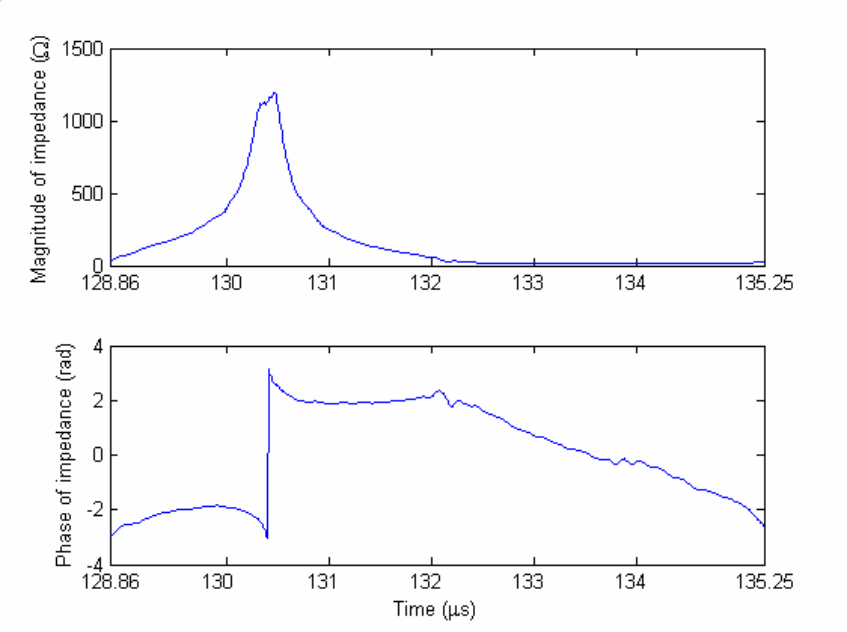

Figure 3-11 Magnitude and phase of input electrical impedance of pulse 3

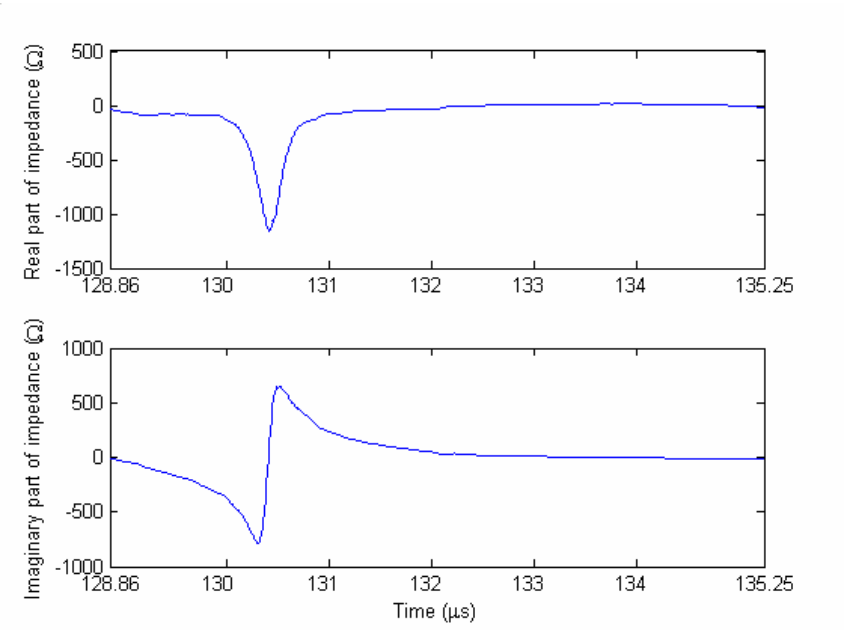

Figure 3-12 Real part and imaginary part of input electrical impedance of pulse 3

ATTENTION: The Singapore Copyright Act applies to the use of this document. Nanyang Technological University Library

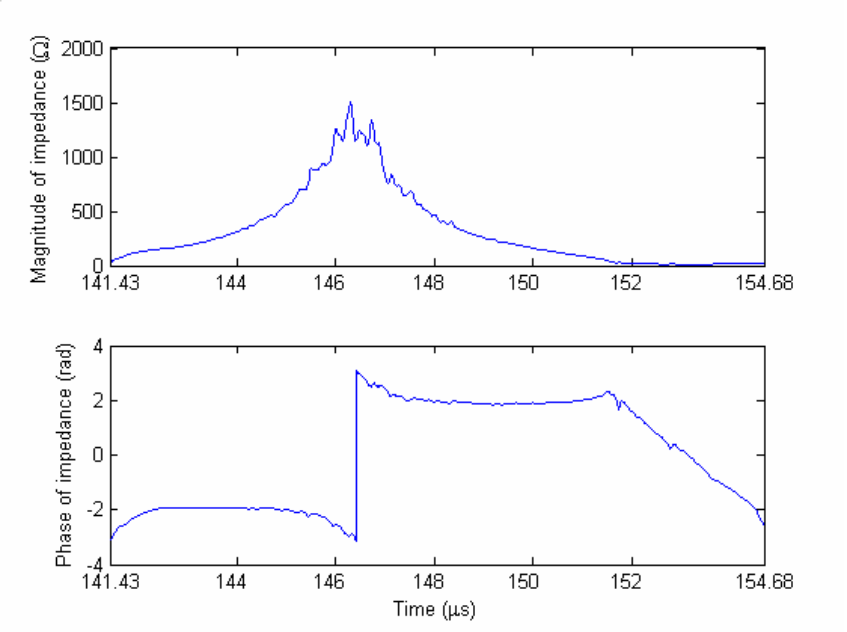

Figure 3-13 Magnitude and phase of input electrical impedance of pulse 4

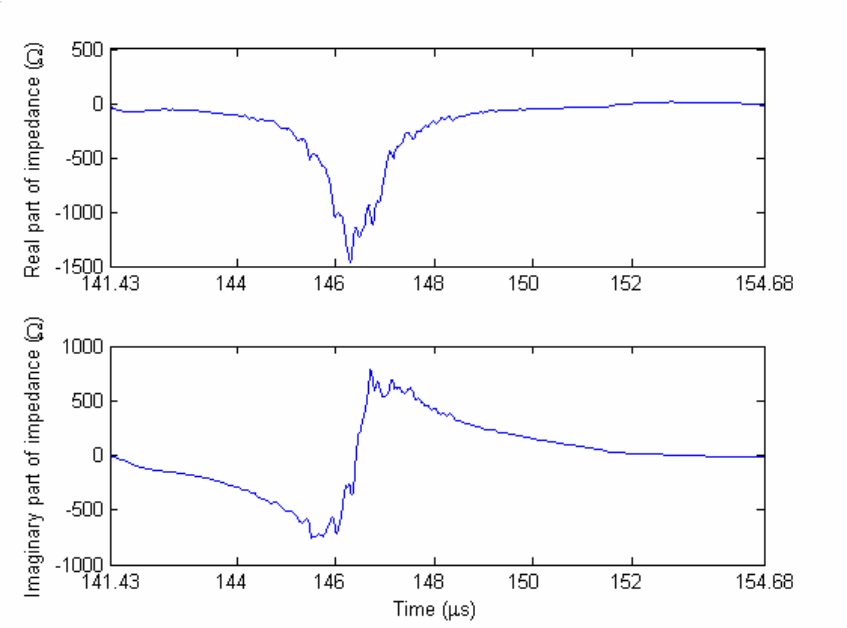

Figure 3-14 Real part and imaginary part of input electrical impedance of pulse 4

ATTENTION: The Singapore Copyright Act applies to the use of this document. Nanyang Technological University Library

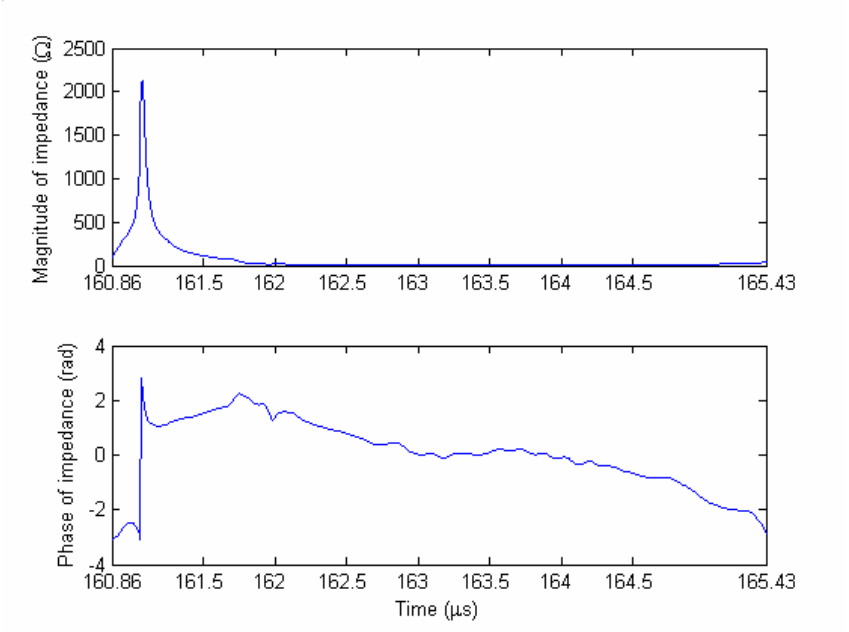

Figure 3-15 Magnitude and phase of input electrical impedance of pulse 5

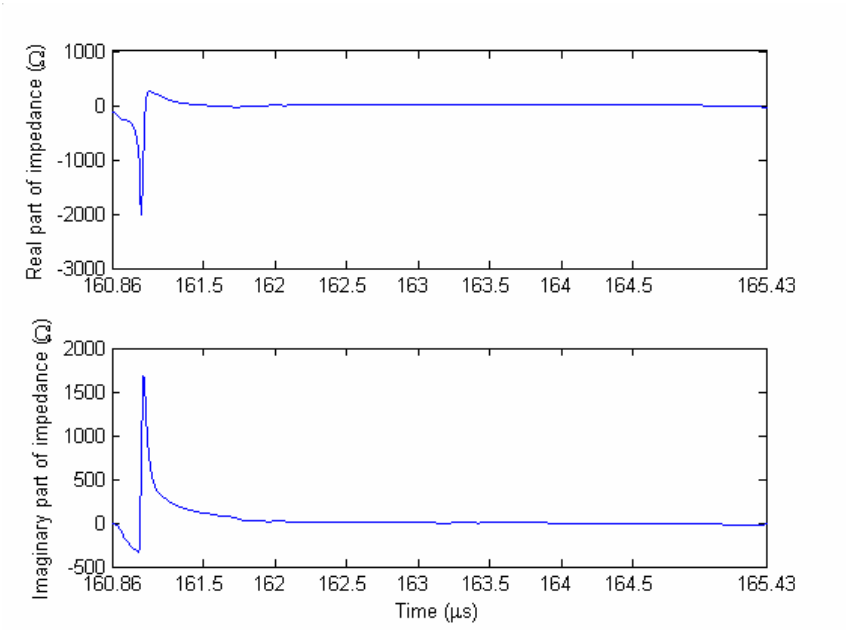

Figure 3-16 Real part and imaginary part of input electrical impedance of pulse 5

ATTENTION: The Singapore Copyright Act applies to the use of this document. Nanyang Technological University Library

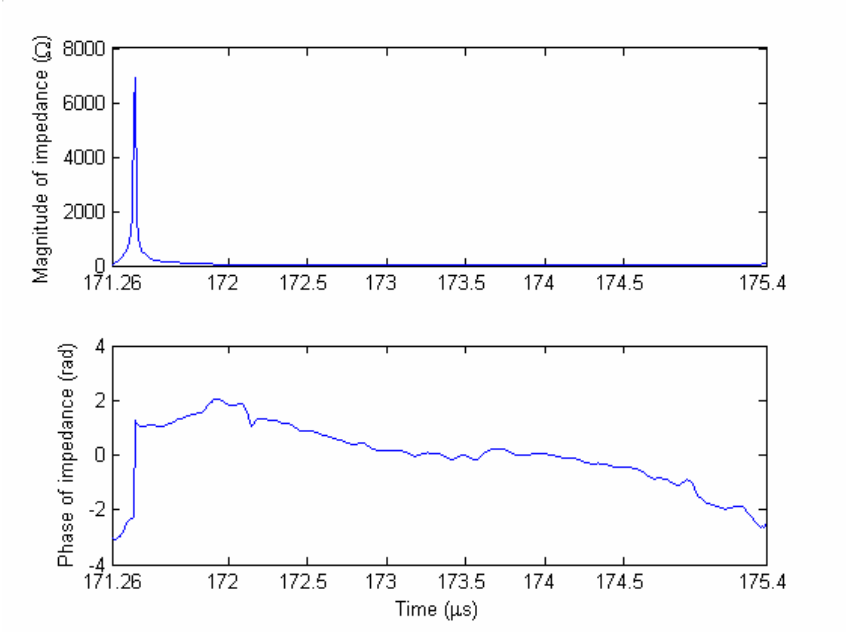

Figure 3-17 Magnitude and phase of input electrical impedance of pulse 6

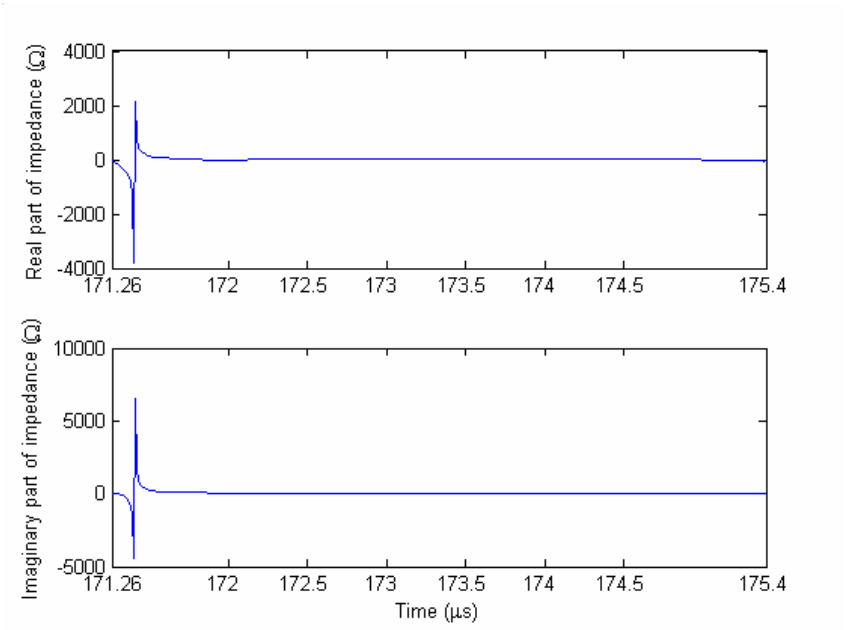

Figure 3-18 Real part and imaginary part of input electrical impedance of pulse 6

ATTENTION: The Singapore Copyright Act applies to the use of this document. Nanyang Technological University Library

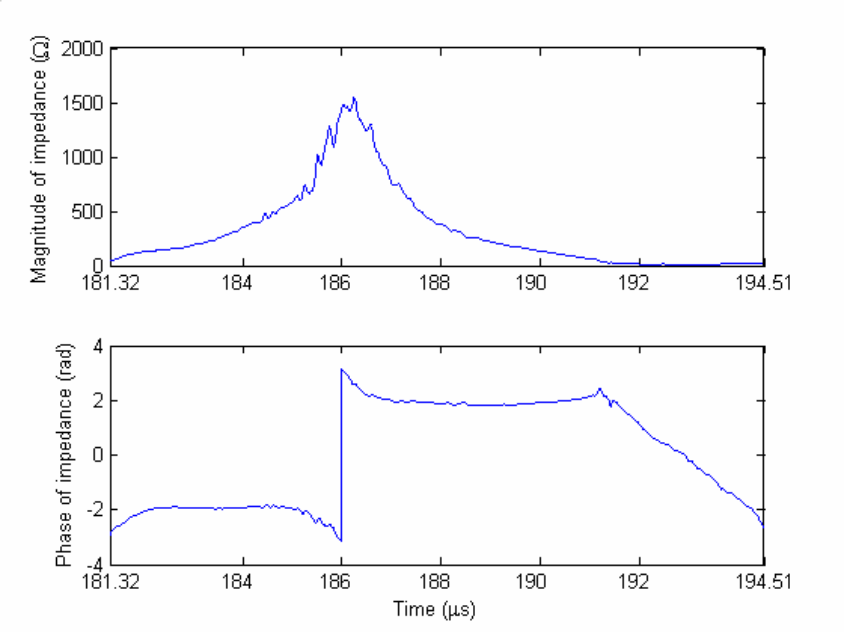

Figure 3-19 Magnitude and phase of input electrical impedance of pulse 7

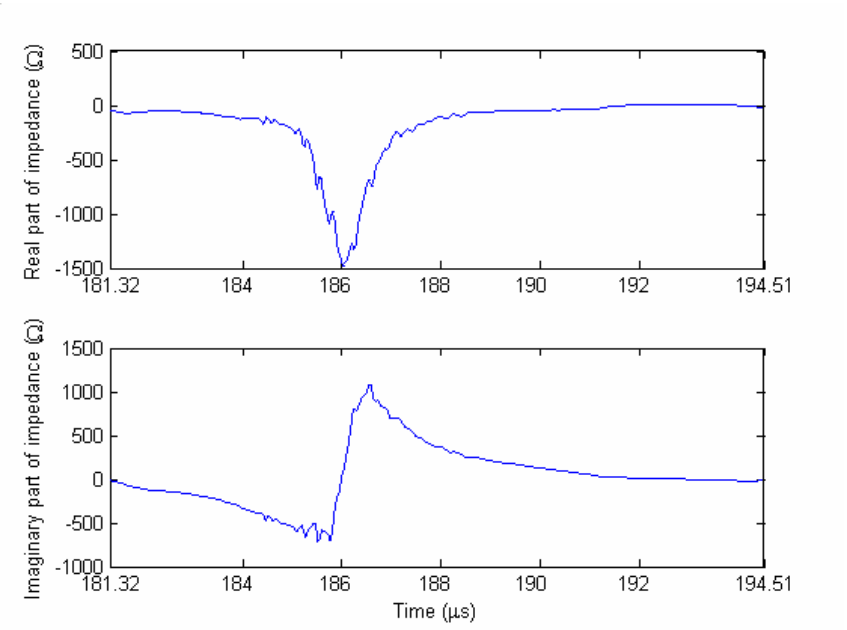

Figure 3-20 Real part and imaginary part of input electrical impedance of pulse 7

ATTENTION: The Singapore Copyright Act applies to the use of this document. Nanyang Technological University Library

Chapter Four

Mechanism of Electrical Discharge Machining

EDM is a nontraditional machining process, during which, material is eroded away by localized melting and evaporation due to high temperature caused by a series of recurring electrical discharges between electrode and workpiece in the presence of a dielectric media. Its applications have been found from traditional aerospace to modern electronic, photonics and biomedical industries. In spite of its widespread applications, the discharge mechanism has not been well understood due to the complex nature of this process, and the lack of comprehensive experimental investigations and robust signal processing methods. A deeper understanding of the discharge mechanism involved is of great significance for the development of effective monitoring systems. Previous research efforts were thus largely directed towards the development of theories in attempt to explain the phenomenon of "erosive discharging" and several theories have been forwarded for this purpose, however for the complicated nature of EDM process, these theories cannot describe the discharge mechanism successfully and been supported by experimental evidences [3, 5].

ATTENTION: The Singapore Copyright Act applies to the use of this document. Nanyang Technological University Library

On the other hand, to understand what happens in the discharge gap during machining, many researchers tried to model the discharge gap using basic electrical parameters. For example, Henderikus [107] treated the discharge gap as a time-varying resistance, and studied the discharge process using electrical circuit analysis method. Guenter etc. [108] modeled the discharge gap using more complicated electrical circuit based on the prediction that the gap resistance and an assumed discharge voltage vary with the time pattern of the discharge pulse. However, because electrical discharges involved in an EDM process is so complicated that normal electrical parameters is insufficient to simulate the its intrinsic nature. At the same time, it is difficult or even impossible to determine the values of those electric parameters.

Previous works also used process signals, such as discharge voltage and current, discharge delay time and radio frequency, to study the discharge mechanism [65, 68, and 74]. However these signals do not represent the inherent characteristics of discharging process and thus cannot exactly describe the discharge mechanism. To gain a deeper understanding of the discharging process, new signals that can describe discharge mechanism more essentially and accurately than the above mentioned ones, are required.

As indicated in last chapter, input electrical impedance is possibly be utilized to investigate discharging mechanism because it is an inherent characteristic of EDM system. This chapter discussed the discharge mechanism of sparks and arcs, the dominant discharge pulses of EDM process, detailedly. In addition, the effects of working parameters on input electrical impedance and the identification of these parameters using input electrical impedance were been addressed at the same time.

ATTENTION: The Singapore Copyright Act applies to the use of this document. Nanyang Technological University Library

4.1 Discharge Mechanism of Spark

The five types of discharge pulse in EDM process are sparks, arcs, opens, offs and short-circuits. The discharge mechanisms of opens, offs and short-circuits are easy to be understood, but it is difficult to investigate what is happening during sparks and arcs because the characteristics of these two types of pulse are quite similar.

Figure 4-1 shows the discharge voltage and current of a typical spark. From the time history of this pulse, four phases can be observed, that is rising, delay, falling and machining. After calculating using the method discussed in last chapter, the magnitude and phase, and the real part and imaginary part of input electrical impedance of this pulse are shown in Figure 4-2 and Figure 4-3, respectively. The input electrical impedance apparently provides more information than the time histories of voltage and current. As shown in Figure 4-3, the imaginary part of input electrical impedance clearly indicates that spark discharging consists of five phases.

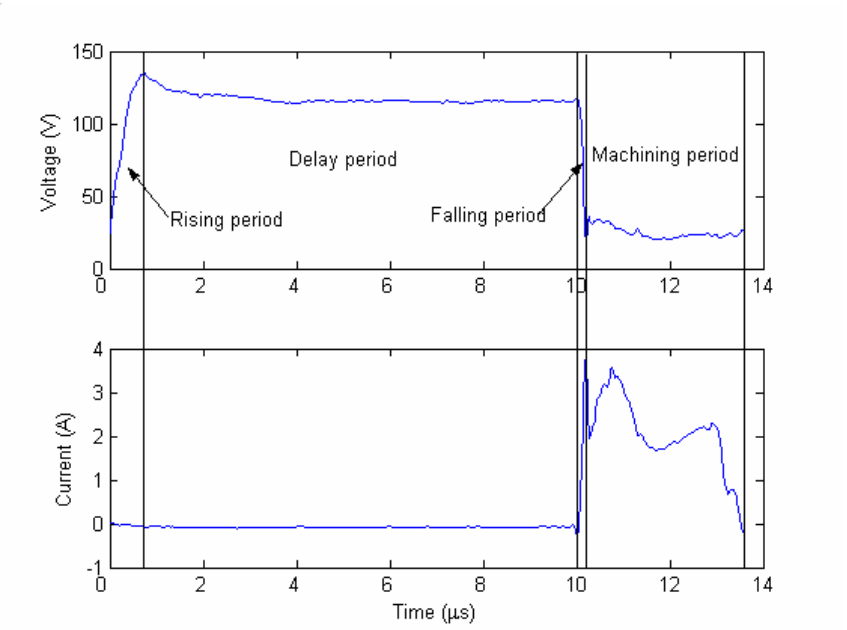

Figure 4-1 Voltage and current of a typical spark

ATTENTION: The Singapore Copyright Act applies to the use of this document. Nanyang Technological University Library

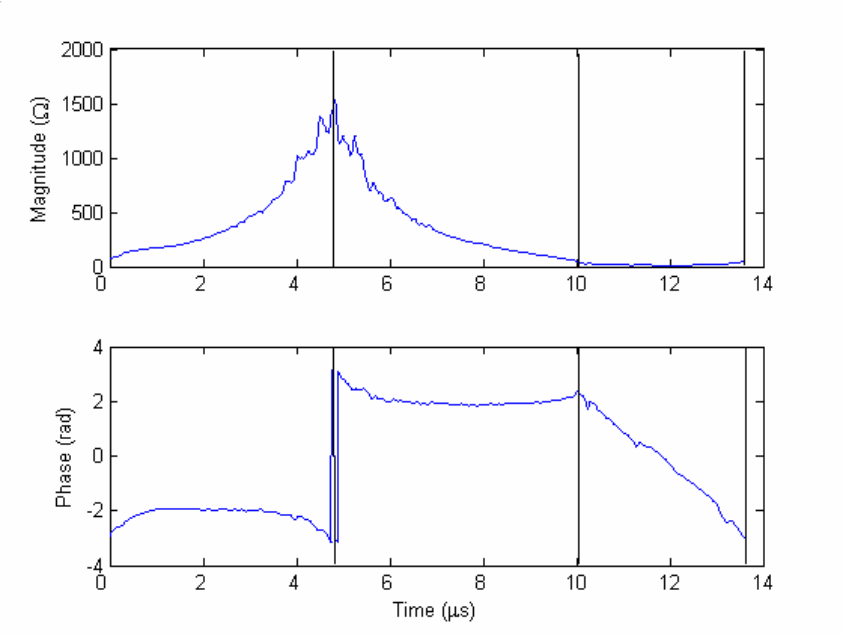

Figure 4-2 Magnitude and phase of input electrical impedance of a typical spark

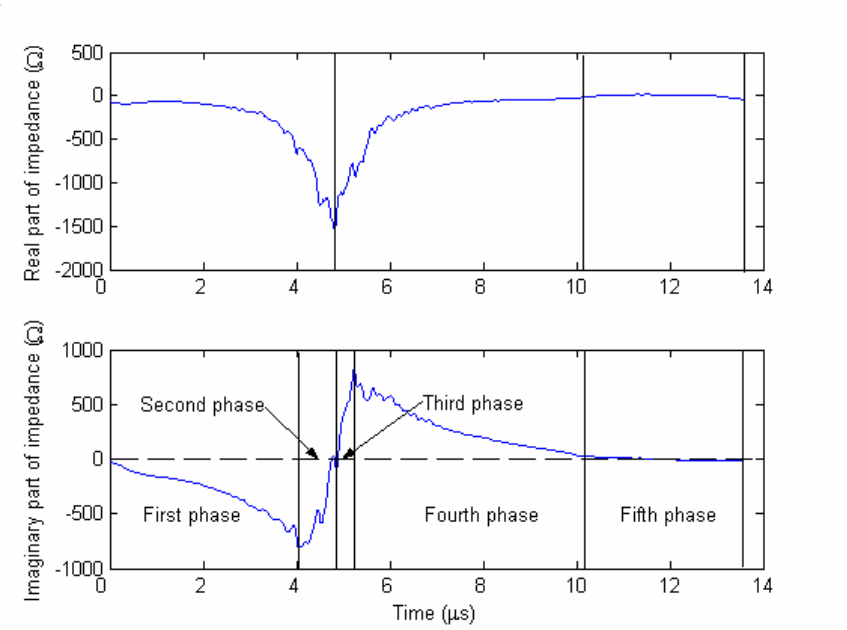

Figure 4-3 Real part and imaginary part of input electrical impedance of a typical spark

ATTENTION: The Singapore Copyright Act applies to the use of this document. Nanyang Technological University Library

In the first phase, voltage is applied on the capacitor that consists of the electrode and the workpiece, the capacitor is being charged as illustrated in Figure 4-4 (a). At the beginning of the charging cycle, the capacitor effectively acts as a DC short-circuit, thus resistance is very small. The intensification of electrical field between the most closely situated peaks of the plate surfaces causes the polarization, as well as orientation of the molecules and ions of the dielectric media. This decreases the effective electric field between the plate surfaces and results the increase of capacitance. Along with the becoming stronger of the polarization, factor k in equation (3-1) increases and sequentially, capacitance keeps increasing till attaining its maximum value. With more and more charges accumulate on the plates, charging slows down and the moving velocity of the electrons in the leading wire decreases. Therefore resistance keeps increasing. As both capacitance and resistance increase, the magnitude of input electrical impedance increases in this phase. The phase of input electrical impedance in this phase is almost a constant value close to –2, which means voltage lags current a constant phase because electrical field is formed due to the accumulation of electrons and ions. Here we define the capacitance at the end of phase one as *maximum capacitance*.

Theoretically, at the end of charging, when capacitance attains its maximum value, resistance should also reach its maximum value because no electrons flow in the leading wire. However, in the first phase, at some predetermined value, the individual electrons break loose from the surface of the cathode and are impelled towards the anode under the influence of field forces. While moving in the inter-electrode space, the electrons collide with the neutral molecules of dielectric media, detaching electrons from them and causing ionization. The detached electrons and ions are attracted to

ATTENTION: The Singapore Copyright Act applies to the use of this document. Nanyang Technological University Library

anode and cathode respectively and been neutralized there. As more and more dielectric media been ionized, the attracted electrons and ions cannot be neutralized efficiently and the net charges on anode and cathode surfaces starts to decrease, which means the ability to store charges of the parallel plate surfaces decreases and results the decrease of capacitance. The non-neutralized electrons and ions accumulated at the plate surfaces form an inverse electrical field. As shown in Figure 4-4 (b), this electrical field tries to stop the fleeing of the electrons from the cathode. Hence the moving velocity of the electrons in the wire keeps decreases, in other words, the resistance increases. As more and more electrons flow to anode and ions flow to cathode, the net charges on plate surfaces keep decreasing. The net electrical field becomes zero when the net charges on the plate surfaces become zero. Only at that time the moving velocity of the electrons in the leading wire decreases to the minimum value, capacitance decreases to zero and resistance attains its maximum value. So in the second phase, capacitance decreases from its maximum value to zero and resistance keeps increasing. At the same time, magnitude of input electrical impedance keeps increasing till attaining its maximum value. The phase of input electrical impedance in this phase is a constant value close to -2, which is almost same as that in the first phase. Here, we define the duration from the start of this pulse to the end of the second phase as *first balance time* or *static balance time*.

Because of overshooting, the flowing of the electrons and ions in dielectric media won't stop immediately when the net electrical field becomes zero. The anode surface gains more electrons than positive charges and the cathode surface gains more positive ions than electrons, anode starts to accumulate electrons and cathode starts to accumulate positive ions, in other words, the capacitor is charged in an inverse

ATTENTION: The Singapore Copyright Act applies to the use of this document. Nanyang Technological University Library

direction. As the ability to store charges of the parallel plates structure increases again, capacitance starts to increase in this phase. With overshooting lasting, the inversed electrical field becomes stronger and stronger and the net electrical field in the gap inversed and keeps increasing till attains its maximum value in inverse direction. To neutralize the electrons and ions on the plate surfaces, the moving velocity of the electrons in leading wire increases again and as a result of this, resistance decreases. When the net charges on plate surfaces reach its maximum value, capacitance reaches the maximum value in inverse direction. Hence in the third phase, capacitance keeps increasing, while resistance and the magnitude of input electrical impedance keep decreasing. At the beginning of phase three, the direction of electrical field is reversed while the flow of electrons and ions in the leading wire keeps the same direction, which is same as voltage leads current a phase. It can be seen from Figure 4-2, the phase of input electrical impedance is a constant value close to 2 and it turns from negative to positive at the beginning of this phase. The schematic representation of the accumulated charges and electrical field of this phase is shown in Figure 4-4 (c). Here we define the capacitance at the end of phase three as *inverse maximum capacitance*.

Under the force of the inversed electrical field, the flowing velocity of the electrons in dielectric media slows down and the moving velocity of the electrons in the leading wire keeps increasing, hence the accumulated electrons at anode and ions at cathode start to decrease, as shown in Figure 4-4 (d). As a result of this, capacitance starts to decrease and resistance keeps decreasing. Same as in the third phase, the phase of input electrical impedance in this phase is a constant close to 2. The inversed electrical field decreases till the net charges on plate surfaces become zero again at the end of this phase. Then, the charging, fleeing, ionization and accumulation of the ions and

ATTENTION: The Singapore Copyright Act applies to the use of this document. Nanyang Technological University Library

electrons attain a dynamic balance. The capacitance becomes zero again and the resistance becomes a very low value. Here, we defined the time from the start of this pulse to the end of the fourth phase as *second balance time* or *dynamic balance time*.

At the end of phase four, the ionization of the dielectric media reaches a certain degree, breakdown of the dielectric media occurs, a high current bridge established and machining starts. The liberation of energy accompanying the collisions of the electrons and ions on plate surfaces leads to the generation of extremely high temperature, causing fusion or partial vaporization of the metal and the dielectric media at the point of discharge. The flow of high-intensity current still furthers the ionization and produces a strong magnetic field that attracts the ions towards the axis of the discharge channel. These ions compress the current beam causing additional heating of the channel. Hence, in the fifth phase, capacitance is zero and both resistance and magnitude of input electrical impedance are low values. The dielectric media effectively acts as a conductor till the end of this pulse, whose value can be approximately calculated using the average voltage divided by the average current in machining duration.

From the discussion above, the spark discharging process can be summarized as following: It consists five phases. In the first phase, both capacitance and resistance increase. In the second phase, capacitance decreases and resistance increases. In these two phases, resistance and magnitude of input electrical impedance keeps increasing, the phase of input electrical impedance is a negative value close to -2. In the third phase, capacitance increases and resistance decreases. In the fourth phase, both capacitance and resistance decrease. In these two phases, resistance and the magnitude

ATTENTION: The Singapore Copyright Act applies to the use of this document. Nanyang Technological University Library

of input electrical impedance keeps decreasing and the phase is a positive value close to 2. In the fifth phase, capacitance is zero while resistance and magnitude of input electrical impedance are very small constants.

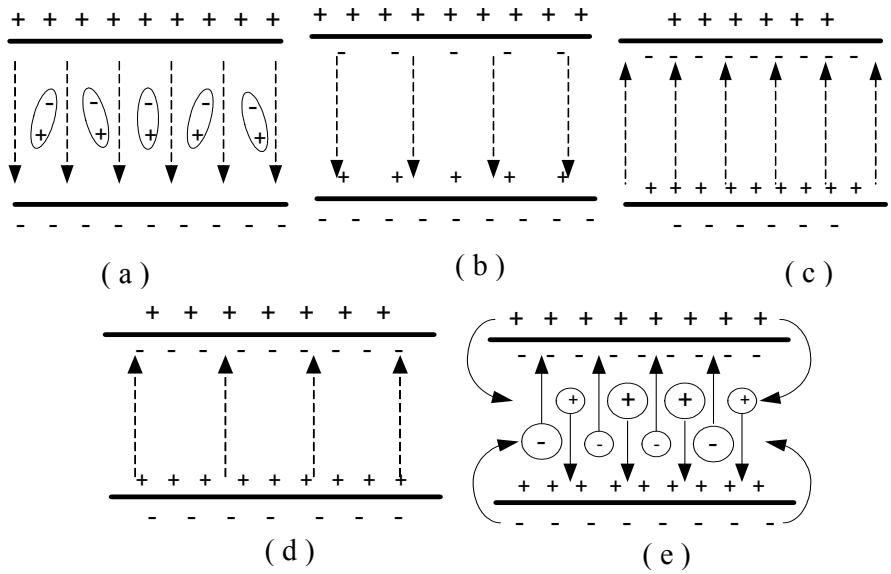

Figure 4-4 Schematic representation of discharging phases

4.2 Discharge Mechanism of Arc

The voltage and current of a typical arc are shown in Figure 4-5. The magnitude and phase, real part and imaginary part of its corresponding input electrical impedance are shown in Figure 4-6 and Figure 4-7, respectively. From Figures 4-7, it can be seen that the generation of the arc pulse can be divided into five phases too. In the first phase, both capacitance and resistance increase, and capacitance reaches its maximum value at the end of this phase. However, because the dielectric media is not fully deionized, there are lots of free electrons and ions left, under the influence of electrical field, these electrons and ions are attracted toward anode and cathode and been partly neutralized, which causes the ability to store charges of the parallel plates structure lower. As a

ATTENTION: The Singapore Copyright Act applies to the use of this document. Nanyang Technological University Library

result of this, the maximum capacitance of arc is lower than that of spark. In addition, the duration of the first phase in arc is shorter than that in spark because the capacitor needs shorter time to reach its maximum ability of storing charges.

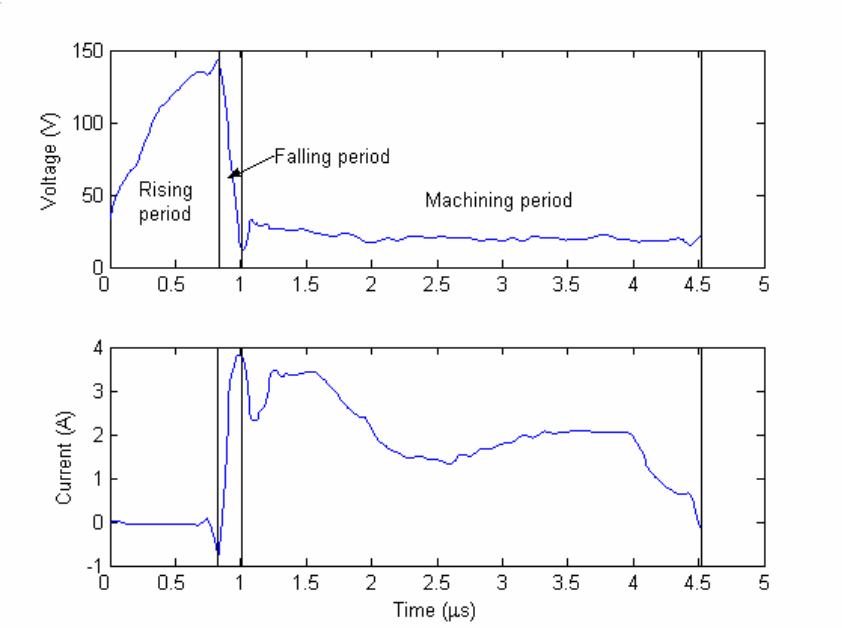

Figure 4-5 Voltage and current of a typical arc

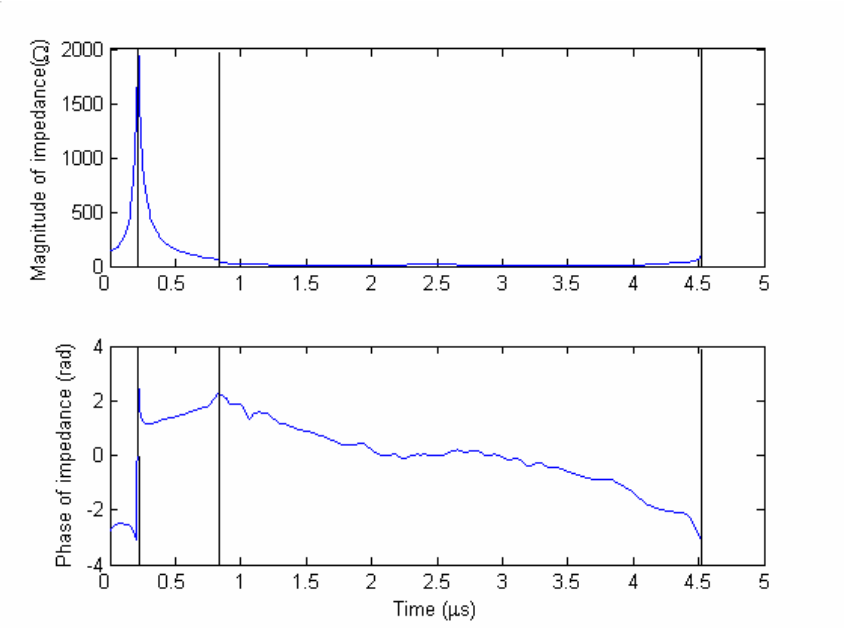

Figure 4-6 Magnitude and phase of input electrical impedance of a typical arc

ATTENTION: The Singapore Copyright Act applies to the use of this document. Nanyang Technological University Library

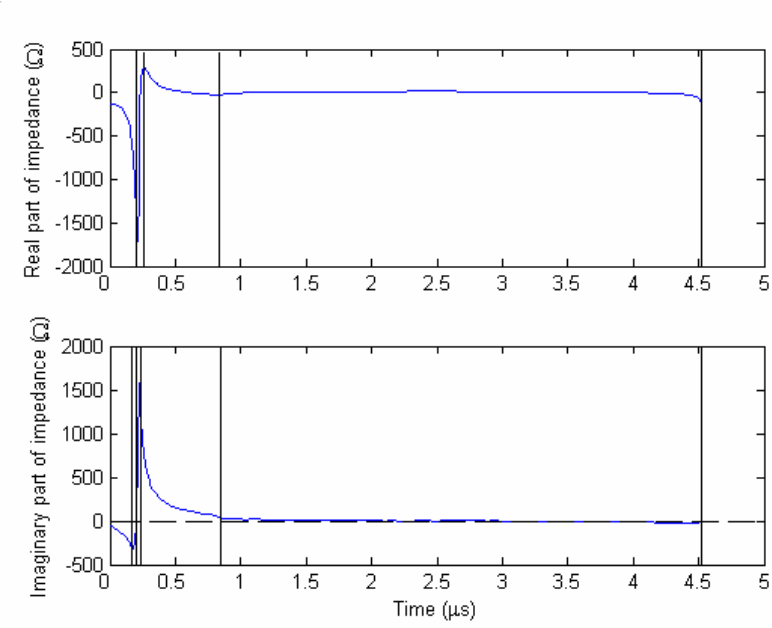

Figure 4-7 Real part and imaginary part of input electrical impedance of a typical arc

The second phase of arc is similar to that of spark except that the duration of this phase is shorter because the accumulation of the numerous free electrons and ions on anode and cathode surfaces is too fast to be neutralized in time. Hence, the ability to store charges of the parallel plates structure, in other words, the capacitance decreases to zero more quickly than that of spark. Since the first and the second phases of arc are both shorter than that of spark, the first balance time or static balance time of arc is much shorter than that of spark. In addition, as can be seen from Figure 4-6, in the first two phases, the phase of input electrical impedance of arc (close to –2.5) is smaller than that of spark (close to –2) due to the residual electrons and ions in dielectric.

In the third phase, the varying trend of the capacitance is same as that of spark, rising from zero to the inverse maximum capacitance. However, different to spark, the resistance of arc turns from its maximum value to the inverse maximum value first,

ATTENTION: The Singapore Copyright Act applies to the use of this document. Nanyang Technological University Library

and then decreases. This phenomenon is also caused by the insufficient deionization of dielectric media. Because the electrons from ionization, residual and fleeing away from cathode surface are so abundant that the inverse electrical field is stronger enough to stop the moving of electrons in the leading wire and even make the electrons move in inverse direction. As the non-neutralized electrons and ions of arc are much more than that of spark, the ability to store charges of the parallel plates structure is higher, the inverse maximum capacitance of arc is higher than that of spark. At the same time, because the overshooting of the electrons and ions in dielectric media when arc occurs is stronger, the duration of this phase is shorter than that of spark.

In the fourth phase, same as that of spark, capacitance decreases from the inverse maximum capacitance to zero and resistance decreases to a low value. However, the duration of this phase of arc is also shorter than that of spark because the strong inversed electrical field when arc occurs can even makes the electrons flow from anode to cathode. Thus, the inversed electrical field decreases more quickly and it needs shorter time to attain the state that the net charges on anode and cathode become zero. As the durations of the first four phases of arc are all shorter than that of spark, the time required attaining the second balance or dynamic balance is shorter. In addition, as can be seen from Figure 4-6, in the third and fourth phases, the phase of input electrical impedance of arc (close to 1.5) is smaller than that of spark (close to 2).

The fifth phase of arc has no much difference with that of spark. In this phase, both resistance and magnitude of input electrical impedance are small values and the capacitance is close to zero. In addition, the resistance and the magnitude of input electrical impedance are equal to that of spark if the gap size is exactly same.

ATTENTION: The Singapore Copyright Act applies to the use of this document. Nanyang Technological University Library

4.3 Effects of Working Parameters on Input Electrical Impedance

It is known that an EDM process is significantly affected by EDM working parameters. To further test whether these parameters would not influence the discharge mechanism and the input electrical impedance could sensitively identify the effects of these parameters, experiments under various machining conditions were carried out. As the analyzed input electrical impedance represents the input-output relationship of the discharge gap, it is found that only the following parameters have effects on input electrical impedance and will be studied respectively in this section, including the polarity of electrode, the materials of electrode and workpiece, the gap size and the materials of dielectric media. In these experiments, the EDM working parameters, such as open voltage, peak current, pulse on-time, pulse interval remained unchanged. The electrode polarity, electrode material, workpiece material, gap size and dielectric material were varied individually too see their effects on input electrical impedance.

Except for the working parameters mentioned above, the deionization status of the dielectric media also has significant influences on input electrical impedance. Theoretically, under the same machining conditions, if the dielectric media is perfectly deionized, all the discharge pulses are spark and the input electrical impedances of discharge pulses have no difference. However, it is very difficult even impossible to keep the deionization status of dielectric media for different experiments same, which makes the comparison of input electrical impedance for different working parameters difficult. To overcome this problem, it is assumed that pulses with same first balance time have same deionization status. Discharge pulses with close first balance time were extracted from the collected data that obtained from experiments carried out under

ATTENTION: The Singapore Copyright Act applies to the use of this document. Nanyang Technological University Library

different machining conditions. Theirs corresponding input electrical impedance signals were calculated.

4.3.1 Effects of Electrode Polarity

Figure 4-8 shows the voltage and the current for different electrode polarities. Their corresponding magnitude and phase, real part and imaginary part of input electrical impedance are shown in Figure 4-9 and 4-10, respectively. Figure 4-8 shows that the voltage and current from positive and negative polarities have no much difference, which means they cannot identify electrode polarity successfully. While from Figure 4-9 and 4-10, it can be seen that the maximum magnitude of input electrical impedance, maximum resistance and capacitance of positive polarity are much bigger than that of negative polarity. This is because when machining with negative polarity, copper cathode cannot provide sufficient electrons to carry the current, there are fewer charges can be stored on the surfaces of electrode and workpiece, which results a lower maximum capacitance. At the same time, the fleeing electrons from copper are insufficient to effectively ionize the dielectric media, the formed inverse electrical field is not strong enough to stop the moving of the electrons, which results a lower maximum resistance. As both real part and imaginary part of input electrical impedance are bigger, the maximum magnitude of input electrical impedance of positive polarity is bigger than that of negative polarity. Hence using input electrical impedance can successfully identify the electrode polarity. In addition, it can be seen from Figure 4-10 that the electrode polarity will not affect the discharge mechanism obtained in last section. The monitoring system of discharge conditions, which will be developed in next chapter, can be used in spite of the electrode polarities.

ATTENTION: The Singapore Copyright Act applies to the use of this document. Nanyang Technological University Library

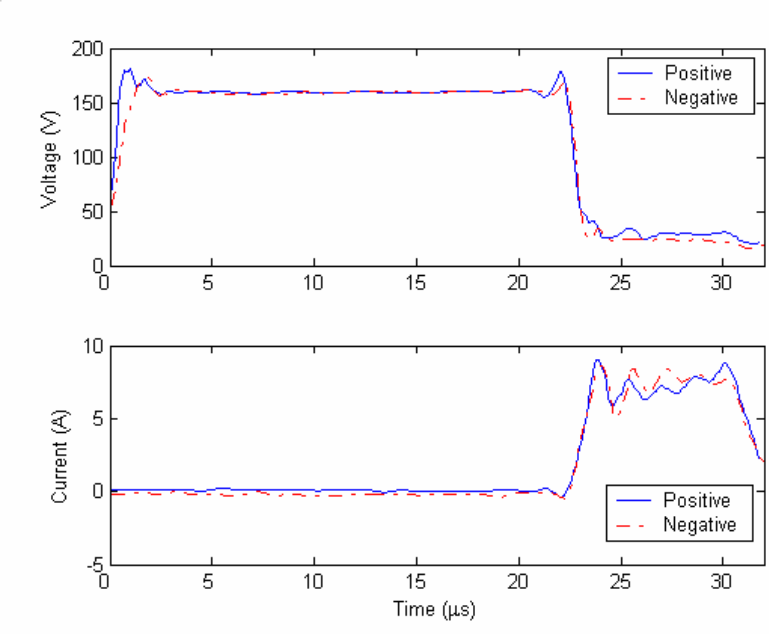

Figure 4-8 Voltage and current for different polarities

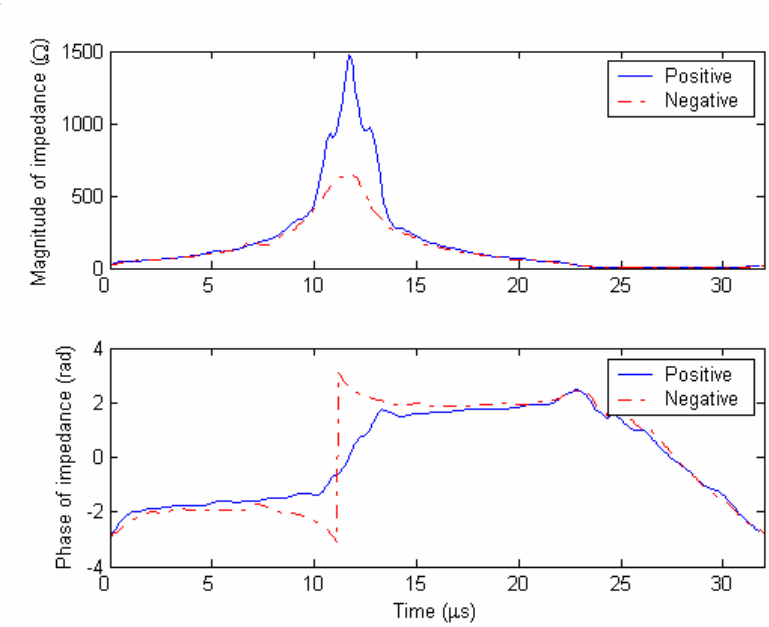

Figure 4-9 Magnitude and phase of input electrical impedance for different polarities

ATTENTION: The Singapore Copyright Act applies to the use of this document. Nanyang Technological University Library

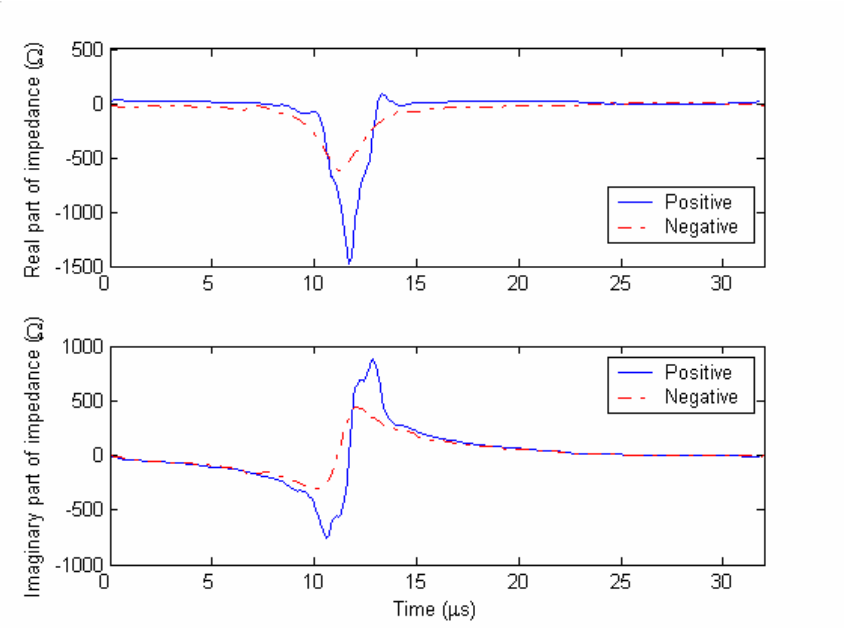

Figure 4-10 Real part and imaginary part of input electrical impedance for different polarities

4.3.2 Effects of Electrode Material

Actually, it is quite difficult to study the effects of the properties of electrode material because there are so many of them have influence on the input electrical impedance. While before the breakdown of dielectric media, input electrical impedance is mainly influenced by the atomic structure of the electrode material. In other words, the resistivity of this material plays the major role. Copper and copper tungsten were used to study the effects of electrode material on input electrical impedance. The resistivity of these two types of material is 9μΩcm and 5.5μΩcm respectively.

The voltage and current for different electrodes shown in Figure 4-11 almost have no difference and thus cannot identify the electrode material successfully. Figure 4-12 and Figure 4-13 show the magnitude and phase, real part and imaginary part of input

ATTENTION: The Singapore Copyright Act applies to the use of this document. Nanyang Technological University Library

electrical impedance. From these two figures, it can be seen that using copper electrode has bigger maximum magnitude of input electrical impedance, maximum resistance and maximum capacitance because copper has bigger resistivity. When copper is used as electrode, there are less electrons flee from the cathode to ionize the dielectric media and the accumulated ions and electrons on the surfaces of electrode and workpiece cannot be neutralized in time, which means the capacitor can store more charges, and thus the capacitance is bigger. In addition, for the bigger resistivity, at the first balance time, there are fewer electrons moving in the leading wire, which means the maximum resistance using copper electrode is bigger than that of using copper tungsten electrode. Hence using input electrical impedance can successfully identify electrode materials. Electrode with bigger resistivity has bigger maximum magnitude of input electrical impedance, maximum resistance and maximum capacitance. In addition, it can be obviously seen that the material of electrode will not influence the discharge mechanism.

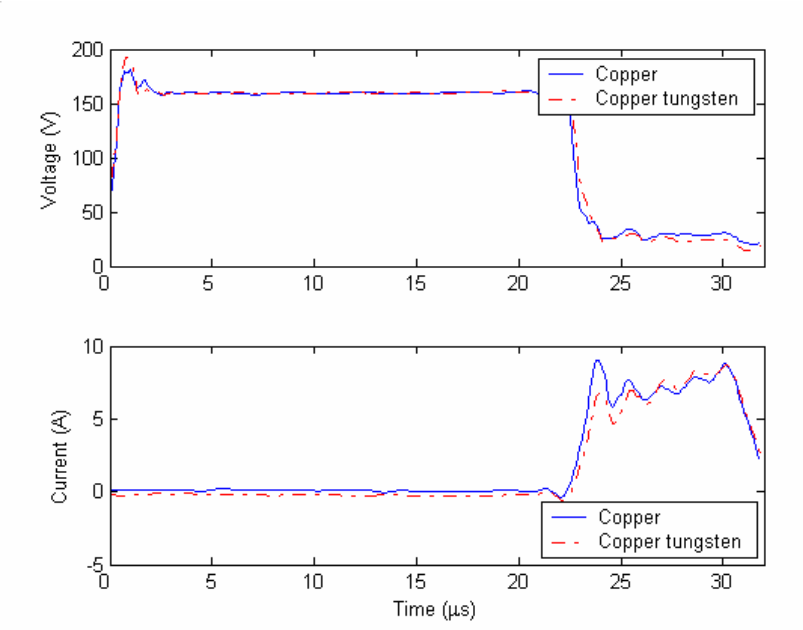

Figure 4-11 Voltage and current for different electrodes

ATTENTION: The Singapore Copyright Act applies to the use of this document. Nanyang Technological University Library

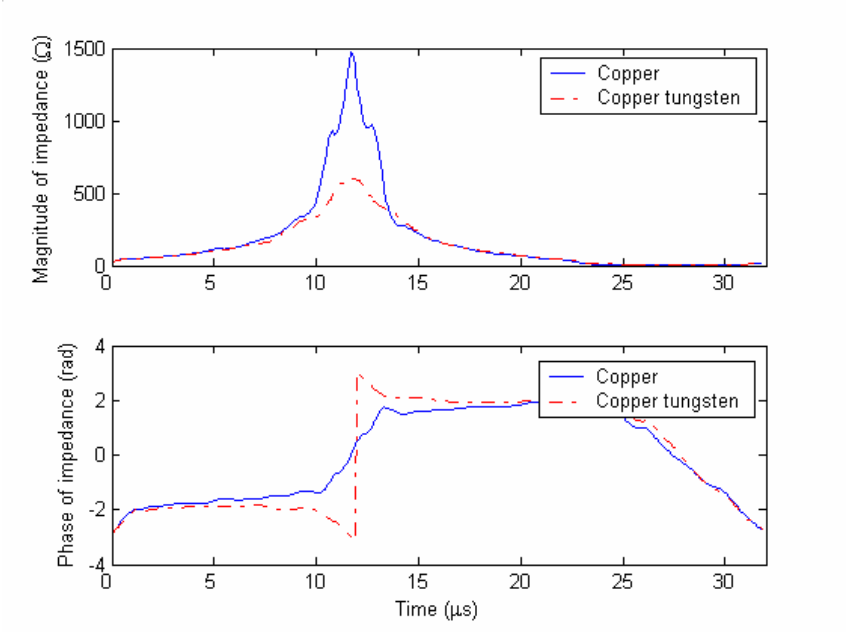

Figure 4-12 Magnitude and phase of input electrical impedance for different electrodes

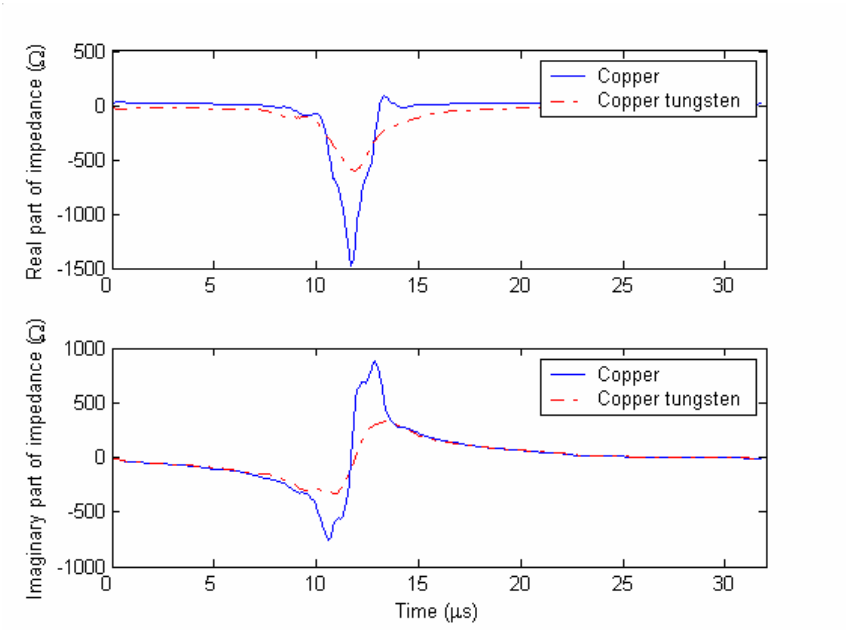

Figure 4-13 Real part and imaginary part of input electrical impedance for different electrodes

ATTENTION: The Singapore Copyright Act applies to the use of this document. Nanyang Technological University Library

4.3.3 Effects of Workpiece Material

The effects of workpiece material on input electrical impedance are some like that of electrode material, which are mainly due to the different resistivity of the materials. Steel, titanium and tungsten carbide are employed to investigate the effects of workpiece material on input electrical impedance. The resistivity of these three types of material is listed in Table 4-1.

Figure 4-14 shows using voltage and current cannot identify the workpiece material successfully as few differences can be observed. While from the input electrical impedances shown in Figure 4-15 and Figure 4-16, it can be observed that the maximum magnitude of input electrical impedance, maximum resistance and maximum capacitance of steel workpiece has the biggest values because steel has the biggest resistivity. As the resistivity of titanium and tungsten carbide are quite close, the values of the maximum magnitude of input electrical impedance, maximum resistance and maximum capacitance of these two types of workpiece have no much difference. Therefore base on electrical resistivity, input electrical impedance can effectively identify workpiece material. Workpiece with bigger resistivity has bigger maximum magnitude of input electrical impedance, maximum resistance and maximum capacitance.

Table 4-1 Resistivity of workpiece materials

	Steel	Titanium	Tungsten carbide
Resistivity (μΩcm)	7.2	5.56	5.4

ATTENTION: The Singapore Copyright Act applies to the use of this document. Nanyang Technological University Library

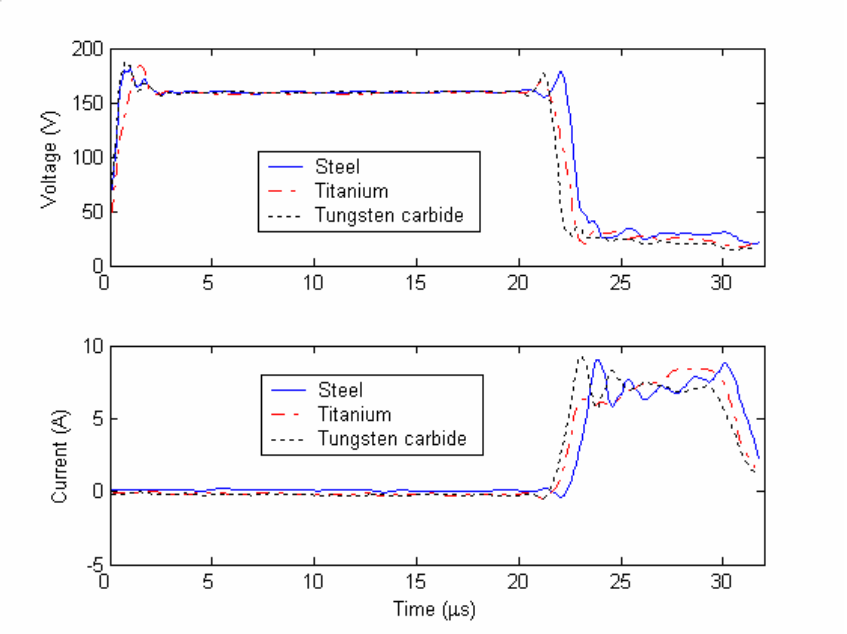

Figure 4-14 Voltage and current for different workpieces

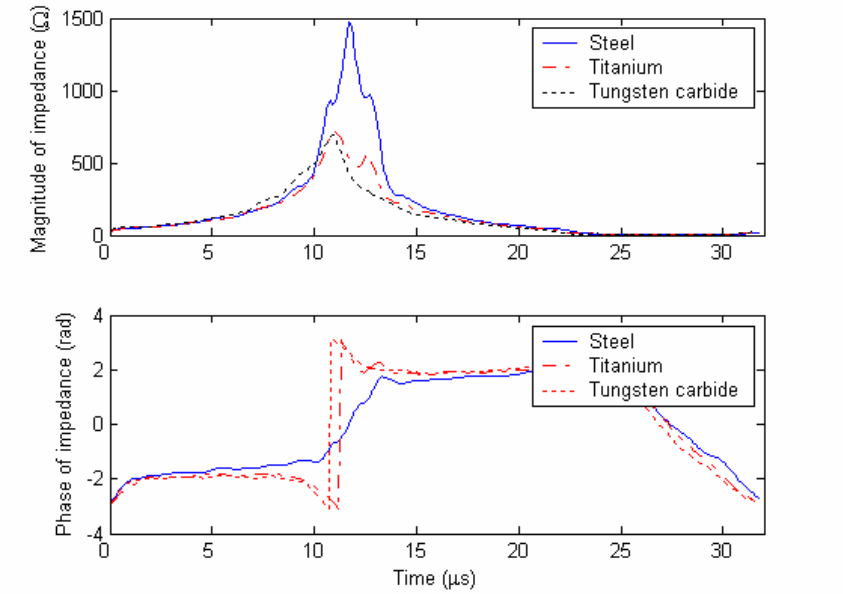

Figure 4-15 Magnitude and phase of input electrical impedance for different workpieces

ATTENTION: The Singapore Copyright Act applies to the use of this document. Nanyang Technological University Library

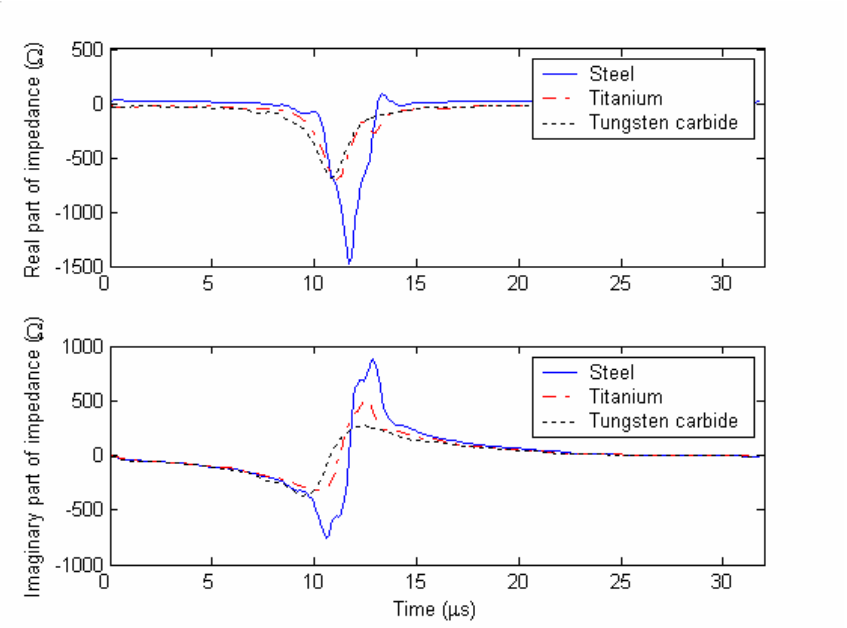

Figure 4-16 Real part and imaginary part of input electrical impedance for different workpieces

4.3.4 Effects of Dielectric Media

The material of dielectric media is the most important working parameter that has influence on input electrical impedance. The dielectric media actually act as a conductor after breakdown. Hence the input electrical impedances in the fifth phase for different dielectric media have no much difference. While before breakdown, the input electrical impedances for different dielectric media do have different characteristics because the insulation abilities of these media are quite different.

There types of dielectric media were used to investigate their effects on input electrical impedance, including total 300 EDM oil, deionized water and air. Figure 4-17 shows the voltage and current, and Figure 4-18 and Figure 4-19 show the magnitude and phase, real part and imaginary part of input electrical impedance for different dielectric

ATTENTION: The Singapore Copyright Act applies to the use of this document. Nanyang Technological University Library

media. Because EDM oil has the biggest insulation ability, it is most difficult to be ionized, the electrons and charges accumulated on cathode and anode surfaces cannot be neutralized in time, which means the ability of storing electrons and ions of the surfaces of electrode and workpiece is the biggest one and thus results the biggest maximum capacitance. In addition, because there are less electrons moving toward the cathode at the first balance time, the maximum resistance of EDM oil also has the biggest value. As both resistance and capacitance have the biggest values, the maximum magnitude of impedance of EDM oil has the biggest value too. Among these three types of dielectric media, because deionized water has the smallest insulation ability, its maximum magnitude of impedance, maximum resistance and maximum capacitance have the smallest values. Hence using input electrical impedance can effectively identify the materials of dielectric media. The bigger of the insulation ability of the dielectric media, the bigger will be the maximum magnitude of impedance, maximum resistance and maximum capacitance.

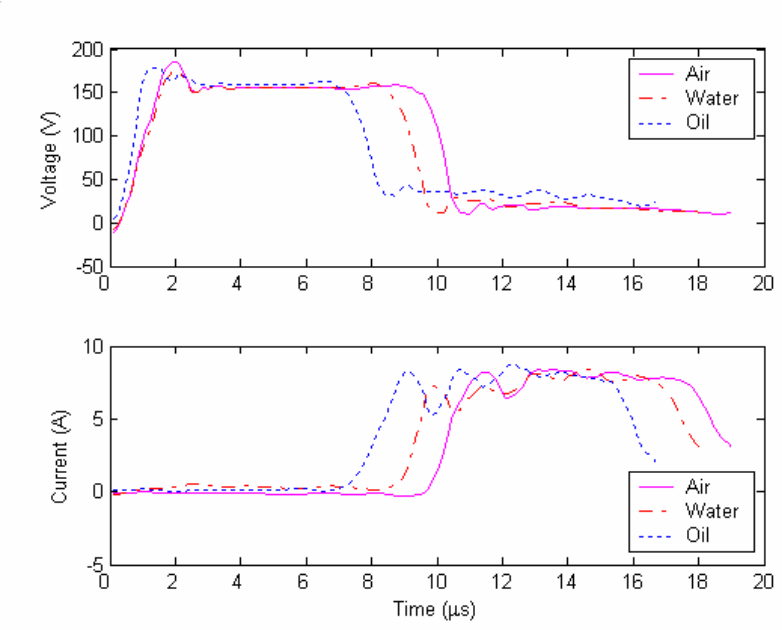

Figure 4-17 Voltage and current for different dielectric

ATTENTION: The Singapore Copyright Act applies to the use of this document. Nanyang Technological University Library

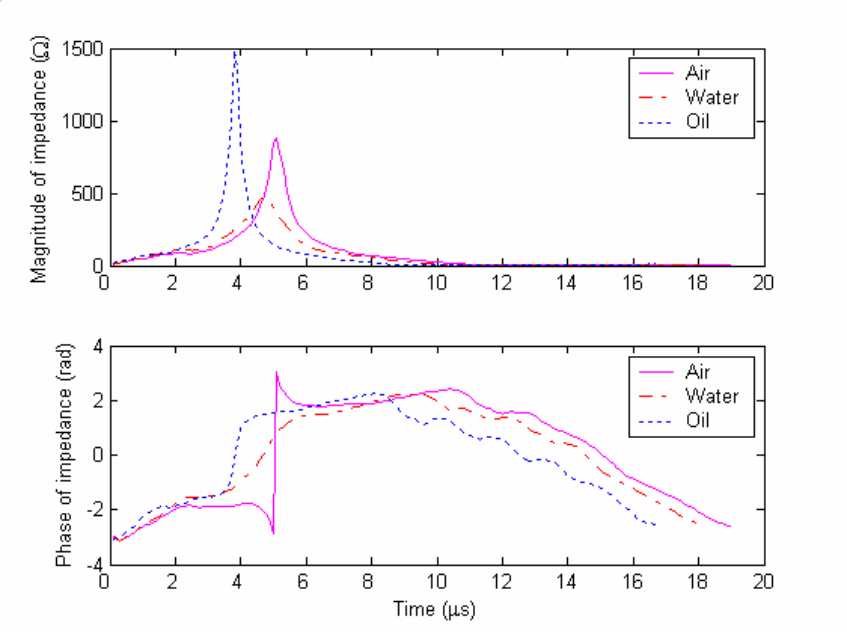

Figure 4-18 Magnitude and phase of input electrical impedance for different dielectric

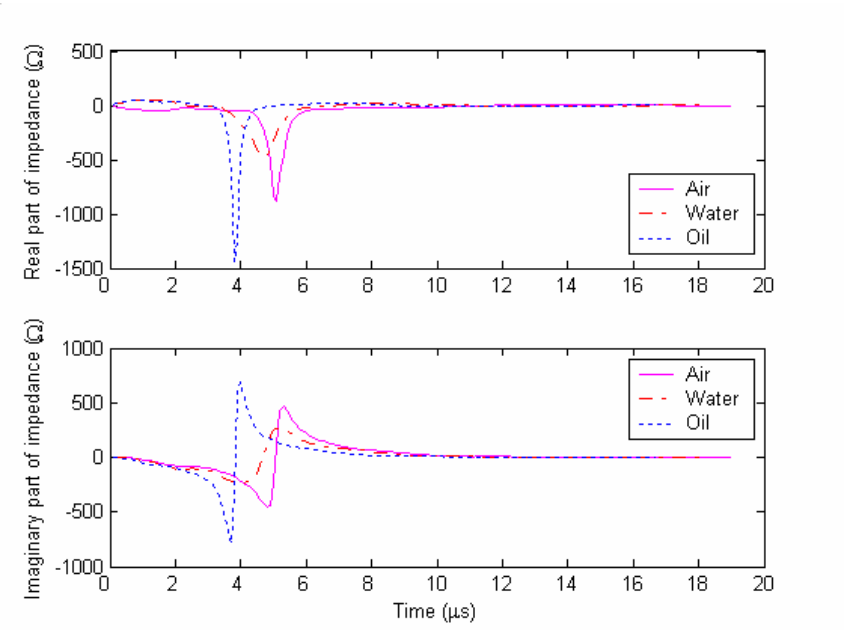

Figure 4-19 Real part and imaginary part of input electrical impedance for different dielectric

ATTENTION: The Singapore Copyright Act applies to the use of this document. Nanyang Technological University Library

4.3.5 Effects of Gap Size

Gap size is another working parameter that has most importance influences on input electrical impedance. With wider gap size, the dielectric media inside discharge gap is thicker, thus it is more difficult to be ionized. Figure 4-20 shows using voltage and current cannot identify the gap size successfully because no much difference can be found from them.

Figure 4-21 and Figure 4-22 show the magnitude and phase, real part and imaginary part of input electrical impedance for difference gap size, respectively. It can be seen from these two figures that the maximum magnitude of impedance, maximum resistance and maximum capacitance increase with gap size. When machining with bigger gap size, because the electrical field inside the gap is weaker, there are less molecules of the dielectric media been ionized. The positive charges and electrons accumulated on the surfaces of electrode and workpiece are more difficult to be neutralized, which means the capacitor can store more charges and thus has bigger maximum capacitance. In addition, as the moving velocity of electrons in the wire at the first balance time is lower for bigger gap size, the maximum magnitude of impedance and the maximum resistance also increases with gap size. It can be observed that the values of the maximum magnitude of impedance, maximum resistance and maximum capacitance almost have a linear relationship with gap size. If the deionization status of the dielectric media is absolutely same, the linear relationship will be more perfect. Hence, input electrical impedance can successfully identify the gap size, which is impossible for using voltage and current.

ATTENTION: The Singapore Copyright Act applies to the use of this document. Nanyang Technological University Library

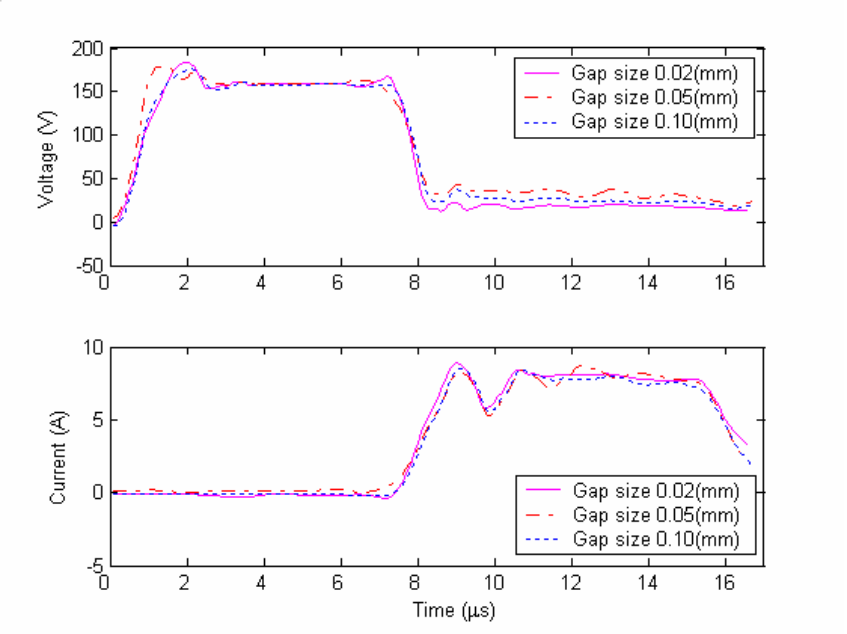

Figure 4-20 Voltage and current for different gap size

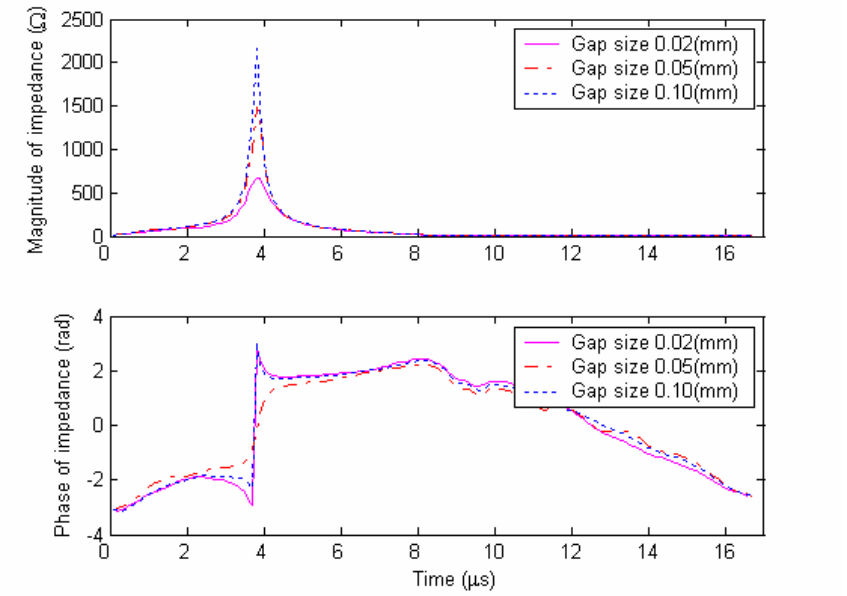

Figure 4-21 Magnitude and phase of input electrical impedance for different gap size

ATTENTION: The Singapore Copyright Act applies to the use of this document. Nanyang Technological University Library

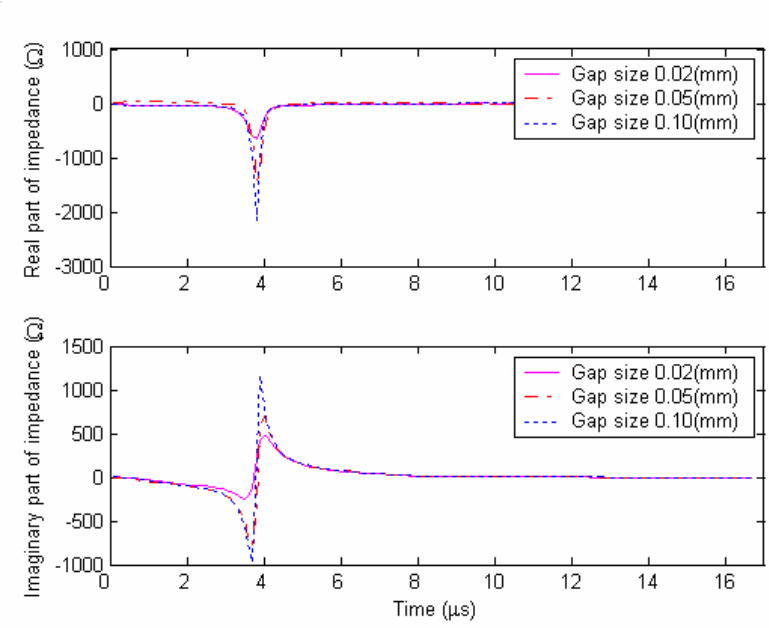

Figure 4-22 Real part and imaginary part of input electrical impedance for different gap size

4.4 Summary

In this chapter, the discharge mechanisms of sparks and arcs were investigated using input electrical impedance. Some conclusions can be obtained from this study: (1) the discharging process can be divided into five phases after investigating the imaginary part of input electrical impedance; (2) the discharge mechanism is more reliable than that obtained using conventionally signals because input electrical impedance is an inherent signal of the discharging process; (3) the input electrical impedance for difference working parameters has different maximum magnitude, capacitance and resistance. Thus it can effectively identify these working parameters, which is almost impossible if using other signals. In addition, the reliability of the discharge mechanism can be guaranteed because these working parameters have no influences on discharging process.

ATTENTION: The Singapore Copyright Act applies to the use of this document. Nanyang Technological University Library

Chapter Five

Monitoring of Discharge Conditions

An effective monitoring system is very important for the purpose of improving performance of EDM process. However due to the complicated and stochastic nature of this process, a reliable monitoring system still has not been achieved because of the difficulties in selecting suitable monitoring signatures. Previous studies have proved that although the performance of EDM process can be influenced by many factors in a complex way, the discharge conditions have overwhelming influences on them [108]. In other words, the ratio of normal discharge to abnormal discharge determines the effectiveness of EDM process. Hence to obtain good process performance, stable and favorable discharge conditions must be achieved through on-line adjusting the controllable working parameters. Discharge conditions are conventionally denoted as series of discharge pulses. Therefore it is desirable to develop a pulse discriminator to detect deleterious discharge pulses effectively.

The discharge pulses can be classified into opens, sparks, arcs, and short-circuits, plus the intervals between two successive pulses that can be treated as off pulses. Among

ATTENTION: The Singapore Copyright Act applies to the use of this document. Nanyang Technological University Library

these types of pulse, opens, short-circuits and offs can be easily detected due to their distinct characteristics. However, it is difficult to differentiate sparks and arcs because these two types of pulse exhibit quite similar characteristics. The monitoring systems are often based on the identification of adverse arcing occurring during machining because arcs usually cause surface damage of workpiece and decrease machining efficiency. It is believed that arcs occur at the same spot as previous pulses because the dielectric media inside discharge gap is not fully deionized. This phenomenon leads to a lot of differences between sparks and arcs, such as discharge voltage, delay time, discharge frequency, etc. As indicated in chapter 2, though many monitoring methods have been developed using these differences as monitoring signatures, they have unavoidable disadvantages and are insufficiently effective to differentiate sparks and arcs. Hence, a new signature, which can differentiate sparks and arcs more effectively than the usually used ones, is required.

The research group of Professor Ling has utilized input electrical impedance to successfully monitor spot welding, arc welding, wire bonding, and etc. systems. The results proved that compared with conventional monitoring methods, input electrical impedance has distinctive advantages [99-102]. Provided that the differences between sparks and arcs are mainly due to the different deionization status of dielectric media, the input electrical impedances of these two types of pulses absolutely have different characteristics. Hence, input electrical impedance of discharge pulse is possibly been employed to differentiate sparks and arcs, and finally monitor the discharge conditions.

In this chapter, the monitoring of discharge conditions using input electrical impedance is comprehensively investigated. To obtain quantified monitoring results, the first step

ATTENTION: The Singapore Copyright Act applies to the use of this document. Nanyang Technological University Library

is segmenting the discharge train into separate pulses. As wavelet analysis has distinctive ability in doing this kind of task, signal segmentation by continuous wavelet transform is studied first. After segmenting the pulse train, the opens, offs and short-circuits can be detected and the left pulses (including sparks and arcs) are classified as discharging pulses initially. Based on the understanding of discharge mechanism, several features are extracted from the input electrical impedance of each pulse and a fuzzy classifier is developed to classify this pulse as spark or arc. The proposed on-line monitoring system is shown in Figure 5-1. The monitoring results of discharge conditions are the time percentage of each type of discharge pulse.

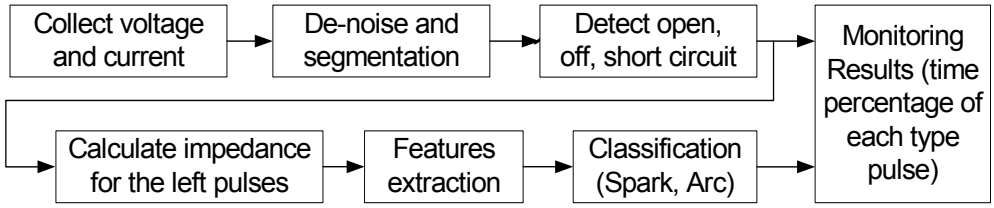

Figure 5-1 Structure of on-line monitoring system

5.1 Wavelet Analysis for Signal De-noise and Segmentation

To precisely obtain the time percentage of each type of discharge pulse, it requires the monitoring method can process the discharge pulses individually. To achieve this purpose, the pulse train should be segmented into separate pulses first. As the collected voltage and current contain background noise, de-noise is essential to filter off the noise from the original signals before the segmentation.

Fourier transform is known to be an effective tool for signals processing. It has been used in almost every engineering field, including signal de-noise and edge detection.

ATTENTION: The Singapore Copyright Act applies to the use of this document. Nanyang Technological University Library

FT can transfer the signal from the temporal field to frequency field. However, data related to the time domain disappear after the signal is transferred to the frequency domain. Furthermore, Fourier transform is suitable for stationary signal analysis and it is not suitable for processing non-stationary or transient signals. To solve these problems, short-time-Fourier-transform (STFT) has been developed. STFT can analyze signal in both time and frequency domain, but the length of the window will affect its accuracy and cannot be determined easily. To overcome this drawback, wavelet transform was developed.

Wavelets form a 2-d family of functions that derived from an original function called mother wavelet. They are scaled, dilated and shifted versions of the mother wavelet. It is a 2-d family because they are described by two parameters: the scaling and the shifting factor. The extra parameter, scaling, introduces flexibility into the construction of wavelets, which makes it suitable for processing different type of signals. Wavelet transform also can analyze signal in both time and frequency domain. It presents a windowing technique with variable-sized regions in contrast to STFT. It can adjust the window in both time and frequency domain for local analysis, which means it employs longer time intervals where more precise low frequency information is required and shorter regions for high frequency information. This allows wavelet transform to capture aspects like trends, breakdown points, and discontinuities in higher derivatives and self-similarity that are missed by the other signal analysis techniques.

Wavelet transform (WT) can be categorized into continuous wavelet transform (CWT) and discrete wavelet transform (DWT). In this study, DWT will be employed for signal de-noising and CWT will be employed for signal segmentation.

ATTENTION: The Singapore Copyright Act applies to the use of this document. Nanyang Technological University Library

5.1.1 Signal De-noise by Discrete Wavelet Transform

Discrete Wavelet Transform (DWT) is a special case of the WT that provides a compact representation of a signal in time and frequency domain that can be computed efficiently. The DWT is defined by the following equation:

$$W(j,k) = \sum_{j}\sum_{k} x(k) \times 2^{-j/2} \psi(2^{-j} n - k) \tag{5-1}$$

Where $\psi(t)$ is a time function with finite energy and fast decay called the mother wavelet. The DWT analysis can be performed using a fast, pyramidal algorithm related to multirate filterbanks [109].

As a multirate filterbank, the DWT can be viewed as a constant Q filterbank with octave spacing between the centers of the filters. Each subband contains half the samples of the neighboring higher frequency subband. In the pyramidal algorithm the signal is analyzed at different frequency bands with different resolution by decomposing the signal into a coarse approximation and detail information. The coarse approximation is then further decomposed using the same wavelet decomposition step. This is achieved by successive highpass and lowpass filtering of the time domain signal and is defined by the following equations:

$$y_{high}[k] = \sum_{n} x[n] g[2k - n] \tag{5-2}$$

$$y_{low}[k] = \sum_{n} x[n] h[2k - n] \tag{5-3}$$

Where $y_{high}[k]$, $y_{low}[k]$ are the outputs of the highpass (g) and lowpass (h) filters, respectively after sub-sampling by 2. The down-sampling process is to throw away every alternate data point to ensure that the size of the data S remains the same after

ATTENTION: The Singapore Copyright Act applies to the use of this document. Nanyang Technological University Library

wavelet transform. In wavelet analysis, approximations and details are often used for describing the upper and lower portions of the frequency. The approximations are the high-scale, low frequency components of the signal. The details are the low scale, high frequency components. The filtering process, at its most basic level, is shown as in Figure 5-2. The decomposition process can be iterated. In DWT, with successive approximations being decomposed in turn, one signal is broken down into many lower resolution components. For example, if we decompose a signal S at level 3, then S can be represented as: S=A3+D3+D2+D1

In engineering field, the real signals almost are low frequency or stationary signals, while noise commonly is high frequency signal. So in order to de-noise the original signal, one way is abandon all the detail coefficients and take the approximate signal as the de-noised signal, this method is called forcible de-noise. Another way is gives a threshold to the detail coefficients and obtains the de-noised signal by reconstructing from the approximate and details that after been applied threshold. Forcible de-noise may lose some useful information, which will influence the accuracy of segmentation, hence, the second way is used to de-noise the collected voltage and current. There are three kinds of thresholding, including hard thresholding, soft thresholding and semi-soft thresholding. In most cases, the performance of noise removal of soft thresholding and hard thresholding method are the same because both methods force the lower magnitude coefficients to zero. Convenience for the segmentation, here hard thresholding is used because this method does not attenuate the higher magnitude coefficients.

ATTENTION: The Singapore Copyright Act applies to the use of this document. Nanyang Technological University Library

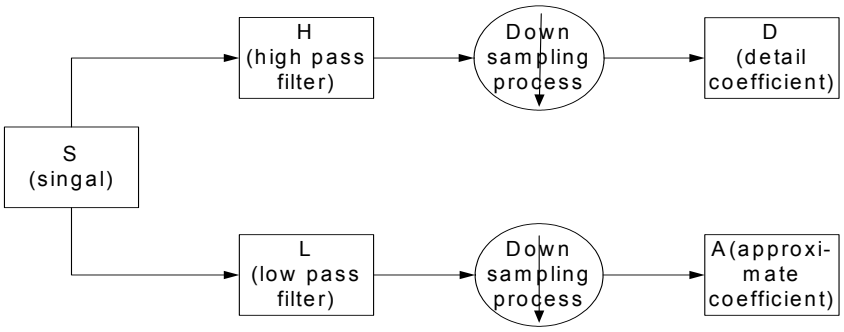

Figure 5-2 Single level wavelet decomposition

Figure 5-3 shows 200μs's voltage and current trains collected from experiment, and Figure 5-4 shows the voltage and current after de-noising, respectively. In this application, "db4" mother wavelet function is chosen. From these two figures, it can be seen that this train contains seven discharge pulses. Figure 5-4 also shows that most noise was removed with the sharp changing points of original signals keep untouched. Though some background noise still exists, it has no much influence on the segmentation results.

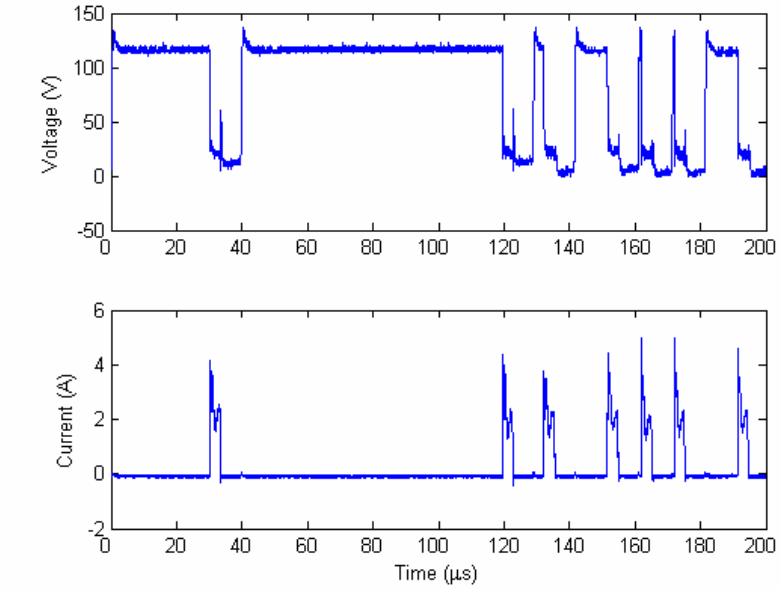

Figure 5-3 Original voltage and current trains

ATTENTION: The Singapore Copyright Act applies to the use of this document. Nanyang Technological University Library

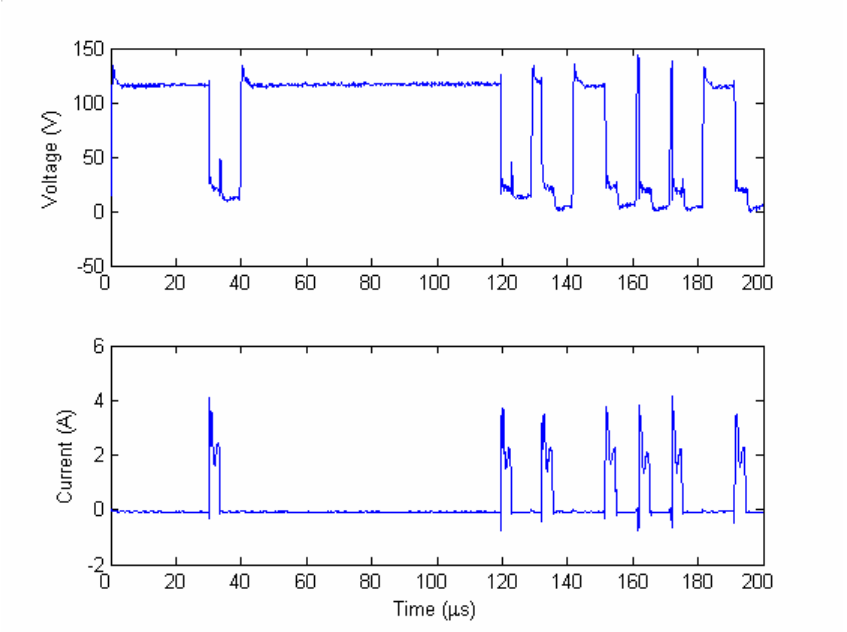

Figure 5-4 Voltage and current after de-noising

5.1.2 Signal Segmentation by Continuous Wavelet Transform

There is an interval between two successive discharge pulses, during which dielectric media is de-ionized and prepared for the next discharge. After this interval, voltage applied, discharge voltage rises from zero to open voltage quickly. When the dielectric is sufficiently ionized to establish a current bridge, dielectric breakdown occurs, discharge voltage falls from open voltage to machining voltage and discharge current rises from zero to peak current immediately. After machining duration, electrical power is cut off, discharge voltage falls from machining voltage to zero and current falls from peak current to zero in a short time. If these abrupt changes of the voltage and current signals can be detected precisely, each discharge pulse can be extracted accurately. Abrupt change is a kind of edge information, or singularities. Taking advantages of the distinctive ability in singularities detection of wavelet transform,

ATTENTION: The Singapore Copyright Act applies to the use of this document. Nanyang Technological University Library

continuous wavelet transform is employed to complete the segmentation task. This signal segmentation method developed partitions the voltage and current of the discharge train into time slices representing separate discharge pulses.

The continuous wavelet transform of a function is defined as:

$$W_f(a,b) = |a|^{-1/2} \int f(t) h(\frac{t-a}{b}) dt \tag{5-4}$$

Here, $f(t)$ is the function to apply wavelet transform, a is scaling factor, b is shifting factor and $h(\frac{t-a}{b})$ is wavelet mother function. The difference between continuous and discrete wavelet transform is that, unlike discrete wavelet transform, continuous wavelet transform can operate at every scale. Therefore continuous wavelet transform is continuous in terms of shifting during computation and analyzing, wavelet is shifted smoothly over the full domain of the analyzed function. As singularities contain high frequency information, using the low scale coefficients of CWT, the location of the singularities can be located correctly.

Calculation of the wavelet transform is a key process in applications. The fast algorithm of computing $W_s f(x)$ for detecting edges and reconstructing the signal can be found in [110] when $\psi(x)$ is a dyadic wavelet defined in that article. However, for some applications such as edge detection in this case, the reconstruction of signals is not required. Therefore, the choice of the wavelet function will not be restricted in the conditions that were presented in [110]. Many wavelets other than dyadic ones can be utilized. In fact, almost all the general integral wavelets satisfy this particular application. In this segmentation method, "Haar" wavelet mother function is chosen because after transformation using this function, the sharp rising edges in original

ATTENTION: The Singapore Copyright Act applies to the use of this document. Nanyang Technological University Library

signal corresponding to big negative coefficients and the sharp falling edges corresponding to big positive coefficients, which makes the realization of this segmentation algorithm using software easier.

Figure 5-5 shows the CWT coefficients of the voltage and current trains shown in Figure 5-4 at scale 10. From this figure, all the seven pulses can be extracted correctly by locating their corresponding maximum and minimum coefficients. Inevitably the extracted discharge pulses have some differences with the original discharge pulses due to the effect of Wavelet transform itself, but the differences are insignificant and will not influence the calculation of input electrical impedance.

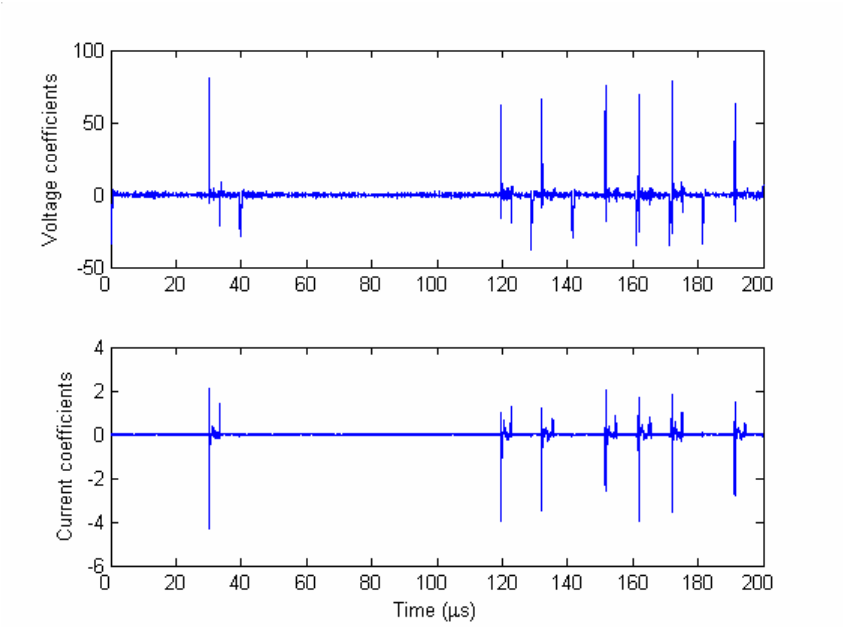

Figure 5-5 Coefficients of CWT at scale 10

ATTENTION: The Singapore Copyright Act applies to the use of this document. Nanyang Technological University Library

5.2 Detection of Opens, Offs, Short-Circuits

Open pulse occurs when the discharge gap is too wide to establish a current bridge, for this type of pulse, discharge voltage equals to open voltage and discharge current is zero. Off pulse is actually the interval between two successive pulses during which power supply has been cut off. Both discharge voltage and discharge current in off pulse are zero. Short-circuit occurs when electrode contacts workpiece directly or due to the debris existed in the discharge gap. Discharge voltage is very small and discharge current equals to peak current for this type of pulse. Hence, the characteristics of opens, offs and short-circuits can be summarized as: opens have high average voltage and low average current, offs have low average voltage and low average current, and short-circuits have low average voltage and high average current. Based on these distinctive characteristics of the three types of pulse, after segmenting the discharge train, the average voltage and average current of each pulse can be calculated. Then opens, offs and short-circuits can be detected easily by setting thresholds to the average voltage and average current. The thresholds are determined mainly by open voltage and peak current used during machining.

5.3 Identification of Sparks and Arcs

After detecting opens, offs and short-circuits, the left pulses, including sparks and arcs, are classified as discharging pulses first. The next also the most important step of this monitoring method is classifying these discharging pulses as sparks and arcs respectively. As sparks and arcs exhibit quite similar characteristics, it is difficult to differentiate them effectively using conventional signatures. To overcome this

ATTENTION: The Singapore Copyright Act applies to the use of this document. Nanyang Technological University Library

difficulty, input electrical impedance is used. The calculation of input electrical impedance and the study of discharge mechanism using this signal have been comprehensively investigated in previous two chapters. In this section, the classification of sparks and arcs using input electrical impedance will be discussed.

5.3.1 Features Extraction

The input electrical impedance of the seven pulses shown in Figure 5-4 has been calculated and shown in Figure 3-9 ~ 3-22. Based on the understanding of discharge mechanism and signal processing knowledge, several features from the input electrical impedance are extracted and some of them are chosen as the determinant features for classification. A feature here is defined to be any property of the input electrical impedance of a discharging pulse that is useful for describing normal or abnormal behavior of this pulse. There are many features can be extracted and it is found that the following ones are suitable for determining whether a pulse is spark or arc.

First balance time or static balance time: this is the time required to attain the first neutralization balance of the charges on the surfaces of electrode and workpiece. As the dielectric media is not fully deionized when arc occurs, there are lots of free ions and electrons left. Under the effect of electrical field, the dielectric media need less time to be polarized and ionized, and the accumulation of the free ions and electrons in dielectric media is much faster, which makes the durations of phase one and phase two of arc both shorter than that of spark. As a result of this, the static balance time of arc is shorter than that of spark. The more insufficient deionization of the dielectric media, the shorter will be this balance time.

ATTENTION: The Singapore Copyright Act applies to the use of this document. Nanyang Technological University Library

Second balance time or dynamic balance time: actually, this time is equal to the breakdown delay time, which can be easily obtained from the voltage or current signal when partition the discharge train. Second balance time is the duration from the start of a discharging pulse to the breakdown of dielectric media of this pulse. For the insufficient deionization of the dielectric media, all the first four phases of arc are shorter than that of spark. Consequently, the dynamic balance of neutralization when arc occurs needs shorter time to be attained. Commonly, spark is believed to have much longer second balance time than arc.

Converting time: this is the duration that capacitance turns from maximum value to inverse maximum value, or in other words, the total duration of phase two and three. The converting time of arc is much shorter than that of spark because the dielectric media is not fully deionized. There are a lot of ions and electrons left in dielectric media when arc occurs, under the effect of electrical field, these electrons and ions move to the electrode and workpiece respectively. The numerous electrons and ions in dielectric media causes the overshooting of arc is much stronger and faster than that of spark, which results the shorter converting time.

Average magnitude of input electrical impedance: from input electrical impedance, it can be seen that during converting, the magnitude of input electrical impedance is very big. As the converting time of spark is much longer than that of arc, the average magnitude of input electrical impedance of spark is much bigger than that of arc. Obviously, the longer the converting time is, the bigger the average magnitude of input electrical impedance will be. In addition, the average real part and the average imaginary part of input electrical impedance have the same characteristic.

ATTENTION: The Singapore Copyright Act applies to the use of this document. Nanyang Technological University Library

Ratio of valley to peak of the imaginary part of input electrical impedance: for spark pulses, as the ions and electrons mainly come from the ionization of the dielectric media, which is much slower than that of arcs. Before attaining the static balance, the capacitor can store more charges, which means the maximum capacitance of spark is bigger than that of arc. On the contrary, when overshooting starts, because the ions and electrons of spark are less than that of arc, the inverse maximum capacitance of spark is smaller than that of arc. Hence, the ratio of maximum capacitance to inverse maximum capacitance of spark is bigger than that of arc.

Phase of input electrical impedance: in the first two phases, voltage lags current almost a constant phase and in the third and fourth phase, voltage leads current a constant phase. When arc occurs, the absolute value of the phase of input electrical impedance in the first and second phases are bigger than that of spark, while in the third and fourth phases, the phase of input electrical impedance of arc is smaller than that of spark.

There are many other features that can be used for classification, such as the pulse duration, the maximum magnitude of input electrical impedance, the average real part and imaginary part of input electrical impedance, or some features extracted from voltage and current, etc. However, most of them are not the inherent ones of the discharging process. Taking into account of the classification speed, only three features are selected here, including first balance time, average magnitude of input electrical impedance and the ratio of valley to peak. These three features of each discharging pulse will be used as the inputs of the fuzzy classifier developed in next section to

ATTENTION: The Singapore Copyright Act applies to the use of this document. Nanyang Technological University Library

determine whether this pulse is spark or arc. Table 5-1 lists the values of some features for the seven pulses shown in Figure 5-4.

Table 5-1 Features extracted for pulse 1 to pulse 7

Features	Pulse1	Pulse2	Pulse3	Pulse4	Pulse5	Pulse6	Pulse7
Duration (μs)	33.55	83.19	6.85	13.6	4.52	4.12	13.26
First balance (μs)	15.00	39.09	1.42	4.82	0.22	0.17	5.00
Second balance (μs)	30.35	80.13	3.40	10.14	1.01	0.84	10.01
Average magnitude (Ω)	572.2	885.9	164.6	322.6	77.3	48.9	324.7
Average real part (Ω)	377.83	595.69	103.44	189.62	12.72	9.95	170.29
Valley/Peak	1.2840	0.9712	1.2801	0.9899	0.1974	0.3184	0.6818

5.3.2 Fuzzy Inference System for Classification

Presently, Fuzzy logic system has been widely and successfully used in monitoring and controlling EDM process [91-93]. The theory of fuzzy logic is proposed by Zadeh [111] and aimed at the development of a set of concepts and techniques for dealing with sources of uncertainty, imprecision and incompleteness. The nature of fuzzy rules and the relationship between fuzzy sets of different shapes provides a powerful capability for incrementally modeling a system whose complexity makes traditional expert systems, mathematical models, and statistical approaches very difficult. The most challenging problem in differentiating sparks and arcs is that many characteristics of these two types of pulse are similar and the knowledge about how to differentiate them is incomplete and vague due to the complexity of discharging process. Though several features have been extracted from the input electrical impedance, how to classify a discharging pulse using these features is still not fully understood and a

ATTENTION: The Singapore Copyright Act applies to the use of this document. Nanyang Technological University Library

mathematical model is even more difficult to be obtained. These reasons lead us to seek a solution of using fuzzy inference method to classify these discharging pulses.

Fuzzy logic systems (FLS) are one of the main developments and successes of fuzzy sets and fuzzy logic. A FLS is a rule-base system that implements a nonlinear mapping between its inputs and outputs. A FLS is characterized by four modules, fuzzifier, defuzzifier, inference engine and rule base. The operation of a FLS is based on the rules contained in the rule base. The *l*-th rule in the rule-base has the following form:

$$R^{(l)}: \text{ If } u_1 \text{ is } A_{1l} \text{ and } u_2 \text{ is } A_{2l} \text{ and } \ldots u_n \text{ is } A_{nl}, \text{ then } v \text{ is } B_l \qquad (5\text{-}5)$$

The first n terms are called the antecedents of the rule while the last term (the one after the "then") is the consequent of the rule. The terms u_i are fuzzy variables and the terms A_{il} are linguistic variables.

It can be noted that the inputs to a FLS somehow correspond to the antecedents of the rules in the rule base. A difference exists though, indeed, the inputs to the FLS, as can be seen in Figure 5-6, come from the outside world (e.g., controlled process) and are crisp variables in general. On the contrary, the antecedents of the fuzzy rules are always fuzzy sets. The role of the fuzzifier in a FLS is to convert a crisp input variable into a fuzzy set that is ready to be processed by the inference engine. The inference engine using the fuzzified inputs and the rules stored in the rule base processes the incoming data and produces an (fuzzy) output. This output needs to be used in the outside world and thus needs to be converted from fuzzy to crisp; the defuzzifier performs this operation. We will now expand on the operations of every module in order to finally formulate the nonlinear parameterized mapping realized by the FLS.

ATTENTION: The Singapore Copyright Act applies to the use of this document. Nanyang Technological University Library

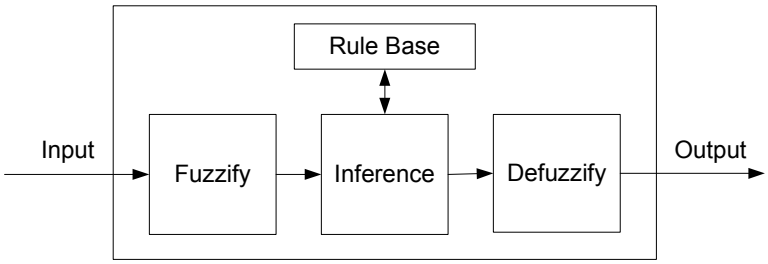

Figure 5-6 Structure of a fuzzy logic system

Fuzzification can be defined as the operation that maps a crisp object to a fuzzy set, i.e., to a membership function. Fuzzifiers are generally divided in singleton and non-singleton ones. A singleton fuzzifier maps an object to the singleton fuzzy set centered at the object itself (i.e., with support and core being the set containing only the given object). A non-singleton fuzzifier, maps an object to a fuzzy set generally centered at the object itself (i.e., the core of the fuzzy set contains the object) and with support containing the object but being a set bigger than only the object itself. A non-singleton fuzzifier maps an object into a non-singleton fuzzy set generally centered at the object itself. Typically, the use of a singleton fuzzifier is very common. Non-singleton fuzzifiers are also used, especially in the presence of e.g., noisy measurements. Indeed, in this case the input crisp value is affected by some uncertainty, thus, the corresponding input fuzzy set can reflect this uncertainty by allowing non-zero membership values around the (noisy) measurement. Therefore, when a non-singleton fuzzifier is used, the width of the corresponding fuzzy set is generally proportional to the amount of noise affecting the measurement. Figure 5-7 shows an example of singleton and non-singleton fuzzification.

ATTENTION: The Singapore Copyright Act applies to the use of this document. Nanyang Technological University Library

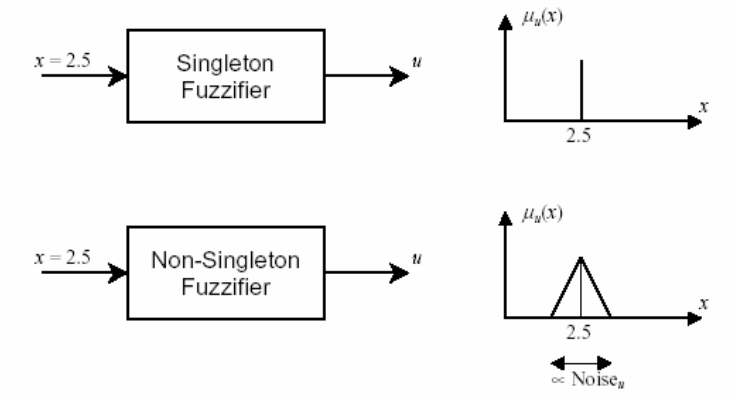

Figure 5-7 Example of singleton and non-singleton fuzzifiers

Once the inputs are fuzzified, the corresponding input fuzzy sets are passed to the inference engine that processes current inputs using the rules retrieved from the rule base. The outcome of these rules in generalized modus ponens will be an output fuzzy set B^{l*} close to B^l. The input in this case is different, not being a scalar anymore, but a vector. Thus in this case we have $A = A^l = A_{1l} \times A_{2l} \times \ldots \times A_{nl}$ and $B = B^l$, but still the fuzzy engine would be mapping fuzzy sets into fuzzy sets. Thus we obtain

$$\mu_{B^{l*}}(y) = \sup_{x \in A^*} \left[\mu_{A^*}(x) \otimes \mu_{A^l \to B^l}(x, y) \right] = \mu_{B^l}(y) \otimes \sup_{x \in A^*} \left[\mu_{A^*}(x) \otimes \mu_{A^l}(x) \right] \tag{5-6}$$

using a *t-norm* as the and connector for antecedents and denoting by x_i the observation corresponding to A^*, we have

$$\begin{aligned} \mu_{A^*}(x) &= \mu_{x_{il}}(x_1) \otimes \mu_{x_{i2}}(x) \otimes \cdots \otimes \mu_{x_{in}}(x_n) \\ \mu_{A^l}(x) &= \mu_{A_{1l}}(x_1) \otimes \mu_{A_{2l}}(x) \otimes \cdots \otimes \mu_{A_{nl}}(x_n) \end{aligned} \tag{5-7}$$

Substituting (5-7) in (5-6) and rearranging we obtain

$$\mu_{B^{l*}}(y) = \mu_{B^l}(y) \otimes \sup_{x \in A^*} \left\{ \begin{array}{l} \left[\mu_{x_{i1}}(x_1) \otimes \mu_{A_{1l}}(x_1) \right] \otimes \left[\mu_{x_{i2}}(x_2) \otimes \mu_{A_{2l}}(x_2) \right] \\ \otimes \cdots \otimes \left[\mu_{x_{in}}(x_n) \otimes \mu_{A_{nl}}(x_n) \right] \end{array} \right\} \tag{5-8}$$

Recalling that the $\mu_{x_{ij}}$ in (5-8) are singletons, that unity is neutral with respect to any *t-norm*, and thus that the argument of the sup operator is independent of x, allows us to

ATTENTION: The Singapore Copyright Act applies to the use of this document. Nanyang Technological University Library

ignore the sup operation (maybe one of the best reasons for the success of singleton fuzzification), and Equation (8) greatly simplifies in

$$\mu_{B^{l*}}(y) = \mu_{B^l}(y) \otimes \mu_{A_{1l}}(x_{i1}) \otimes \mu_{A_{2l}}(x_{i2}) \otimes \cdots \otimes \mu_{A_{nl}}(x_{in}) \tag{5-9}$$

Equation (5-9) is the final expression for the membership function of the fuzzy set output by the *l*-th fuzzy rule when an engineering implication operator is used along with singleton fuzzification.

At the output of the fuzzy inference there will always be a fuzzy set $\mu_Y(y)$ that is obtained by the composition of the fuzzy sets output by each of the rules using Equation (5-8). In order to be used in the real world, the fuzzy output needs to be interfaced to the crisp domain by the defuzzifier. The output fuzzy set indicates what the output is in fuzzy terms. This fuzzy output will be a membership function that provides the degree of membership of several possible crisp outputs. Thus, the point corresponding to the highest degree of membership in the fuzzy output has to be sought. This operation would correspond to a type of defuzzification, called max defuzzification. Unfortunately, in most practical cases the situation is not so simple, since there might be many points having the same maximum degree of membership in the fuzzy output, and an indecision on which one of these points to choose arises. Moreover, choosing the maximum point of the membership function is an operation that discards most of the information contained in the membership function itself.

There is the need for a technique that summarizes the information contained in the membership function. The crisp output corresponding to a certain fuzzy output set should be a number that takes into account all the points in the support of this fuzzy output, weighing the points with high membership degree more than the ones with

ATTENTION: The Singapore Copyright Act applies to the use of this document. Nanyang Technological University Library

small or no membership degree. Thus, one widely used defuzzifier is the centroid defuzzifier that transforms a fuzzy output set into a number that is the *x*-coordinate of the set's center of gravity. The output of this defuzzifier is a number y_d given by

$$y_d = \frac{\int_S y\mu_Y(y)dy}{\int_S \mu_Y(y)dy} \tag{5-10}$$

Where S is the support of $\mu_Y(y)$. One drawback of this kind of defuzzification is the complexity involved with finding the center of gravity (i.e., integration). For this and other reasons (see [112] for a more detailed account of defuzzification approaches), easier defuzzification schemes are generally employed for reduced computational burden. One of the most popular defuzzifiers is the center of area (COA) defuzzifier (also called height defuzzifier). In this approach the overall center of gravity is approximated by the center of gravity of "point-masses" located at the center of gravity of each individual rule's output fuzzy set, with "mass" equal to the membership degree at that point. This is not an approximation if the supports of the fuzzy sets corresponding to the output of each rule do not overlap and the consequent membership functions are isosceles triangles with equal bases. In the general case of overlap this might be an approximation to the actual center of gravity depending also on the rule connective that is used. Calling δ_l the center of gravity of fuzzy set B^{l*} output of the l-th rule, the output of the COA defuzzifier is given by

$$y_d = \frac{\sum_{l=1}^{R} \delta_l \mu_{B^{l*}}(\delta_l)}{\sum_{l=1}^{R} \mu_{B^{l*}}(\delta_l)} \tag{5-11}$$

Equation (5-11) is very easy to use since the centers of gravity of commonly used membership functions are known ahead of time. Regardless of the *t-norm* used

ATTENTION: The Singapore Copyright Act applies to the use of this document. Nanyang Technological University Library

(minimum or product) the center of gravity for commonly used symmetric membership functions (triangular, Gaussian, trapezoidal, bell shaped) does not change after inference. In other words for commonly used symmetric consequent membership functions, the center of gravity of B^l and B^{l*} is the same, therefore making the application of (5-11) very easy and thus, appealing.

The fuzzy logic systems described in the above sections are commonly referred to as pure fuzzy logic systems or Mamdani fuzzy logic systems [113]. An alternative to these FLSs is offered by Takagi-Sugeno (TS) fuzzy logic systems. Takagi-Sugeno fuzzy reasoning system was first introduced in 1985 [114]. It is similar to the Mamdani method in many respects. In fact the first two parts of the fuzzy inference process, fuzzifying the inputs and applying the fuzzy operator, are exactly the same. The main difference between Mamdani-type of fuzzy inference and Sugeno-type is that the output membership functions are only linear or constant for Sugeno-type fuzzy inference. In a TS-FLS the consequent of each rule is not a fuzzy set but it is a local model of the system (function) to be controlled (approximated). Thus the *l*-th rule of a TS-FLS has the form:

$R^{(l)}$: If u_1 is $A_{1k(1,l)}$ and u_2 is $A_{2\,k(2,l)}$ and … u_n is $A_{n\,k(n,l)}$, then $y = g_l(x_1, x_2, \ldots, x_n)$

A typical fuzzy rule in a zero-order TS-FLS model has the form

If x is A and y is B then $z = k$

Where A and B are fuzzy sets in the antecedent, while k is a crisply defined constant in the consequent. When the output of each rule is a constant like this, the similarity with Mamdani's method is striking. The only distinctions are the fact that all output membership functions are singleton spikes, and the implication and aggregation

ATTENTION: The Singapore Copyright Act applies to the use of this document. Nanyang Technological University Library

methods are fixed and cannot be edited. The implication method is simply multiplication, and the aggregation operator just includes all of the singletons.

In this study, as the fuzzy inference system has only one output, which is whether a pulse belongs to sparks or arcs. It is more convenient to use Sugeno-type inference system than conventional used Mamdani-type system. The fuzzy inference system constructed is shown in Figure 5-8. It has three inputs that corresponding to the three selected features. Every input has three fuzzy terms: low, medium and high. There is only one output, pulse type, which has two values, zero corresponding to arc and one corresponding to spark. The rule table can be easily constructed based on the information discussed in feature extraction. Table 5-2 lists the classification results for the seven pulses shown in Figure 5-4, it can be seen that pulse 5 and 6 are classified as arc and the other five pulses are classified as spark.

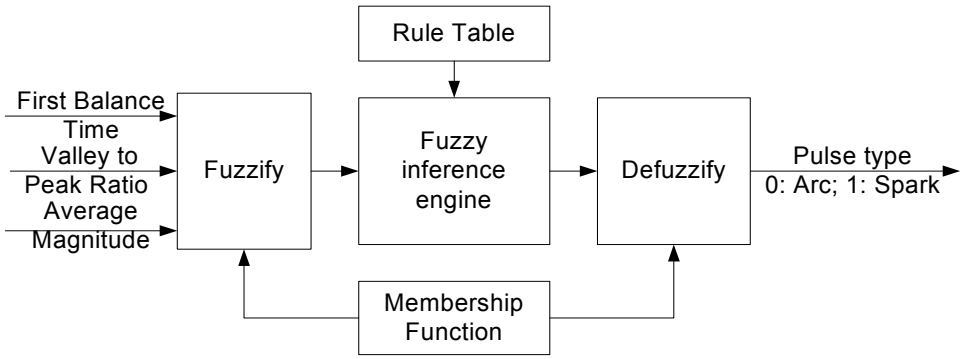

Figure 5-8 Schematic representation of the fuzzy classifier

Table 5-2 Fuzzy reasoning results for pulse 1 to pulse 7

	Pulse 1	Pulse 2	Pulse 3	Pulse 4	Pulse 5	Pulse 6	Pulse 7
Reasoning results	1	1	1	1	0	0	1

ATTENTION: The Singapore Copyright Act applies to the use of this document. Nanyang Technological University Library

5.4 Monitoring Results of Discharge Conditions

After differentiating sparks and arcs successfully using the fuzzy classifier, the monitoring results (the time percentage of each type of pulse) can be obtained. It can be seen from Figure 3-6 that there exist incomplete pulses at the start or the end of the discharge train, which cannot be processed by this monitoring method. Therefore in the monitoring results, the total processed duration is the time from the start of the first integral pulse to the end of the last pulse. In addition, as the power supply is controlled to supply peak current after the breakdown of dielectric media occurs, in the discharge train, there are no real open pulses. Therefore there are only four types of pulses existing in the discharge train, including sparks, arcs, offs and short-circuits. Among these four types of pulse, sparks and arcs are the dominating ones because only these two types of pulses contribute to material removal rate. In the monitoring results of this method, the open duration is defined as the sum of the delay time of all the discharge pulses. In addition, as metal is removed only in machining duration, the spark duration is defined as the total machining time of all the spark pulses and the arc time is defined as the total machining time of all the arc pulses. Off duration is defined as the sum of all the intervals between two successive pulses, which can be easily obtained when segmenting the discharge train. Continue the example discussed in this chapter, the monitoring results of the discharge train shown in Figure 5-4 are calculated and listed in Table 5-3.

Table 5-3 Monitoring results of discharge conditions

	Processed duration	Percentage of spark	Percentage of arc	Percentage of short	Percentage of open	Percentage of off
Monitoring Results	191.52(μs)	6.77%	3.71%	0.00%	70.68%	18.91%

ATTENTION: The Singapore Copyright Act applies to the use of this document. Nanyang Technological University Library

Figure 5-9 shows one millisecond voltage and current collected with 10M sampling frequency from another experiment. The working parameters in this experiment were set as: open voltage 200V, peak current 4A, pulse on time 12.8μs, pulse interval 12.8μs, gap size 0.01mm, copper electrode and steel workpeice. It can be seen that this pulse train contains 21 discharge pulses. After analyzing these pulses using the proposed monitoring method, 14 pulses are classified as spark and 7 of them are classified as arc. The monitoring results are listed in Table 5-4.

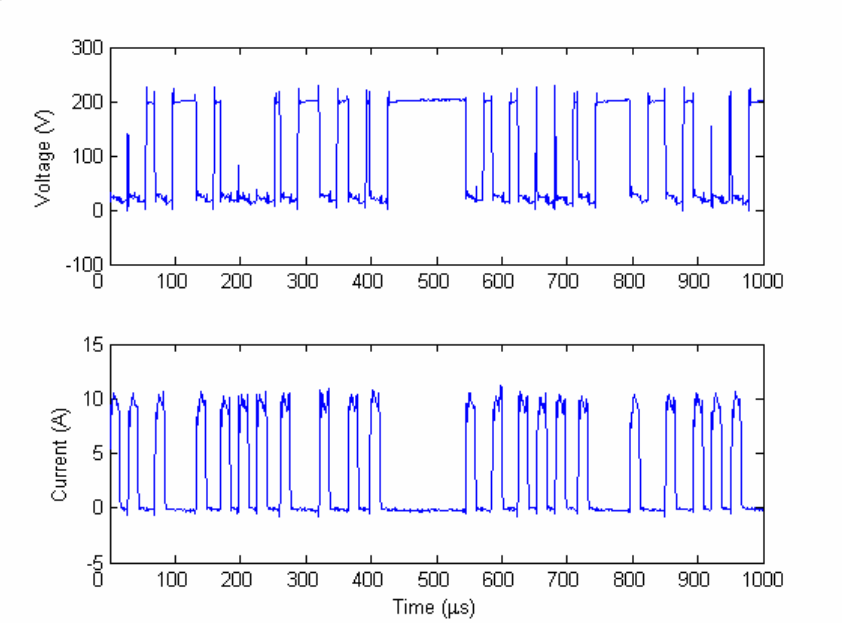

Figure 5-9 Voltage and current trains collected from experiment

Table 5-4 Monitoring results of discharge conditions

	Processed duration	Percentage of spark	Percentage of arc	Percentage of short	Percentage of open	Percentage of off
Monitoring results	940.7(μs)	22.52%	11.17%	0.00%	42.66%	23.63%

ATTENTION: The Singapore Copyright Act applies to the use of this document. Nanyang Technological University Library

5.5 Verification of Monitoring Results

It is known that sparks distribute randomly on the whole workpiece surface, while arcs occur at the same spot as previous pulses, thus arcs will leave a deeper crater on the workpiece surface and thus decrease the machining efficiency. Hence the surface roughness increases with the time percentage of arc and the material removal rate increases with the time percentage of spark, which can be used to verify the correctness of the monitoring results. In the verification experiments, the electrode polarity, electrode material, workpiece material and dielectric material are chosen as positive, copper, steel, total 300 EDM oil. The working parameters of open voltage, peak current, pulse on-time and pulse interval are fixed at 200V, 4A, 12.8μs and 3.2μs, respectively. The gap size varies from 0.01mm to 0.20mm to see the effects of gap size on the time percentage of spark and arc, material removal rate and surface roughness.

Figure 5-10 shows the effect of gap size on material removal rate and the time percentage of spark and Figure 5-11 shows the effect of gap size on surface roughness and the time percentage of arc, respectively. It can be seen from these two figures that the time percentage of spark can trace material removal rate and the time percentage of arc can trace surface roughness successfully, which means the monitoring results of the discharge conditions is correct and thus the reliability of the monitoring system is guaranteed. The little errors between these curves are because arc also has contribution to material removal rate and spark will also influence the surface roughness. In addition, short-circuit has some influence on material removal rate and surface roughness as well though it is commonly very small.

ATTENTION: The Singapore Copyright Act applies to the use of this document. Nanyang Technological University Library

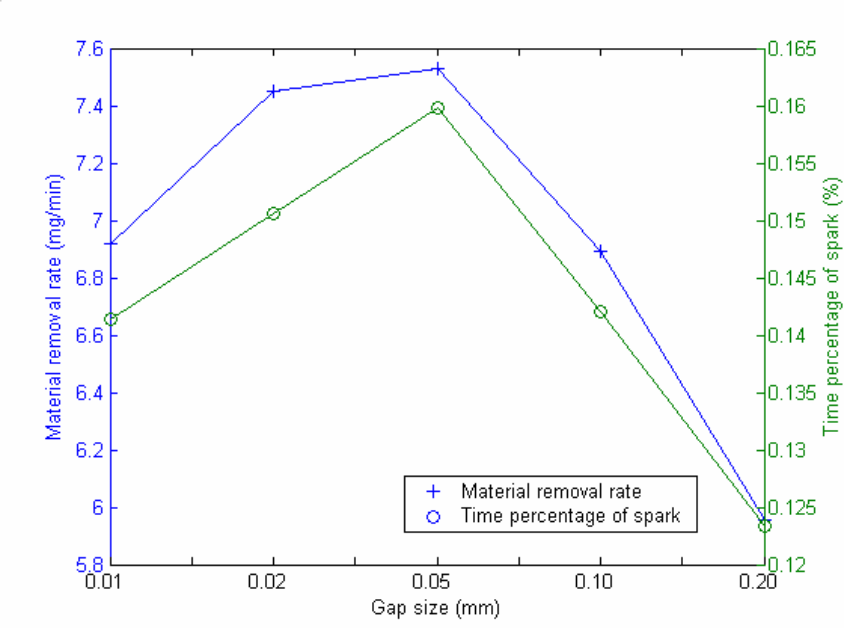

Figure 5-10 Material removal rate and time percentage of spark vs gap size

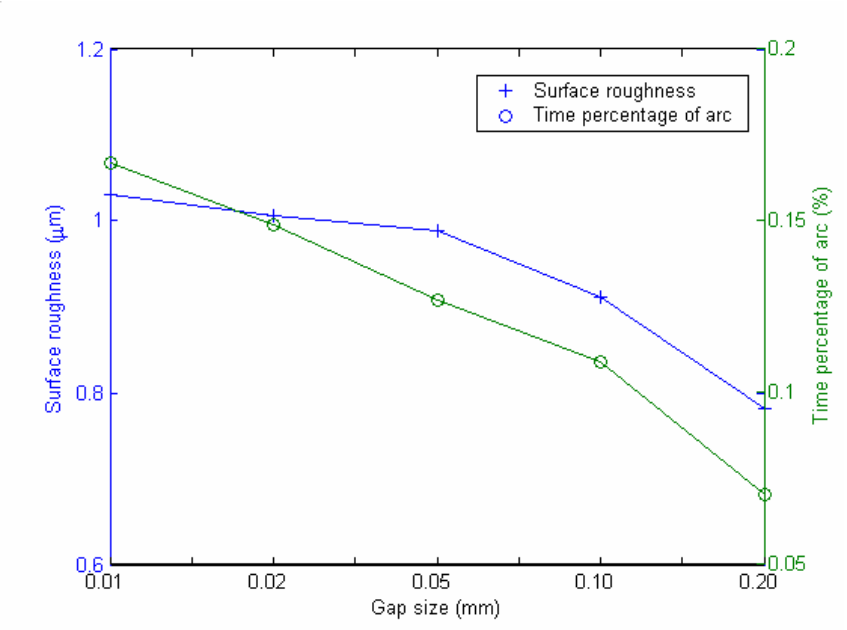

Figure 5-11 Surface roughness and time percentage of arc vs gap size

ATTENTION: The Singapore Copyright Act applies to the use of this document. Nanyang Technological University Library

5.6 Summary

This chapter proposed a new on-line monitoring system for discharge conditions. Through analyzing the input electrical impedance for individual discharge pulse and extracting features from this signature, this method can differentiate sparks and arcs effectively and finally classify all the five types of pulse. Quantified monitoring results are obtained and its correctness is guaranteed through conducting verification experiments. To improve the performance of this monitoring system, it may be necessary to extract more features to assist the classification. This monitoring system has the following advantages: (1) it can process the discharge pulses individually, quantified monitoring results of the discharge conditions (the time percentage of each type of pulse) can be precisely obtained; (2) it can differentiate sparks and arcs effectively; (3) the monitoring signature (input electrical impedance) is an inherent characteristic of EDM process, so the monitoring results can reliably reflect the discharge conditions; (4) An on-line cost-effective monitoring system can be easily realized, which are readily to be used as a module in control systems.

ATTENTION: The Singapore Copyright Act applies to the use of this document. Nanyang Technological University Library

Chapter Six

Influences of Working Parameters on Discharge Conditions and Process Performance

Previous studies have indicated that the discharge conditions plays dominative role on performance of EDM process, but how discharge conditions affect the performance has not been well understood because the discharge conditions were never quantified using the conventional monitoring methods [115]. For the same reason, what are the crucial factors of the performance of EDM process has not been determined. As quantified monitoring results of discharge conditions can be obtained using the method proposed in last chapter, a more essential interpretation of process performance can be achieved, and the crucial factors can be determined by taking into account both working parameters and discharge conditions.

It is known that there are lots of electrical and non-electrical factors have complex influences on discharge conditions and in turn process performance. This very fact makes it impossible to study the influences of these factors using one-case-one-step method. To save experimental cost and time, only those factors that have important

ATTENTION: The Singapore Copyright Act applies to the use of this document. Nanyang Technological University Library

influences on EDM process will be studied, including electrode polarity, open voltage, peak current, gap size, pulse on-time, pulse interval and magnitude of ultrasonic vibration. Those factors that have less influence, such as the temperature of dielectric fluid, are neglected. To ensure these neglects will not influence research results, a repeatability study will be carried out first. Once the repeatability of EDM process has been guaranteed, the effects of electrode polarity on process performance will be studied for the purpose of selecting a suitable polarity for machining steel workpiece with copper electrode to achieve higher material removal rate.

After determining the electrode polarity, open voltage, peak current, gap size, pulse on-time and pulse interval are selected to form the inner array of a Taguchi experiment. Through analyzing the process performance obtained from the Taguchi based experiments, the optimal values of these five working parameters can be determined and are set as the initial values for the screening experiments. By changing these parameters one by one while keeping others at their optimal values and studying theirs influences on discharge conditions and process performance at the same time, the effects of these working parameters can be understood. Finally, the effects of the magnitude of ultrasonic vibration on discharge conditions and process performance will be studied.

Through studying the influences of all these working parameters on discharge conditions and process performance, the relationships among working parameters, discharge conditions and process performance can be understood and a more essential interpretation of the process performance can be obtained. In addition, the crucial factors of the performance of EDM process can be determined.

ATTENTION: The Singapore Copyright Act applies to the use of this document. Nanyang Technological University Library

6.1 Repeatability of Experimental EDM Process

In order to study and monitor EDM process, it should be guaranteed that under the same machining conditions, outputs of this process should be same if the inputs have no differences. In other words, the repeatability of this process should be ensured. However, because electrical discharge machining process is stochastic and there are so many working parameters have influence on it, it is impossible to keep all these parameters unchanged during machining, and some of them have to be neglected. Therefore although machining with exactly same inputs, outputs for several cases will unavoidably have differences. As we know what are the key working parameters that have important influence on EDM process, if all these parameters are kept the same during experiments, the differences of outputs for several cases should lie in an acceptable range and their deviation should be small. Otherwise EDM is an unpredictable process and studying on the monitoring of this process is meaningless.

To test the repeatability of EDM process, ten holes were drilled on steel workpeice with copper electrode. The working parameters were set as: positive electrode polarity, open voltage 160V, peak current 3A, pulse duration 6.4μs, pulse interval 6.4μs, gap size 50μm, machining time 3.2s, withdraw time 0.8s, servo voltage 65V, etc. The studied outputs are material removal rate, electrode wear ratio and surface roughness, plus the monitoring results of discharge conditions. Figure 6-1 ~ 6-3 show the process performance and Figure 6-4 shows the monitoring results of the ten holes, respectively. From these figures, it can be seen that process performance and monitoring results of the ten holes are at a same level and their deviations are very small, which means process performance and monitoring results can be repeated very well.

ATTENTION: The Singapore Copyright Act applies to the use of this document. Nanyang Technological University Library

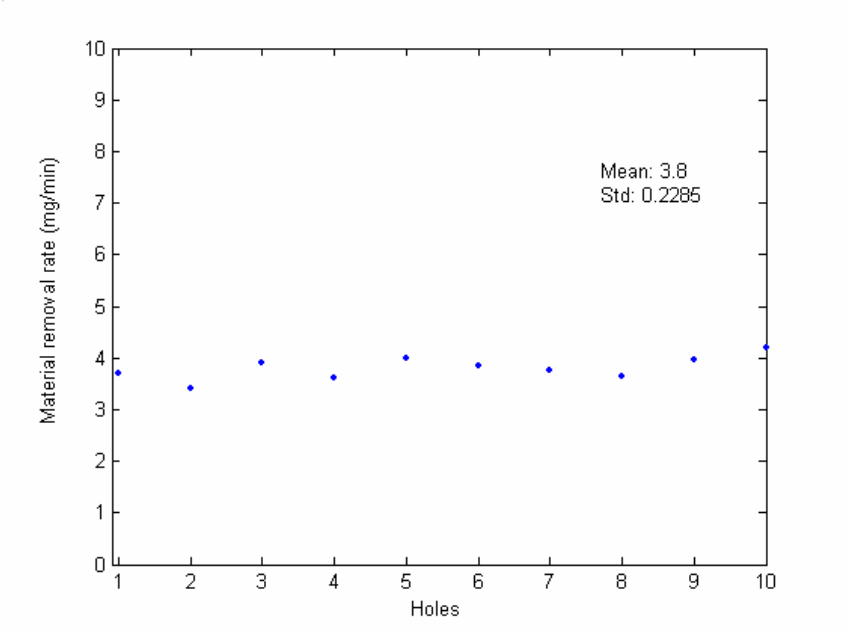

Figure 6-1 Material removal rate

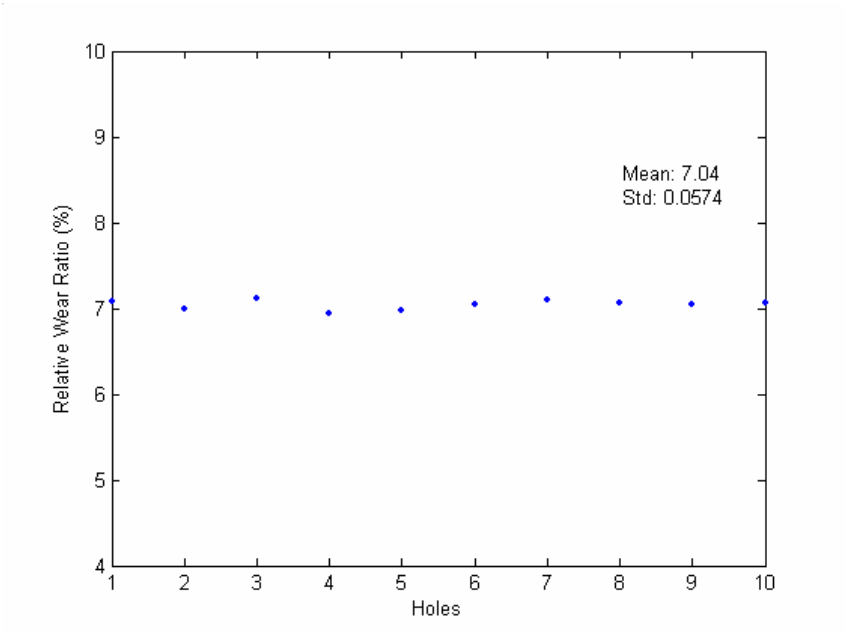

Figure 6-2 Relative wear ratio

ATTENTION: The Singapore Copyright Act applies to the use of this document. Nanyang Technological University Library

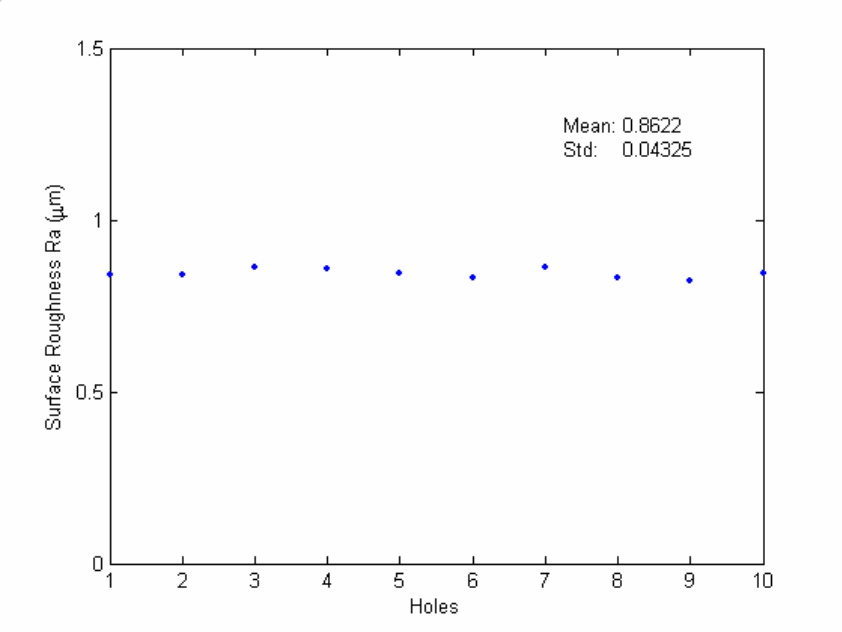

Figure 6-3 Surface roughness

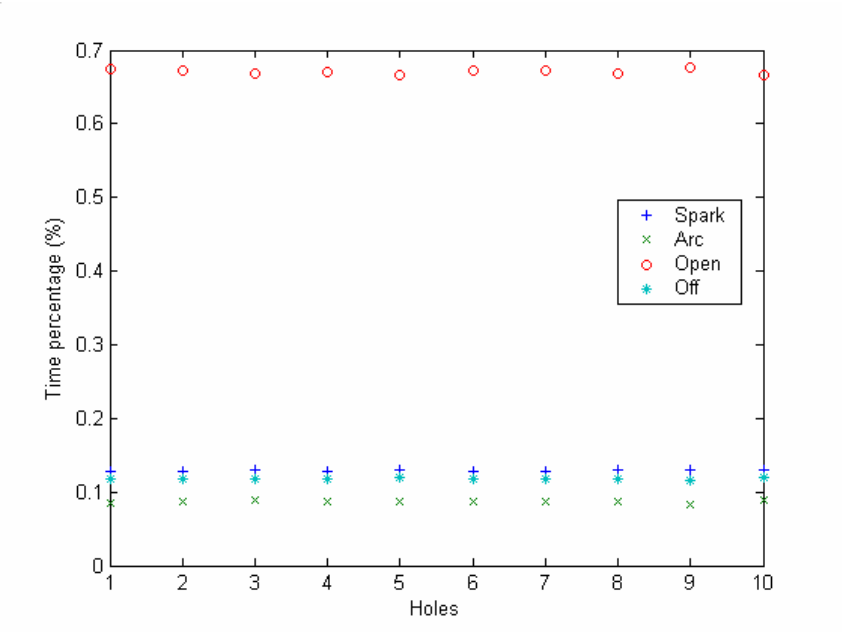

Figure 6-4 Monitoring results of discharge conditions

ATTENTION: The Singapore Copyright Act applies to the use of this document. Nanyang Technological University Library

The repeatability study discussed above is based on an average view, however the repeatability in time domain is also very important and should be guaranteed too. In other words, the process performance and the monitoring results of discharge conditions of the ten holes should have similar varying trend versus time. As electrode wear ratio and surface roughness cannot be measured on-line during machining, only material removal rate and monitoring results of discharge conditions are studied. Figure 6-5 shows the machining depth and Figure 6-6 shows the material removal rate of the ten holes versus time, from these two figures, it can be seen that the performance of EDM process has good repeatability. Figure 6-7 and Figure 6-8 show the time percentage of spark and the time percentage of arc versus time. Same results can be obtained from these two figures that the monitoring results have good repeatability too. Thus, the repeatability of EDM process is ensured.

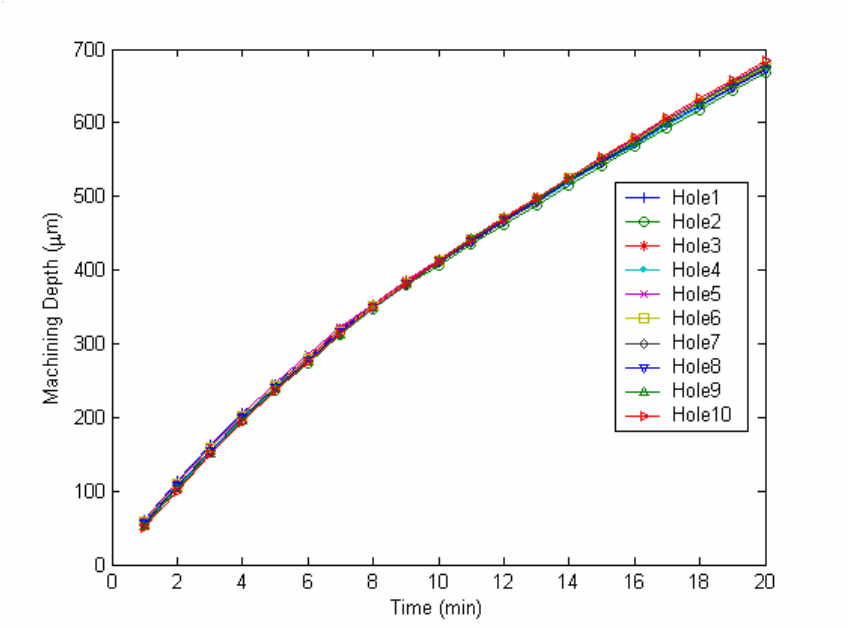

Figure 6-5 Machining depth vs time

ATTENTION: The Singapore Copyright Act applies to the use of this document. Nanyang Technological University Library

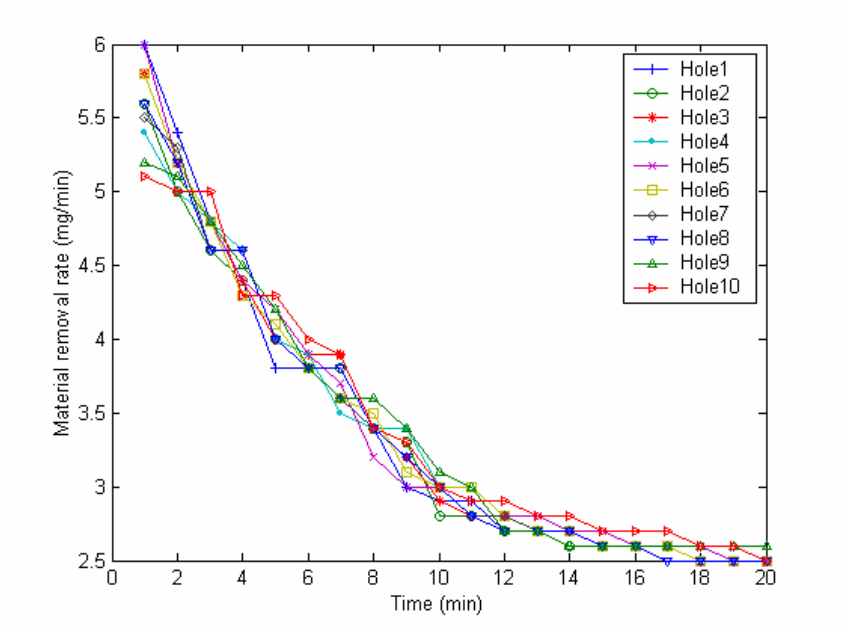

Figure 6-6 Material removal rate vs time

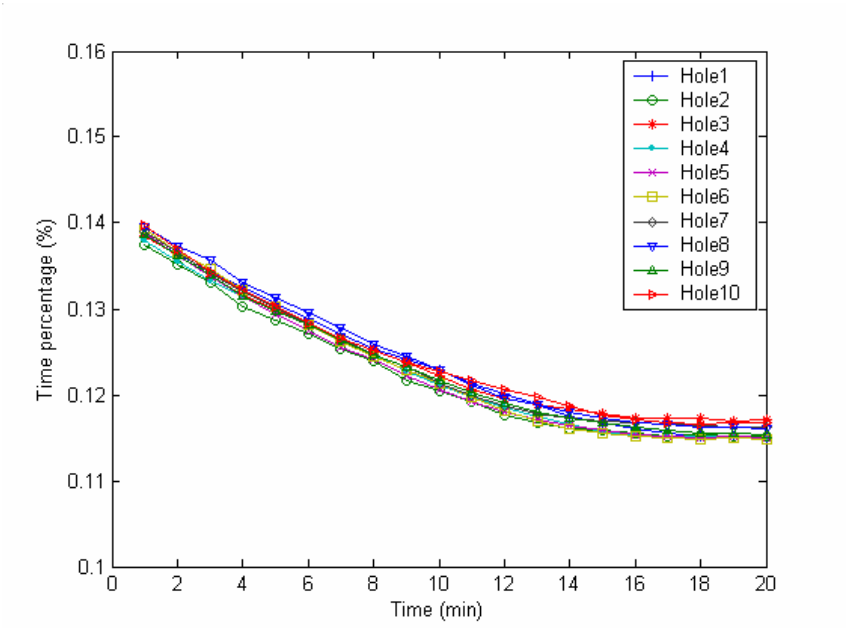

Figure 6-7 Percentage of spark vs time

ATTENTION: The Singapore Copyright Act applies to the use of this document. Nanyang Technological University Library

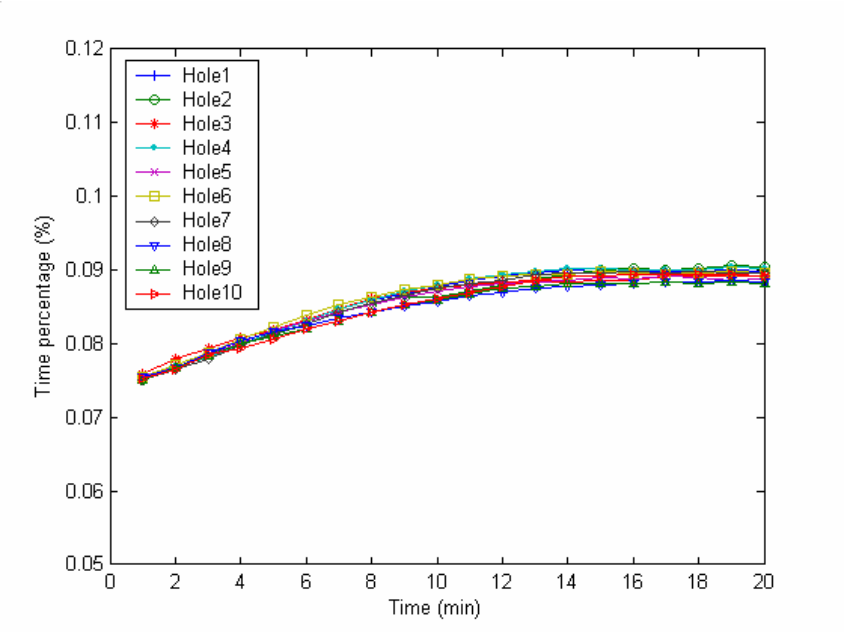

Figure 6-8 Percentage of arc vs time

6.2 Determination of Electrode Polarity

In EDM, the choice of electrode polarity is an important factor. The polarity of an EDM operation is quoted as the polarity of the electrode. The choice of polarity depends on the required material removal rates and electrode wear in addition to the materials of the electrode and workpiece. Electrode polarity guidance covers a range of electrode-workpiece combinations and type of EDM operations, which is usually provided by the machine manufacturers.

For positive polarity, electrode is anode and steel is cathode, the removal of the workpiece material is resulted from the collisions of the ions. While for negative polarity, electrode is cathode and workpiece is anode, the removal of the workpiece material is caused by the collisions of the electrons. At low current density, the amount of the ionized dielectric media is insufficient, there are few electrons and ions exist in

ATTENTION: The Singapore Copyright Act applies to the use of this document. Nanyang Technological University Library

the gap. As the energy brought by the electrons and ions are very low, the material removal rates for positive and negative polarity are both small and have no much difference. At high current density, much more dielectric media is ionized, there are sufficient electrons and ions existed in the gap. As the weight of the ion is much bigger than that of electron, most energy is gained by the ions, which results the higher material removal rate of the positive polarity. In addition, because the energy brought by the electrons is much lower than that of ions, the craters left on the workpiece surface by each collision of electrons are much flatter than that of ions, which results the lower surface roughness of negative polarity.

The influences of electrode polarity on material removal rate and surface roughness are illustrated in Figure 6-9 and Figure 6-10 respectively. Figure 6-9 shows the material removal rates of positive and negative polarity both increase with current density, but the increase of positive polarity is much faster than that of negative polarity. This figure also shows when current density is lower than 1A, the material removal rates for negative polarity and positive polarity are quite close, while when current density is bigger than 1A, positive electrode polarity gives a much higher material removal rate than negative polarity. Figure 6-10 shows the surface roughness of positive and negative polarity both increases steadily with current density, but the surface roughness of negative polarity is much lower than that of positive polarity in spite of the current density. Therefore when machine steel workpiece with copper electrode, using positive electrode polarity is more desirable for achieving higher material removal rate. However negative polarity should be selected if the machining purpose is to obtain a better surface finish. In this research, as material removal rate is the most important performance, positive polarity will be selected.

ATTENTION: The Singapore Copyright Act applies to the use of this document. Nanyang Technological University Library

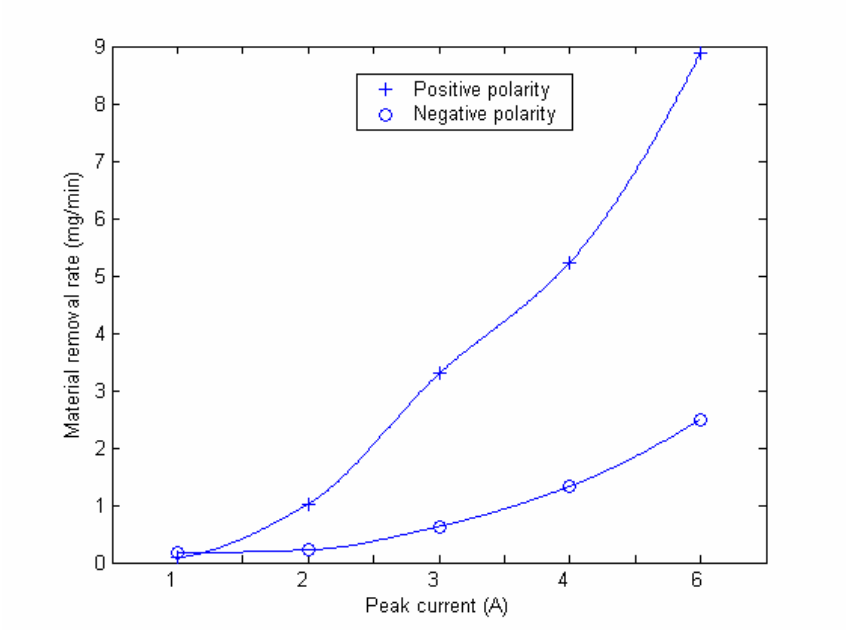

Figure 6-9 Influences of electrode polarity on MRR

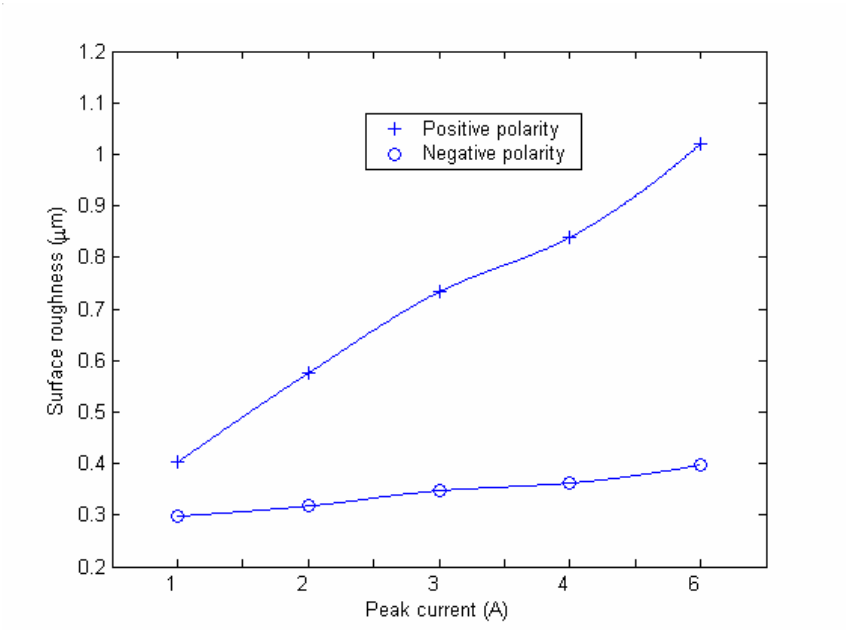

Figure 6-10 Influences of electrode polarity on SR

ATTENTION: The Singapore Copyright Act applies to the use of this document. Nanyang Technological University Library

6.3 Taguchi Method for Experimental Design

The concept of experiment design method [116] was developed originally by Fisher [117]. However, classical experimental design methods are too complex and not easy to use. Furthermore, a large number of experiments have to be carried out as the process parameter increases. To solve this important task, Taguchi method uses a special design of orthogonal arrays to study the entire parameter space using only a small number of experiments [118]. The experiment results are then transformed into a signal-to-noise (S/N) ratio. The S/N ratio for each level of process parameters is computed based on the S/N analysis, which can be used to measure the deviation of the performance characteristics from the desired values.

Usually, there are three categories of performance characteristics in the analysis of the S/N ratio, which is, the lower-the-better, the higher-the-better and the nominal-the-better. Regardless of the category of the performance characteristic, a large S/N ratio indicates a better performance characteristic. Therefore, the optimal level of the process parameters is the level with the highest S/N ratio. By computing the average effect of process parameters on the S/N ratio, the rough influences of the process parameters on performance characteristics can be obtained. Furthermore, a statistical analysis of variance (ANOVA) is performed to see which process parameters are statistically significant. With the S/N ratio and ANOVA analysis, the optimal combination of the process parameters can be determined. Finally, a confirmation experiment is conducted to verify the optimal process parameters obtained from the parameter design.

ATTENTION: The Singapore Copyright Act applies to the use of this document. Nanyang Technological University Library

Loss function is defined to calculate the deviation between the experimental value and the desired value. The loss functions of the smaller-the-better, higher-the-better and nominal-the-better can be expressed as equations 6-1~6-3:

$$L_{ij} = \frac{1}{n}\sum_{1}^{n} y_{ijk}^2 \tag{6-1}$$

$$L_{ij} = \frac{1}{n}\sum_{1}^{n} \frac{1}{y_{ijk}^2} \tag{6-2}$$

$$L_{ij} = \frac{1}{n}\sum_{1}^{n} (y_{ijk} - y_o)^2 \tag{6-3}$$

Here, L_{ij} is the loss function of the *i*th process response in the *j*th experiment, *n* is the number of tests, and y_{ijk} is the experimental value of the *i*th performance characteristic in the *j*th experiment at the *k*th test. Loss function is further transformed into a S/N ratio, which is used to determine the process response deviating from the desired value. The S/N ratio η_{ij} for the *i*th process response in the *j*th experiment can be expressed as:

$$\eta_{ij} = -10\log(L_{ij}) \tag{6-4}$$

The procedure of parameter design using Taguchi method can be summarized into following steps:

1. Identify the performance characteristics and process parameters to be evaluated
2. Determine the number of levels for the process parameters.
3. Select the appropriate orthogonal array and assign the process parameters to the orthogonal array.
4. Conduct experiments based on the arrangement of the orthogonal array.
5. Analyze the experimental results using the S/N and ANOVA analysis.
6. Select the optimal levels of the process parameters.

ATTENTION: The Singapore Copyright Act applies to the use of this document. Nanyang Technological University Library

7. Verify the optimal process parameters through a confirmation experiment

After parameter design using Taguchi method, several objectives can be achieved. The optimal process parameters can be determined, the contribution of each process parameters to the performance characteristic can be estimated and the performance characteristics based on the optimal process parameters can be predicted.

In this research, five working parameters are selected to make the inner array, including open voltage, peak current, pulse on-time, pulse interval and gap size. All these five parameters have three levels, as shown in Table 6-1.

Table 6-1 Process parameters and their levels

Symbol	Parameters	Unit	Level 1	Level 2	Level 3
A	Open voltage	V	80	160	200
B	Peak current	A	2	3	4
C	Gap size	mm	0.02	0.05	0.10
D	Pulse on-time	μs	3.2	6.4	12.8
E	Pulse interval	μs	3.2	6.4	12.8

To handle five process parameters which each has three levels, an L_{18} orthogonal array has to be used [118]. Actually this array can handle one two-level process parameter and seven three-level process parameters, and only 18 experiments are needed to study the entire machining parameter space. Hence an L_{18} array has 8 columns and 18 rows. However as there are only 5 process parameters will be studied in this research, three columns of the array are left empty, which will not lose the orthogonality of this array. The experimental layout for the process parameters using the L_{18} orthogonal array is shown in Table 6-2.

ATTENTION: The Singapore Copyright Act applies to the use of this document. Nanyang Technological University Library

Table 6-2 Experimental layout using an L_{18} orthogonal array.

Number	Process parameters				
	A	B	C	D	E
1	1	1	1	1	1
2	1	2	2	2	2
3	1	3	3	3	3
4	2	1	1	2	2
5	2	2	2	3	3
6	2	3	3	1	1
7	3	1	2	1	3
8	3	2	3	2	1
9	3	3	1	3	2
10	1	1	3	3	2
11	1	2	1	1	3
12	1	3	2	2	1
13	2	1	2	3	1
14	2	2	3	1	2
15	2	3	1	2	3
16	3	1	3	2	3
17	3	2	1	3	1
18	3	3	2	1	2

Table 6-3 shows the experimental results of the material removal rate, surface roughness and theirs signal-to-noise ratio based on the experimental layout. Since the experimental design is orthogonal, it is then possible to separate out the effect of each working parameter at different levels. The mean S/N ratio for each level of the working parameters is summarized and called the S/N response for the corresponding process performance (Table 6-4 and Table 6-5).

As mentioned above, the optimum level of the working parameters is the level with the highest S/N ratio, which means the performance is closer to the desired value. From Table 6-4 and Table 6-5, it can be seen that the optimum level of the working

ATTENTION: The Singapore Copyright Act applies to the use of this document. Nanyang Technological University Library

parameters for material removal rate is A3B3C1D3E1, the S/N ratio of the predicted material removal rate at the optimum level is 17.518, corresponding to a material removal rate of 7.514mg/min. While for surface roughness, the optimum level of the working parameters is A2B1C3D1E3, the S/N ratio at the optimum level is 6.427, corresponding to a surface roughness of 0.475. The results of the confirmation experiments are listed in Table 6-6, it can be seen, the confirmation experiment results are very close to the predicted optimum values.

Table 6-3 Process performance of Taguchi experiments

Trial condition	Surface roughness, R_a (μm)			Material removal rate (mg/min)		
	Sample 1	Sample 2	S/N ratio (db)	Sample 1	Sample 2	S/N ratio (db)
1	0.5641	0.5443	5.128	0.92	0.91	-0.772
2	0.7940	0.7551	2.216	2.21	2.18	6.828
3	0.8574	0.8493	1.38	3.38	3.42	10.629
4	0.5650	0.5349	5.197	1.05	0.99	0.16
5	0.7934	0.8151	1.894	3.605	3.64	11.179
6	0.8418	0.8736	1.338	4.385	4.32	12.774
7	0.5223	0.5439	5.471	0.89	0.90	-0.964
8	0.8526	0.8287	1.513	3.79	3.80	11.584
9	1.0193	1.0371	-0.241	7.04	7.085	16.979
10	0.6158	0.6235	4.166	0.96	0.975	-0.288
11	0.7121	0.7368	2.804	1.815	1.83	5.213
12	0.8655	0.8986	1.094	4.385	4.32	12.774
13	0.5366	0.5076	5.651	1.015	1.0	0.059
14	0.7083	0.7211	2.919	2.325	2.28	7.242
15	0.8440	0.8299	1.55	4.295	4.23	12.592
16	0.5197	0.4948	5.905	1.035	1.07	0.44
17	0.8888	0.9168	0.894	4.615	4.71	13.371
18	0.8573	0.8388	1.436	4.29	4.30	12.659

ATTENTION: The Singapore Copyright Act applies to the use of this document. Nanyang Technological University Library

Table 6-4 Signal-to-noise response table for material removal rate

Symbol	Machining parameter	Mean S/N ratio (dB)			
		Level 1	Level 2	Level 3	Max-Min
A	Open voltage	4.926	7.117	8.195	4.269
B	Peak current	-1.454	7.006	12.686	14.140
C	Gap size	7.616	6.338	5.683	1.933
D	On time	5.203	6.854	8.180	2.977
E	Interval	7.990	6.801	5.446	2.544

Table 6-5 Signal-to-noise response table for surface roughness

Symbol	Machining parameter	Mean S/N ratio (dB)			
		Level 1	Level 2	Level 3	Max-Min
A	Open voltage	2.507	2.973	2.350	0.623
B	Peak current	4.998	2.374	0.859	4.139
C	Gap size	1.953	2.606	3.272	1.319
D	On time	3.461	2.609	1.760	1.701
E	Interval	2.040	2.809	3.481	1.441

Table 6-6 Results of the confirmation experiments

	Material removal rate	Surface roughness
Parameters Level	A3B3C1D3E1	A2B1C3D1E3
Prediction	7.514 mg/min	0.475μm
Experiment	7.450 mg/min	0.515μm

Thus, the optimum values of the working parameters for process performance are obtained. For material removal rate, the highest value occurs at: positive polarity, open voltage 200V, peak current 4A, pulse on-time 12.8μs, pulse interval 3.2μs and gap size 0.02mm. These values will be set as the initial values of the working parameters in the screening experiments. In fact, the optimum parameters are based on the analysis of the average effect of working parameters on process performance. There may be some differences between them with the real optimum parameters from experiments.

ATTENTION: The Singapore Copyright Act applies to the use of this document. Nanyang Technological University Library

6.4 Influences of Working Parameters on Discharge Conditions and Process Performance

6.4.1 Open Voltage

The open voltage or generator voltage is usually fixed by the manufacture, being generally between 80 and 200V. To achieve reasonable process performance, high open voltage may be necessary for machining some materials, which have high electrical resistance and high discharge voltage. Figure 6-11 shows the influences of open voltage on material removal rate and surface roughness and Figure 6-12 shows the influences of open voltage on discharge conditions. It can be seen from Figure 6-11 that material removal rate and surface roughness both increase with open voltage due to the increase of the discharge energy. Theoretically, the time percentage of spark will decrease and the time percentage of arc will increase with open voltage because the difficulties to remove the debris from discharge gap and de-ionize the dielectric media increase with discharge energy. However, it can be seen from Figure 6-12 that the time percentages of spark and arc both increase with open voltage. However the time percentage of arc increases faster than that of spark because when machining with a constant gap size, higher open voltage causes dielectric media easier to be breakdown, which results the increase of the number of discharge pulse. Though the increase of discharge energy causes spark to decrease, the overall effect is the time percentage of spark increases with open voltage. As the increase of the discharge energy and the increase of the number of discharge pulse both contribute to the increase of the time percentage of arc, the increase of arc is faster than that of spark. It is known that arc will leave a deeper crater on the workpiece surface. The higher is the time percentage of arc, the higher is the surface roughness.

ATTENTION: The Singapore Copyright Act applies to the use of this document. Nanyang Technological University Library

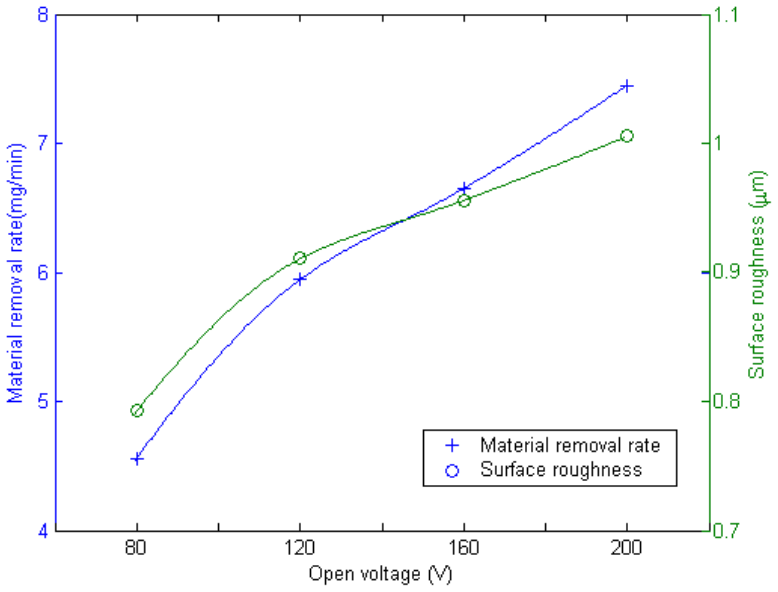

Figure 6-11 Influences of open voltage on MRR and SR

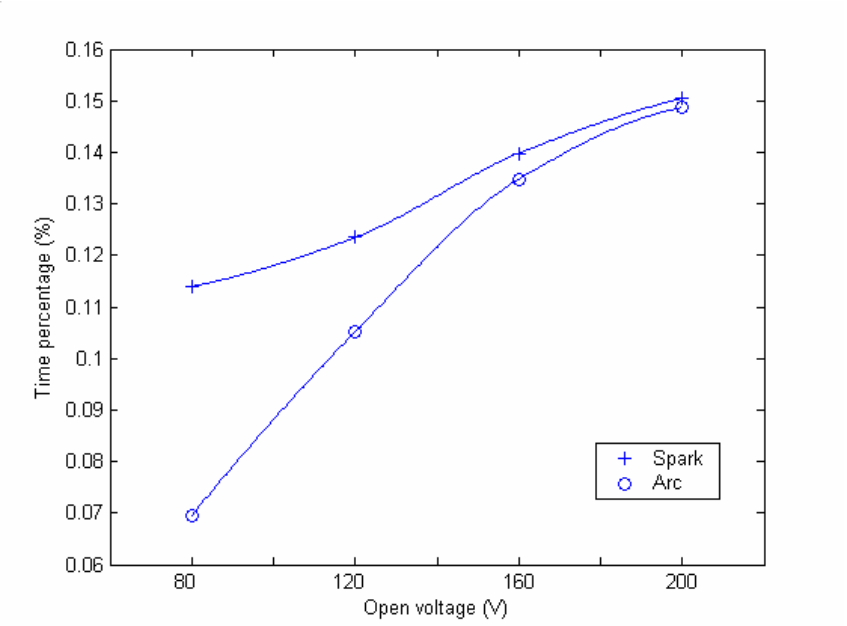

Figure 6-12 Influences of open voltage on spark and arc

ATTENTION: The Singapore Copyright Act applies to the use of this document. Nanyang Technological University Library

6.4.2 Peak Current

Peak current is the factor that has the most significant effect on the performance of EDM process, which is normally selected on the basis of the maximum material remove rate possible within the allowable mean current, electrode wear and surface integrity. Figure 6-13 shows the influences of peak current on material removal rate and surface roughness, and Figure 6-14 shows the influences of peak current on the time percentage of spark and arc, respectively. It can be seen from Figure 6-13 that both material removal rate and surface roughness increase quickly with peak current due to the increase of the discharge energy that depends on the number of discharge pulses and the amount of energy in each discharge. This figure also shows that the material removal rate is proportional to the current intensity, while fine finish is possible only at low amperage. Thus, the finer the required surface, the lower is the material removal rate. In general, high current is used when high material removal rate is required and low current is used when good surface finish is expected. Figure 6-14 shows that the time percentage of spark decreases and the time percentage of arc increase rapidly with current density because the increase of discharge energy makes the debris in discharge gap cannot be flushed away effectively and the dielectric media in discharge gap is difficult to be deionized. Theoretically, material removal rate will decrease with the time percentage of spark. However, because the increase of material removal rate due to the increase of discharge energy exceeds its decrease caused by the decrease of spark, material removal rate still increases with current density. In addition, as the increase of discharge energy and the time percentage of arc both contribute to the increase of surface roughness, surface roughness increases steadily with current density.

ATTENTION: The Singapore Copyright Act applies to the use of this document. Nanyang Technological University Library

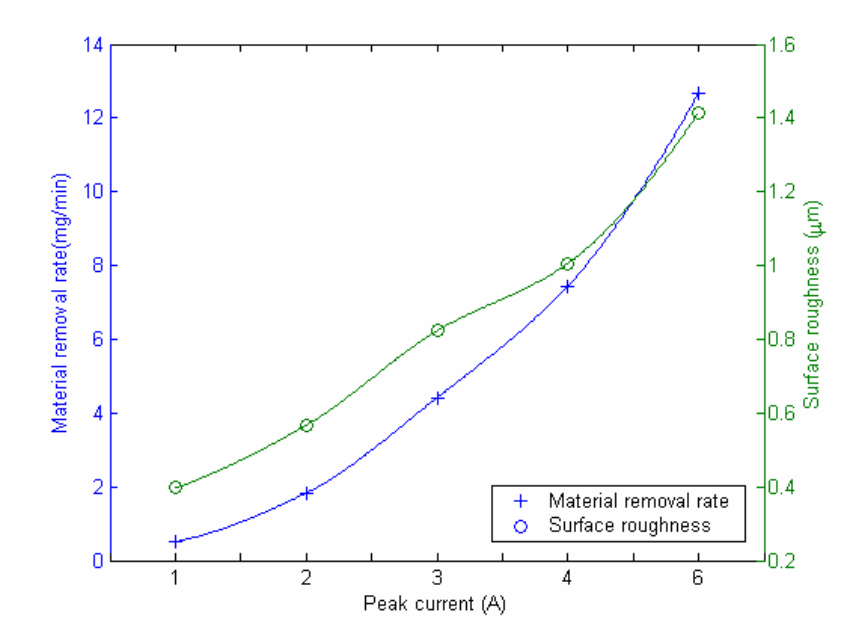

Figure 6-13 Influences of peak current on MRR and SR

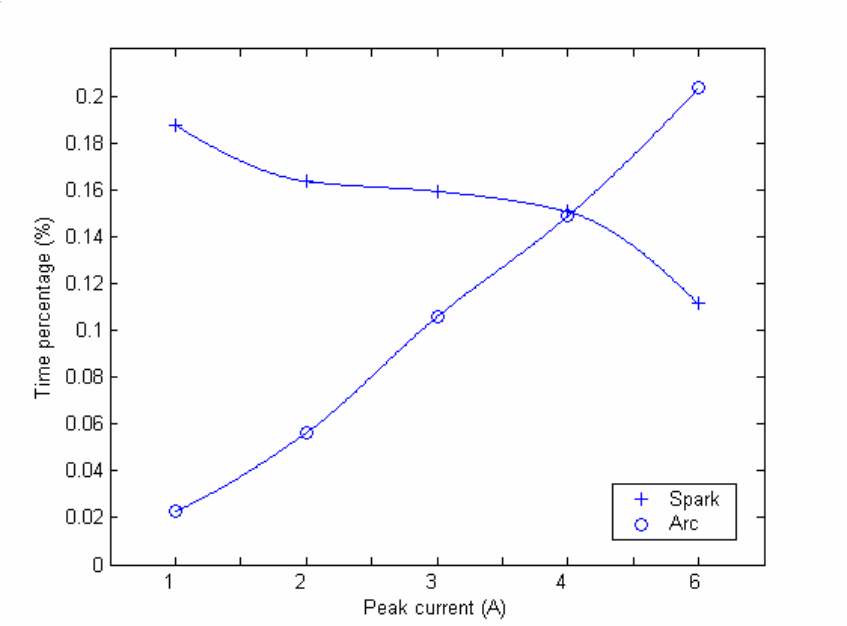

Figure 6-14 Influences of peak current on spark and arc

ATTENTION: The Singapore Copyright Act applies to the use of this document. Nanyang Technological University Library

6.4.3 Pulse On-time

Pulse on-time is another most significant factor of EDM process because all the material is removed during this period. The optimum value of pulse on-time depends on many factors and is difficult to be determined, and is usually selected through experiment. Figure 6-15 shows the influences of pulse on-time on material removal rate and surface roughness, and Figure 6-16 shows the influences of pulse on-time on the time percentage of spark and arc, respectively. It can be seen from Figure 6-15 that material removal rate and surface roughness both increase with pulse on-time due to the increase of the input discharge energy that is directly proportional to the pulse on-time. Figure 6-16 shows the time percentages of spark and arc increase with pulse on-time too, but the increase of arc is faster than that of spark. When pulse on-time is below 12.8μs, the time percentage of spark is bigger than that of arc, while when pulse on-time is bigger than 12.8μs, the time percentage of spark is smaller than that of arc. The increases of spark and arc are due to the increase of the effective machining duration in each pulse. The faster increase of arc is because when the pulse on-time is too big, the large residual debris is difficult to be flushed away and the dielectric media cannot be effectively deionized, which further contribute to the increase of arc. In fact the changes of pulse on-time can be effectively reflected by the time percentage of spark and arc. As the input power (determined by open voltage and peak current) is same while changing pulse on-time, the material removal rate and surface roughness are fully determined by the time percentage of spark and arc. The increase of material removal rate is due to the increases of the time percentage of spark, while the increase of surface roughness is mainly caused by the increase of the time percentage of arc.

ATTENTION: The Singapore Copyright Act applies to the use of this document. Nanyang Technological University Library

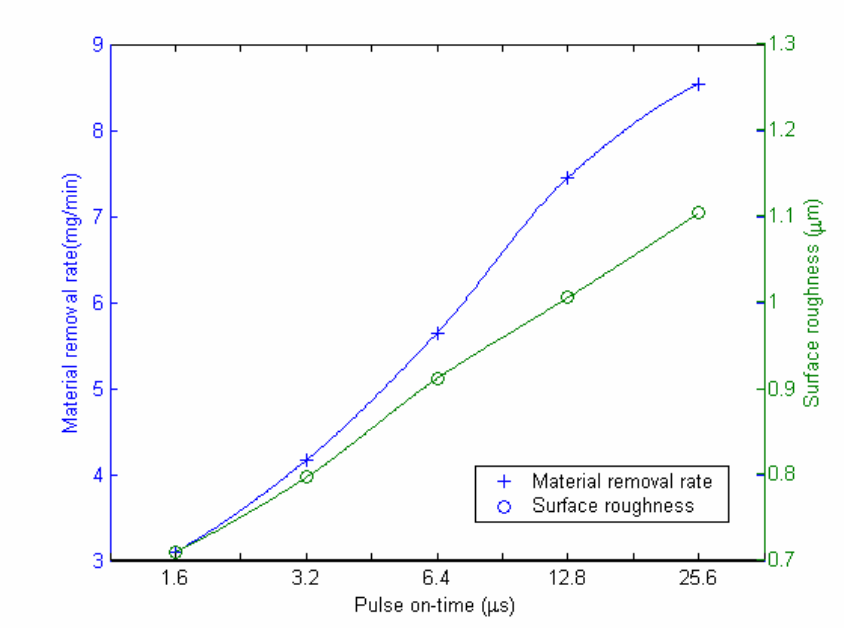

Figure 6-15 Influences of pulse on-time on MRR and SR

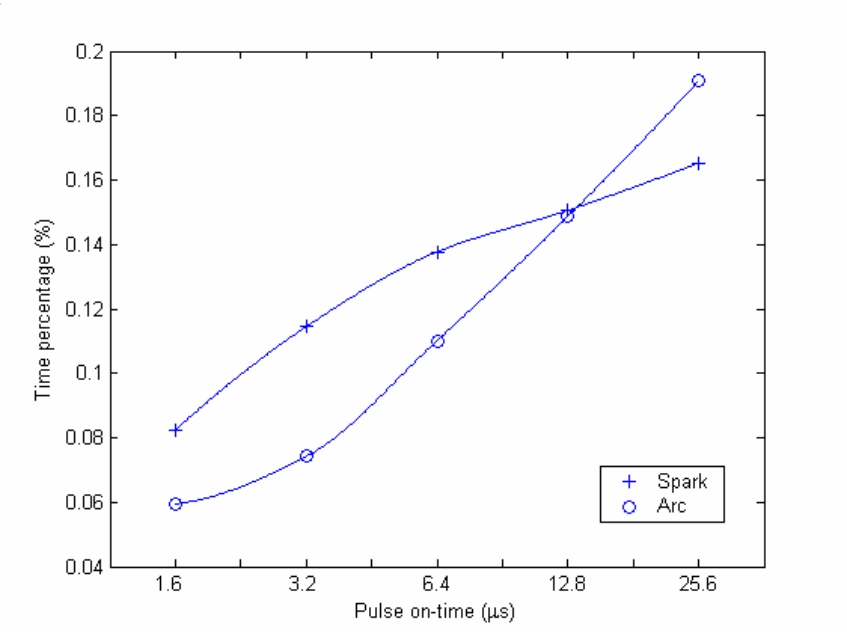

Figure 6-16 Influences of pulse on-time on spark and arc

ATTENTION: The Singapore Copyright Act applies to the use of this document. Nanyang Technological University Library

6.4.4 Pulse Interval

Pulse interval is the time required for the re-establishment of insulation in the discharge gap or de-ionization of the dielectric media at the end of each discharge. It governs the stability of EDM process and is one of the commonly controlled parameters. To prevent arcing while achieving high material removal rate, the pulse interval may have to be adjusted manually or by computer during machining.

The influences of pulse interval on material removal rate and surface roughness are depicted in Figure 6-17, and the influences of pulse interval on the time percentage of spark and arc are shown in Figure 6-18, respectively. Figure 6-17 shows that the material removal rate increases from pulse interval 1.6μs to 3.2μs, and then decreases, while the surface roughness decreases steadily with pulse interval. That is because from pulse interval 1.6μs to 3.2μs, the discharge conditions get better, the time percentage of spark increases and the time percentage of arc decreases very quickly with pulse interval, which results the fast increase of the material removal rate. With the further increase of pulse interval, as the time percentage of spark start to decrease due to the decrease of the number of discharge pulse, the material removal rate decreases with pulse interval. In addition, with the increase of pulse interval, the discharge conditions get better and the number of discharge pulse decreases, thus the time percentage of arc decreases, which results the steadily decrease of the surface roughness. Generally, short pulse interval favors material removal rate but increases surface roughness, whereas long pulse interval improves the surface finish but the material removal rate will decrease significantly. The process performance are mainly determined by the time percentages of spark and arc because the input power is same.

ATTENTION: The Singapore Copyright Act applies to the use of this document. Nanyang Technological University Library

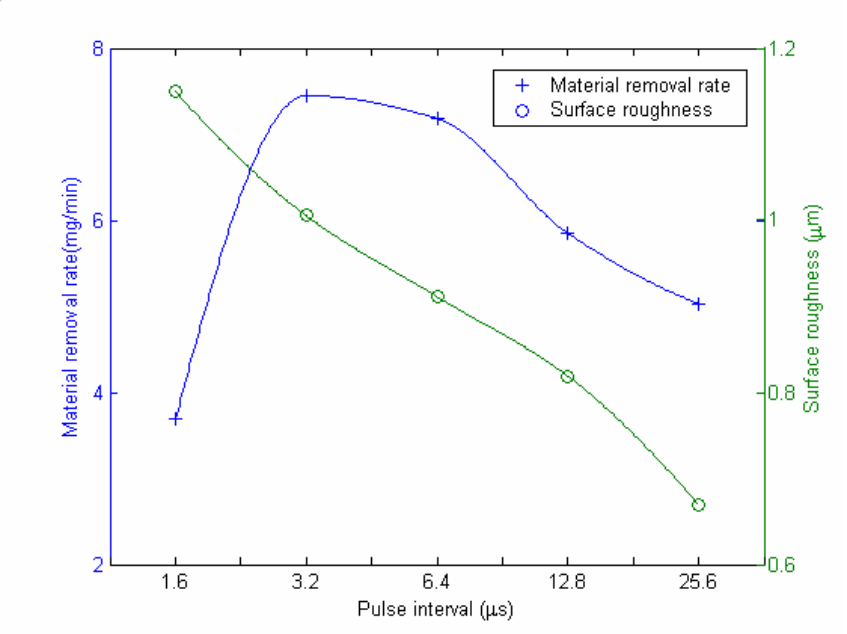

Figure 6-17 Influences of pulse interval on MRR and SR

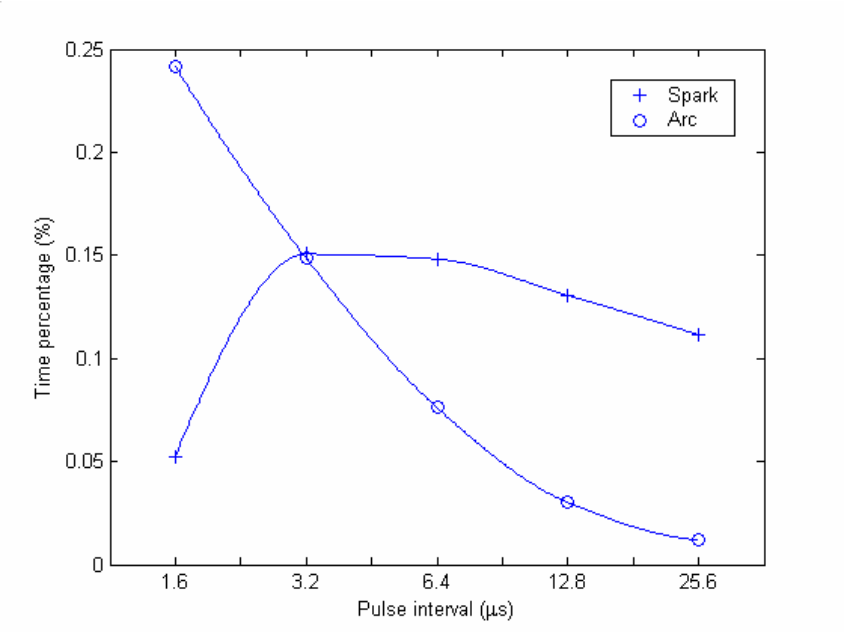

Figure 6-18 Influences of pulse interval on spark and arc

ATTENTION: The Singapore Copyright Act applies to the use of this document. Nanyang Technological University Library

6.4.5 Gap Size

Gap size is one of the most crucial working parameter of EDM process, it has important influences on the performance of EDM process and is another working parameter that be commonly controlled. Most EDM systems employ different control methods for the purpose to maintain the gap size at a constant value during machining. Typical values of the gap size between 10μm to several hundred micrometers can be found depending on the application, current, voltage and the dielectric media. The influences of gap size on material removal rate and surface roughness are shown in Figure 6-19, and the influences of gap size on the monitoring results of discharge conditions are depicted in Figure 6-20, respectively. These two figures show that from gap size 0.01mm to 0.05mm, material removal rate increases with gap size because with wider gap size, the discharge conditions get better and results the increase of the time percentage of spark. While from gap size 0.05mm to 0.20mm, with the further increase of gap size, because the dielectric media in discharge gap gets more and more difficult to be ionized and breakdown, the number of discharge pulse decreases, which results the decrease of the time percentage of spark and thus the decrease of material removal rate. When the open voltage is not high enough, too wide gap size will make the discharge cannot start at all. Hence, to improve the material removal rate, a small gap size is required. However, a too small gap size will cause the difficulties in flushing away the debris from the gap and results more arcing and short circuit, which will decrease the material removal rate on the contrary. In addition, due to the decrease of the number of discharge pulse and the getting better of the discharge conditions, the time percentage of arc decreases steadily with gap size, which results the decrease of the surface roughness for the whole range of gap size.

ATTENTION: The Singapore Copyright Act applies to the use of this document. Nanyang Technological University Library

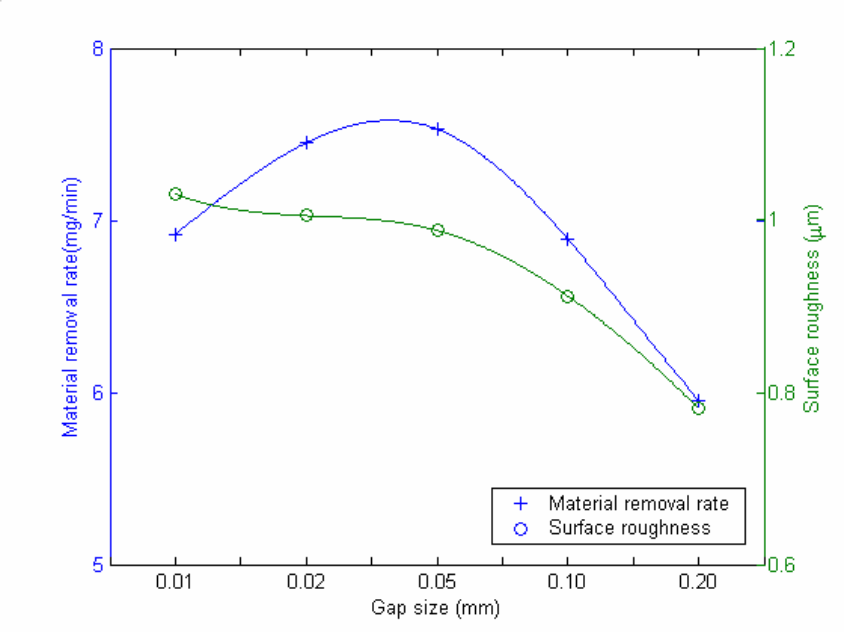

Figure 6-19 Influences of gap size on MRR and SR

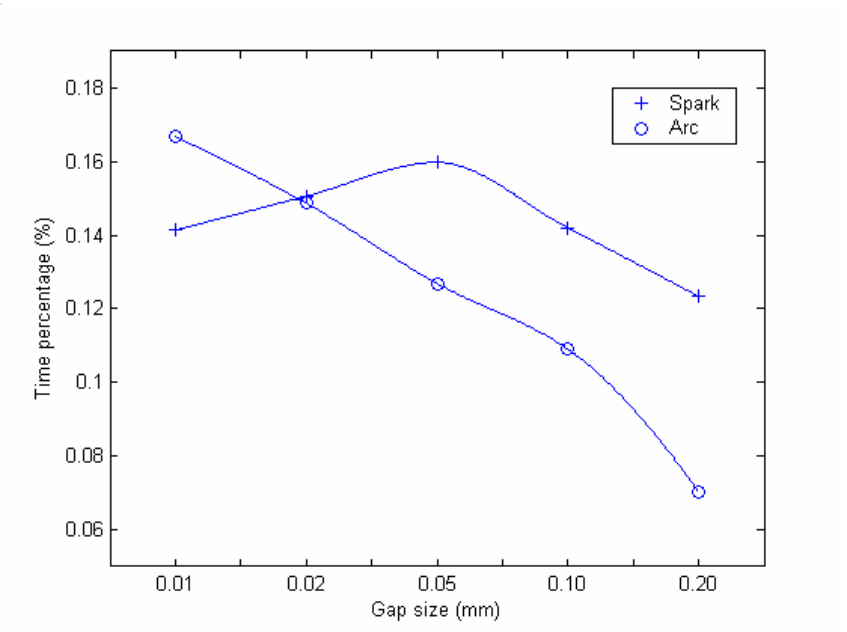

Figure 6-20 Influences of gap size on spark and arc

ATTENTION: The Singapore Copyright Act applies to the use of this document. Nanyang Technological University Library

6.4.6 Ultrasonic Vibration

How to remove the debris effectively from the discharge gap is a widely encountered problem. Among the approaches for solving this problem, ultrasonic vibration of the electrode is an effective method and many researchers had proved that ultrasonic vibration could improve the process performance of EDM to a certain extent. The combination of ultrasonic vibration and EDM are conducive to each other. The high frequency pumping action, by pumping the debris away and sucking the fresh dielectric media into the gap, stoutly ameliorates the discharge conditions, increases its efficiency and gives a higher material removal rate and better surface finish.

Figure 6-21 depicted the influences of ultrasonic vibration on material removal rate and surface roughness, and Figure 6-22 depicted the influences of ultrasonic vibration on the time percentage of spark and arc, respectively. From these two figures, it can be seen that material removal rate increases and surface roughness decreases with the magnitude of ultrasonic vibration steadily due to the increase of the time percentage of spark and the decrease of the time percentage of arc. In addition, these two figures also show that the increase of material removal rate and the decrease of surface roughness at low magnitude of vibration are faster than that at high magnitude of vibration because the discharge conditions improved more obviously at the low magnitude of vibration. With further increase of the magnitude of vibration, the improvement of the discharge conditions slows down, which results the slower increase of the material removal rate and the slower decrease of the surface roughness. From the discussion above, it can be further proved that when machining with same input power, the process performance are mainly determined by discharge conditions.

ATTENTION: The Singapore Copyright Act applies to the use of this document. Nanyang Technological University Library

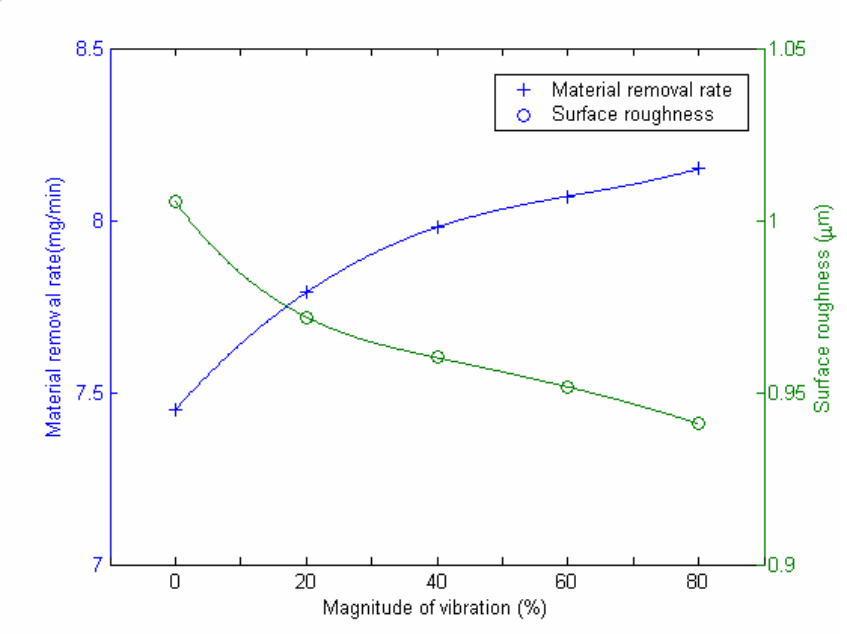

Figure 6-21 Influences of ultrasonic vibration on MRR and SR

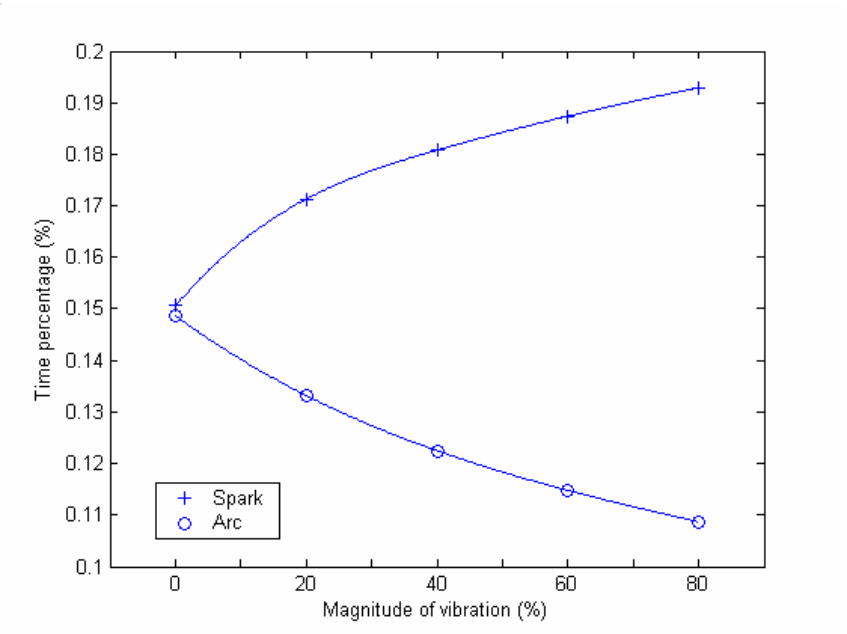

Figure 6-22 Influences of ultrasonic vibration on spark and arc

ATTENTION: The Singapore Copyright Act applies to the use of this document. Nanyang Technological University Library

6.5 Summary

In this chapter, the effects of working parameters on discharge conditions and process performance have been fully studied through conducting screening experiments. From these studies, the following conclusions can be obtained: (1) the repeatability of EDM process is ensured because both the process performance and the discharge conditions have good repeatability from average and time domain views; (2) utilizing working parameters and discharge conditions together gives a more essential interpretation of the process performance; (3) the input power and the discharge conditions (mainly the time percentages of spark and arc) are the crucial factors of the performance of EDM process; (4) if the input power remains the same, material removal rate of EDM process is influenced most significantly by the time percentage of spark, while surface roughness is determined mainly by the time percentage of arc.

ATTENTION: The Singapore Copyright Act applies to the use of this document. Nanyang Technological University Library

Chapter Seven

Development of Performance Predictor for EDM Process

Basically, there are two approaches to study EDM process, either the theoretical or the empirical. The theoretical work is based on solid-state physics, thermodynamics and electrodynamics, and the goal is to describe the physical behavior by making using of a physical model. As electrical discharge machining is basically a stochastic process, those theories put forward to describe this process are still not capable of giving a very convincing explanation of the material removal mechanism. Researchers have encountered lots of difficulties in modeling this process and the inevitable assumptions and simplified approaches push the physical models far from reality [58, 59].

On the other hand, experimentalists have tried to establish empirical or semi-empirical models based on statistical analysis and optimization methods. Various empirical and semi-empirical models for predicting process performance have been proposed in past [62, 64]. In addition, neural network has also gained wide application in modeling EDM process for its outstanding ability to map inputs to outputs for complex and nonlinear systems [60, 61, 63]. In spite of the different modeling approaches, most of

ATTENTION: The Singapore Copyright Act applies to the use of this document. Nanyang Technological University Library

the models are established to correlate the working parameters with the process performance. However, due to a large number of variables and the complicated nature of EDM process, suitable models are difficult to be obtained. In addition, as the process performance is influenced greatly not only by the working parameters, but also the discharge conditions, these models cannot predict the process performance successfully.

In chapter 6, it was proved that the discharge power and the discharge conditions are the determinant factors of the performance of EDM process, hence, a model established between these factors and process performance can give a better prediction result. In this chapter, a neural network model and empirical models are established to predict process performance. Finally, after comparing the performance of these models, the most suitable model for EDM process is obtained and an on-line performance predictor can be achieved.

7.1 ANN Model of EDM Performance

The modeling capability of a neural network is ascribed to its ability to learn the mathematical functions underlying the system operation. If the network is designed and trained properly, it can perform generalization rather than simple curve fitting. It can act as a preprocessor, postprocessor, as a mathematical model or as a baseline control. The use of the neural network as a system model is increasing because it can model a system by example mapping. If accuracy is the only concern for a model, then the neural network may be very well suited for that application. In recent years, neural networks have become a very useful tool in the modeling of the input-output

ATTENTION: The Singapore Copyright Act applies to the use of this document. Nanyang Technological University Library

relationships of complicated systems. Due to the ability of neural networks to approximate any degree of non-linearity with a considerable degree of accuracy, they are widely accepted as a candidate for modeling complex non-linear systems in which traditional modeling strategies fail. According to the successful applications of neural networks in other industry and EDM process, it may be an effective method in establishing the model between monitoring results and process performance. In this research, a feed-forward multi-layer neural network is employed and the back-propagation algorithm is selected for training the NN.

7.1.1 Back-propagation Neural Networks

A neural network is represented by a set of nodes and arrows. A node represents a neuron and an arrow corresponds to a connection, along with the direction of signal flow, between neurons. A typical structure has an input layer, a hidden layer and an output layer. Despite of the structure of neural network, basically, neural networks are composed of simple elements operating in parallel, which are nodes, interconnections and learning rules [119].

A node is a simple device that approximates the function of a biological neuron. The main function of a node is receiving input variables and translating them into an output signal. The translation process includes the evaluation of input signals by weights, the summation of inputs and creating activation value through a chosen activation function.

According to their functions, the nodes used in neural networks can be classified as input nodes, output nodes and hidden nodes. Input nodes are those that receive input

ATTENTION: The Singapore Copyright Act applies to the use of this document. Nanyang Technological University Library

signals from outside the network while output nodes are those that send the results out of the network. Hidden nodes have their inputs and outputs within the network. The input, output and hidden nodes form the corresponding input, output and hidden layers of a multi-layer neural network.

The interconnection scheme is a part of the network architecture definition, which propagates a signal from one node to another, or even to the node itself. If the information flows in one direction, the interconnections are called feed-forward.

The learning rules are the last and also the most import attribute used to define a neural network paradigm. There are several different training algorithms for feed-forward networks. Back-propagation is one of the most important paradigms, which can train multi-layer feed-forward networks with differentiable transfer functions to perform function approximation, pattern association, and pattern classification.

The back-propagation algorithm's strength is its ability to change the values of its weights in response to errors. During training, the input data are passed through the hidden layers to generate values for each node at the output layer. The actual outputs are then compared with the desired outputs to produce the errors. These errors are then passed back to hidden layers. The hidden nodes will use these errors to calculate the errors for this layer. The delta rule that is generalized from the Least Mean Square (LMS) rule is used as a learning law to reduce the errors and change the weights for all the layers. The objective of this procedure is to minimize the sum-squared error of the network and find optimized weights. The set of optimal weights will be preserved after training.

ATTENTION: The Singapore Copyright Act applies to the use of this document. Nanyang Technological University Library

Consider a three-layer network with standard back-propagation architecture shown in Figure 7-1. Input nodes are labeled by *X*, hidden nodes by *H*, output nodes by *O*. Index *i* refers to output nodes, while *j* to hidden nodes and *k* to input nodes. Assuming we have a training set of input-output pairs (X_k^p, Y_i^p). w_{jk} is the weight from *k*th input node to *j*th hidden node, and β_j is the current bias term for the *j*th node. Similarly, w_{ij} is the weight from *j*th hidden node to *i*th output node, and β_i is the current bias term for the *i*th node. We label different patterns by a superscript p. So input *k* is set to X_k^p. We use *N* to denote the number of output nodes and *P* to denote the number of patterns in the training set (*p*=1, 2, …, *P*).

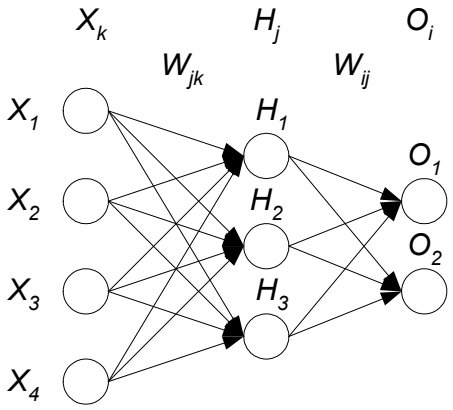

Figure 7-1 Architecture of a feed-forward multi-layer NN

Given pattern *p*, hidden node *j* receives a net input

$$h_j^p = \sum_k w_{jk} X_k^p + \beta_j^p , \tag{7-1}$$

and produces output by taking the transfer (or activation) function f_h of the result.

$$H_j^p = f_h(h_j^p) = f_h(\sum_k w_{jk} X_k^p + \beta_j^p) . \tag{7-2}$$

Similarly, the output node *i* receive an input

ATTENTION: The Singapore Copyright Act applies to the use of this document. Nanyang Technological University Library

$$o_i^p = \sum_j w_{ij} H_j^p + \beta_i^p = \sum_j w_{ij} f_h(\sum_k w_{jk} X_k^p + \beta_j^p) + \beta_i^p , \tag{7-3}$$

and produces the final output if assuming the activation function of the output layer is f_o.

$$O_i^p = f_o(o_i^p) = f_o(\sum_j w_{ij} H_j^p + \beta_i^p) = f_o(\sum_j w_{ij} f(\sum_k w_{jk} X_k^p + \beta_j^p) + \beta_i^p) \tag{7-4}$$

In general, these output values are not equal to the corresponding target values. The training process is to obtain the optimum weights and biases to minimize the errors. Least-mean-squares error function is often used.

$$E(w) = \frac{1}{2} \sum_p \sum_i (Y_i^p - O_i^p)^2 . \tag{7-5}$$

Submitted O_i^p from (7-4) into (7-5), we get

$$E(w) = \frac{1}{2} \sum_p \sum_i [Y_i^p - f_o(\sum_j w_{ij} f_h(\sum_k w_{jk} X_k^p + \beta_j^p) + \beta_i^p)]^2 . \tag{7-6}$$

Obviously, $E(w)$ is a differentiable function of every weight when activation function for every node is a differentiable function. So we can use a gradient descent algorithm to find the weights and minimize $E(w)$. The back-propagation algorithm is designed to take fixed steps u in the direction of steepest descent in order to minimize the error function $E(w)$.

$$\Delta w_{ij} = -u \frac{\partial E}{\partial w_{ij}} , \tag{7-7}$$

Where, u is the learning rate. Hence for the hidden-to-output connections

$$\Delta w_{ij} = -u \frac{\partial E}{\partial w_{ij}} = u \sum_p \delta_i^p H_j^p , \tag{7-8}$$

Where, $\delta_i^p = f_o^{'}(o_i^p)(Y_i^p - O_i^p)$. (7-9)

ATTENTION: The Singapore Copyright Act applies to the use of this document. Nanyang Technological University Library

For the input-to-hidden connections, using the chain rule, we obtain

$$\Delta w_{jk} = -u\frac{\partial E}{\partial w_{jk}} = u\sum_p \frac{\partial E}{\partial H_j^p}\frac{\partial H_j^p}{\partial w_{jk}} = u\sum \delta_j^p X_k^p \,, \tag{7-10}$$

Where, $\delta_j^p = f^{'}(h_j^p)\sum_i w_{ij}\delta_i^p$. (7-11)

The Equation (7-4) and its multi-layer extension are attractive in that the derivatives of an error function $E(w)$ with respect to weights can be calculated recursively from output to input by using the chain rule. Thus, the error signals δ in each layer can be recursively calculated from the upper layer by back-propagating it. That's why the procedure called back-propagation. In all cases, the error function $E(w)$ will be a sum over terms E^p for each learning pattern.

Usually, the activation function must be differentiable, and we normally want it to saturate at both extremes. In the case of a sigmoid function $f(n) = \frac{1}{1+e^{-2\beta n}}$ or $f(n) = \frac{2}{1+e^{-2\beta n}} - 1$ either a (0, 1) or (-1, 1) range can be used. The derivative of the function is readily expressed in terms of function itself as $f^{'}(n) = 2\beta f(1-f)$. Thus, Equation (7-9) can be rewritten as

$$\delta_i^p = O_i^p(1-O_i^p)(Y_i^p - O_i^p)\,, \tag{7-12}$$

and Equation (7-11) becomes

$$\delta_j^p = H_j^p(1-H_j^p)\sum_i w_{ij}\delta_i^p \,. \tag{7-13}$$

The above two equations make it easy to calculate error in each node of each layer, combining with Equation (7-8) and (7-10), the weights and biases are also easy to obtained.

ATTENTION: The Singapore Copyright Act applies to the use of this document. Nanyang Technological University Library

7.1.2 ANN Model Design

In order to model the input-output relationships, the elements and structure of neural networks should be determined before training. In this study only one hidden layer was used because one layer of hidden units can approximate any continuous input-output relation of interest to any desired degree of accuracy provided sufficiently many hidden units are available and most empirical work on modeling using neural network used one hidden layer [120].

In last chapter, it has been proved that the input power (open voltage and peak current) and the discharge conditions (time percentage of spark and time percentage of arc) are the crucial factors of the performance of EDM process. Hence, the input layer has four nodes corresponding to open voltage, peak current, the time percentage of spark and the time percentage of arc. In this study, two process performance including material removal rate and surface roughness need to be modeled, hence the number of nodes of the output layer is two. Linear function is chosen as the activation function (or transfer function) of the output node. This is because sigmoid functions show poor characteristics at the prediction of extreme values when they are used as transfer functions for output nodes.

The number of hidden neurons in the neural network depends on the pattern and complexity of the approximated function and the transfer function of the layers. It can vary widely from application to application and bears a relationship to the number of statistically significant factors that exist in the input data. Using too few neurons in the hidden layer increases the number of iteration required to train the network and

ATTENTION: The Singapore Copyright Act applies to the use of this document. Nanyang Technological University Library

reduces the predictive ability of the neural network or even makes the network not trainable. This is because too few hidden nodes cannot be flexible enough to realize the input-output map for the given data set. It is often named under-fitting. Increasing the number of hidden nodes can improve the situation by decreasing the error level of the training set. However, using too many neurons in the hidden layer extends the training time and tends to make the neural network memorize rather than generalize the training data. The error on the train set is driven to very small value, but when new data is presented to the neural network the error is large and this is often named over-fitting. The number of hidden neurons usually falls between the total of input and output neurons. For most back-propagation networks, the number of neurons in the hidden layer is determined by a trail and error approach.

The avoidance of under-fitting and over-fitting can be achieved by a method called early stopping. In this technique, the available data is divided into three subsets. The first one is the training set that is used to computing the gradient and updating the network weights and biases. The second set is called validation set. The output of this validation set is calculated via the update weights and biases, and the error of this validation set is obtained and monitored during training. The validation error will normally decrease during the initial phases of training, as does the training set error. However, when the network begins to over-fit the data, the validation set error will increase. Once over-fitting is confirmed, the training is stopped. The validation set is actually used to real time testing. The last set is the testing set, its error is not used in training process, but it is used to compare different models. In this research, the first samples in the L_{18} inner array listed in Table 6-3 are used for training, the second samples are used for validation and the screening experimental results are used for

ATTENTION: The Singapore Copyright Act applies to the use of this document. Nanyang Technological University Library

testing. The numbers of the records used for training, validation and testing are listed in Table 7-1.

Table 7-1 Numbers of records for NN model

Number of training (Sample 1)	Number of validation (Sample 2)	Number of testing (Screening experiment)
18	18	20

Once an appropriate network model has been chosen, the next concern of neural network building is the design of reasonable network training strategies and the selection of parameters, like the choice of the error level, the number of iterations and initial conditions on the network parameters, such as learning rate and momentum value. To train the neural network model, the weights associated with the variables need to be assigned some initial values as starting points for the training. When the network is being trained, these values will be adjusted through each of the iterations to reduce the errors so that the predict output will be close to the target output. While it is hard to attach any explicit explanations to the magnitude values of the weights, the initial weight values do matter in starting the training process. Neural network researchers have recommended a number of variations on the initial weight range. Eberhart and Dobbins [121] suggested that it be typical to initialize the weights to random numbers between 0.3 and –0.3, simply because most back-propagation neural networks seem to train faster with these bounds.

The objective of the back-propagations is to minimize the average sum-squared error term by performing a gradient descent in error space. The gradient descent technique is one of the local training techniques. With the gradient descent, the direction of each step is given by the local negative gradient of the performance function, and the step

ATTENTION: The Singapore Copyright Act applies to the use of this document. Nanyang Technological University Library

size is determined by a chosen learning rate. In general, the gradient search toward the nearest valley in the error function is downhill during the training, but there might be a danger that it will gravitate to local minimum happens to be nearest the starting point. If the function has a large number of minimums, most of them may be inferior to some global minimum, and then there will be some danger of getting stuck around one of the local minima. This might be the reason that the initial weight between 0.3 and –0.3 or 1 and –1 did not work with the present problem. Choosing different values for the learning rate and momentum term may help to avoid this situation.

Identification of appropriate values for the learning rate, momentum term, the error level and the number of iterations need to be determined after the initial weight values are determined. The values for the learning rate and momentum term range between 0 and 1 and there are no rules for selecting optimal values for these. Rumelhart and Hinton [122] frequently used 0.5 and 0.9 respectively for the learning rate and momentum term. Eberhart and Dobbins [121] thought that it was best to use small values (0.15 and 0.075) for learning rate and momentum. Other studies showed that the networks would be doing well when both the learning rate and momentum term were assigned at 0.5. After running several training trials with different rates and momentum terms, the 0.5 values seemed to be the most appropriate for both terms in this study.

There are two criteria for terminating network training: one is the specified number of iterations and the other is an error level. The network training is terminated when one of these criteria is reached. The error level or the number of iterations depends on the complexity of the problem and the type of the data. There are two strategies to specify the number of iterations. The first one is to specify a new and larger number of

ATTENTION: The Singapore Copyright Act applies to the use of this document. Nanyang Technological University Library

iterations to resume the training process. The second one is to use the output weight from the network as new input weights and specify an additional number of iterations to resume the training process. This training process can be repeated until the error term is reduced to the specified level or the network output is the closest to the target output. In this study, an initial iteration number of 1000 and an initial error tolerance of 10^{-6} were specified for this problem. After this network was trained successfully, the network was ready to be used as a predicting model for a new data set. The output weights from the trained network would be used as the input parameters for predicting.

7.1.3 Results and Discussion

Finally, a three layers back-propagation neural network model is developed and its structure is shown in Figure 7-2. This neural model has four input nodes to accept the inputs of open voltage, peak current, time percentages of spark and arc, and two output nodes with linear transfer function to output material removal rate and surface roughness. In addition, this model has ten hidden nodes with logsig active function. B_H is the bias of the hidden layer nodes and B_O is the bias of the output layer nodes.

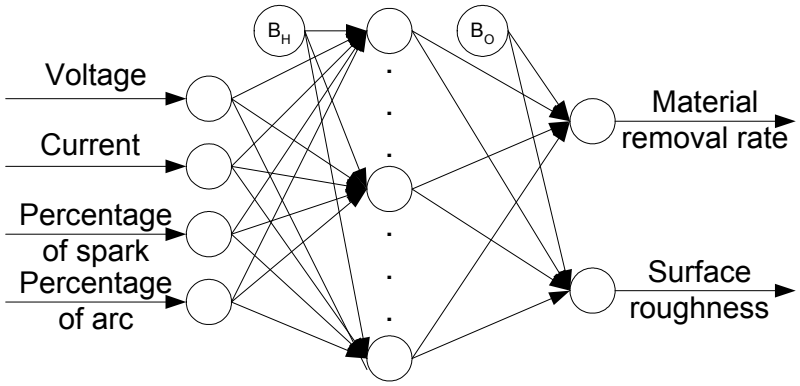

Figure 7-2 Structure of the developed Neural Network

ATTENTION: The Singapore Copyright Act applies to the use of this document. Nanyang Technological University Library

Table 7-2 and 7-3 show the errors of process performance between validation experiments and NN model. The process performance from experiments is quite close to that from neural network model, which means the developed neural network model has been correctly designed. However, before putting into real application, the prediction ability of this model for other working parameters settings that have not contained in the training data must be guaranteed. For this purpose, results from the screening experiments that mentioned in last chapter are used for testing. From table 7-3 and Figure 7-4, it can be seen that the errors of process performance between testing experiments and NN model are very big for the working parameters that not contained in the training data, which means the neural network has not been sufficiently trained.

Table 7-2 Errors of process performance between validation experiments and NN

Trial condition	Material removal rate (mg/min)			Surface roughness, R_a (μm)		
	Experiment	NN	Error (%)	Experiment	NN	Error (%)
1	0.910	1.003	10.18	0.5443	0.5798	6.52
2	2.180	2.157	1.08	0.7551	0.7667	1.54
3	3.420	3.403	0.49	0.8493	0.8485	0.09
4	0.990	1.026	3.66	0.5349	0.5611	4.90
5	3.640	3.638	0.05	0.8151	0.7934	2.67
6	4.320	4.342	0.51	0.8736	0.8401	3.83
7	0.900	0.795	11.66	0.5439	0.5195	4.48
8	3.800	3.816	0.42	0.8287	0.8530	2.93
9	7.085	7.170	1.19	1.0371	1.0249	1.17
10	0.975	1.090	11.82	0.6235	0.6606	5.96
11	1.830	1.826	0.22	0.7368	0.7097	3.68
12	4.320	4.517	4.56	0.8986	0.8703	3.15
13	1.000	1.001	0.03	0.5076	0.5322	4.84
14	2.280	2.411	5.75	0.7211	0.7178	0.46
15	4.230	4.093	3.24	0.8299	0.8319	0.24
16	1.070	0.992	7.29	0.4948	0.5174	4.56
17	4.710	4.679	0.67	0.9168	0.8923	2.67
18	4.300	4.625	7.56	0.8388	0.8784	4.72

ATTENTION: The Singapore Copyright Act applies to the use of this document. Nanyang Technological University Library

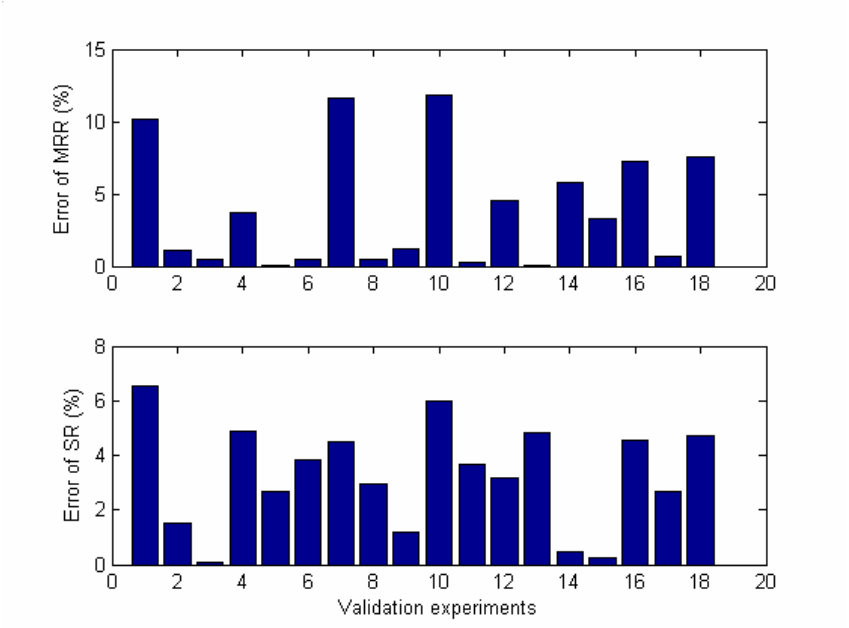

Figure 7-3 Errors of process performance between validation experiments and NN

Table 7-3 Errors of process performance between testing experiments and NN

	Setting		Material removal rate (mg/min)			Surface roughness, R_a (μm)		
			Experiment	Model	Error (%)	Experiment	Model	Error (%)
1	Voltage	80V	4.560	4.067	10.81	0.7927	0.8155	2.88
2		120V	5.945	5.600	5.86	0.9106	0.9205	1.08
3		160V	6.650	5.881	11.57	0.9558	0.9376	1.91
4		200V	7.450	6.807	8.64	1.0054	1.0247	1.92
5	Current	1A	0.515	-0.483	193.72	0.3966	0.1730	56.37
6		2A	1.830	1.640	10.38	0.5666	0.4952	12.60
7		3A	4.415	4.349	1.5	0.8228	0.8693	5.65
8		4A	7.450	6.807	8.64	1.0054	1.0247	1.92
9		6A	12.660	10.770	14.93	1.4146	1.2589	11.00
10	On-time	1.6μs	3.095	-0.039	101.25	0.7107	0.6042	14.92
11		3.2μs	4.165	4.684	12.45	0.7966	0.9038	13.46
12		6.4μs	5.645	5.836	3.38	0.9113	0.9746	6.95
13		12.8μs	7.450	6.807	8.64	1.0054	1.0247	1.92
14		25.6μs	8.540	7.759	9.15	1.1037	1.0685	3.19
15	Interval	1.6μs	3.685	3.167	14.05	1.1496	0.8142	29.18
16		3.2μs	7.450	6.807	8.64	1.0054	1.0247	1.92
17		6.4μs	7.185	5.889	18.04	0.9113	0.9441	3.60
18		12.8μs	5.850	4.762	18.60	0.8190	0.8374	2.25
19		25.6μs	5.035	-6.087	220.90	0.6688	0.2365	64.64

ATTENTION: The Singapore Copyright Act applies to the use of this document. Nanyang Technological University Library

(Continue of table 7-3)

20	Gap size	0.01mm	6.920	6.369	7.97	1.0306	1.0112	1.89
21		0.02mm	7.450	6.807	8.64	1.0054	1.0247	1.92
22		0.05mm	7.530	7.203	4.34	0.9883	1.0297	4.19
23		0.10mm	6.890	6.757	1.93	0.9122	0.9997	9.59
24		0.20mm	5.955	3.126	47.50	0.7850	0.7754	0.78

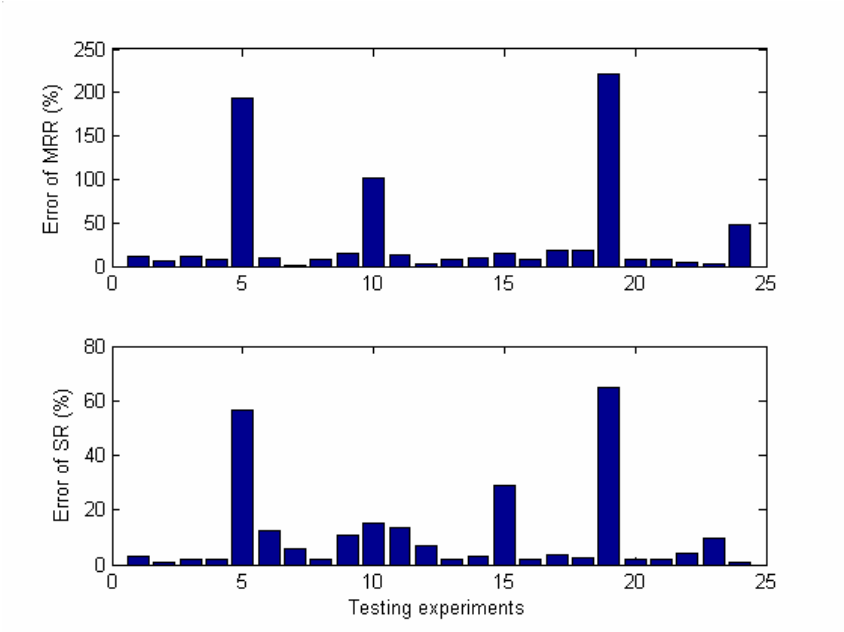

Figure 7-4 Errors of process performance between testing experiments and NN

7.2 Empirical Models of EDM Performance

In this section, two empirical models will be established for predicting process performance of material removal rate and surface roughness respectively. Similar to the ANN model, these two models take the input power (open voltage and peak current) and the discharge conditions (the time percentages of spark and the time percentage of arc) as the input parameters. Before developing the empirical models, several assumptions must be made first.

ATTENTION: The Singapore Copyright Act applies to the use of this document. Nanyang Technological University Library

a) The percentage of the input energy lost in the dielectric media is always a constant.

b) The percentage of the input energy used to remove the material of workpiece is a constant.

c) The energy required to remove a unit of material from the workpiece is a constant.

d) The volume and depth of the craters left on the surface of workpiece by spark or arc are same.

e) Controlled by the power supply, the effective machining time in each spark or arc is same.

f) Only sparks and arcs contribute to the material removal rate and surface roughness. Short-circuits can be neglected because its time percentage is commonly very small.

7.2.1 Empirical Model of Material Removal Rate

From the discussions in last chapter, it is known that the open voltage and peak current both have contributions to the material removal rate, but their contribution coefficients are different. Define the contribution coefficients of open voltage and peak current to material removal rate as c_v and c_i. Assume the time percentage of spark is TP_s, the time percentage of arc is TP_a, the weight of the material removed by a spark and an arc pulse with 1V voltage and 1A current are MR_s and MR_a respectively, the effective machining duration of each spark and arc pulse are T_s and T_a. The material removal rate can be expressed as

ATTENTION: The Singapore Copyright Act applies to the use of this document. Nanyang Technological University Library

$$MRR = V^{c_v} I^{c_i} (MR_s * \frac{TP_s}{T_s} + MR_a * \frac{TP_a}{T_a}) = \frac{MR_s}{T_s} V^{c_v} I^{c_i} (TP_s + \frac{MR_a * T_s}{MR_s * T_a} TP_a) \quad (7\text{-}14)$$

Define $\frac{MR_s}{T_s}$ as machining coefficient c_m and define $\frac{MR_a * T_s}{MR_s * T_a}$ as the contribution coefficient of arc to material removal rate c_a, equation (7-14) can be rewritten as:

$$MRR = c_m V^{c_v} I^{c_i} (TP_s + c_a TP_a) \quad (7\text{-}15)$$

Using the experimental results of the material removal rate listed in Table 6-3 and using curve-fitting method, those coefficients in equation (7-15) can be determined as in equation (7-16).

$$MRR = 0.033 V^{0.12} I^{1.87} (TP_s + 0.13 TP_a) \quad (7\text{-}16)$$

In this equation, the machining coefficient c_m is 0.033, which means the material removal rate for a spark pulse with 1V voltage and 1A current is 0.033mg. It can be seen from this equation that the contribution coefficient of open voltage to material removal rate c_v is 0.12 and the contribution coefficient of current to material removal rate c_i is 1.87 respectively. That means both voltage and current have positive contribution to material removal rate, but compared with the contribution of current, the contribution of voltage is very small. In addition, equation (7-16) also shows that the contribution coefficient of arc to material removal rate is 0.13, which means though arc also contributes to the material removal rate, compared with spark, its contribution is very small. This equation also shows that current and the time percentage of spark are the most crucial factors that have influence on material removal rate of EDM process.

ATTENTION: The Singapore Copyright Act applies to the use of this document. Nanyang Technological University Library

7.2.2 Empirical Model of Surface Roughness

The surface roughness R_a is defined on the basis of the ISO 4287 norm [123] as the arithmetical mean of the deviations of the roughness profile from the central line along the measurement. This definition is set out in equation (7-17), where $y(x)$ is the values of the roughness profile and l is the evaluation length:

$$R_a = \frac{1}{l}\int_0^l |y(x)|dx \tag{7-17}$$

Equation (7-17) can also be expressed in discrete notation as in equation (7-18), where n is the number of measurement points and $y(k)$ is the corresponding profile's value.

$$R_a = \frac{1}{n}\sum_{k=1}^{n} | y(k) | \tag{7-18}$$

Define the contribution coefficients of open voltage and peak current to surface roughness are k_v and k_i. Assume the depth of the craters caused by a spark and an arc pulse with 1V voltage and 1A current is D_s and D_a respectively, and assume that along the central line, only one discharge pulse occurs at each of the measurement point. The surface roughness can be derived as:

$$R_a = \frac{1}{n} V^{k_v} I^{k_i} \left(D_s \frac{TP_s}{T_s} + D_a \frac{TP_a}{T_a}\right) \tag{7-19}$$

However, along the central line, thousands of discharge pulses occur and the craters left on the workpiece overlapped on each other. In addition, the overlap degrees of spark and arc pulses are different. Hence the surface roughness cannot be evaluated by adding the depth of the craters simply as in equation (7-19). Defined o_s as the overlap coefficient of spark and define o_a as the overlap coefficient of arc. Equation (7-19) can be rewritten as:

ATTENTION: The Singapore Copyright Act applies to the use of this document. Nanyang Technological University Library

$$R_a = \frac{1}{n} V^{k_v} I^{k_i} [(D_s * \frac{TP_s}{T_s})^{o_s} + (D_a * \frac{TP_a}{T_a})^{o_a}]$$
$$= \frac{1}{n} (\frac{D_s}{T_s})^{o_s} V^{k_v} I^{k_i} [TP_s^{o_s} + (\frac{D_a}{T_a})^{o_a} (\frac{T_s}{D_s})^{o_s} TP_a^{o_a}] \quad (7\text{-}20)$$

Define $\frac{1}{n}(\frac{D_s}{T_s})^{o_s}$ as machining coefficient k_m and define $(\frac{D_a}{T_a})^{o_a}(\frac{T_s}{D_s})^{o_s}$ as contribution coefficient of arc to surface roughness k_a, equation (7-20) can be expressed as:

$$R_a = k_m V^{k_v} I^{k_i} (TP_s^{o_s} + k_a TP_a^{o_a}) \quad (7\text{-}21)$$

Using the experimental results of the surface roughness listed in Table 6-3 and using curve-fitting method, those coefficients in equation (7-21) can be determined

$$R_a = 0.70 V^{-0.02} I^{0.55} (TP_s^{0.27} + 5.0 TP_a^{1.76}) \quad (7\text{-}22)$$

This equation shows that the contribution factor of voltage to surface roughness k_v is –0.02 and the contribution factor of current to surface roughness k_i is 0.55, which means compared with current, the contribution of voltage to surface roughness is much smaller. In addition, this equation also shows that the contribution coefficient of arc k_a is 5.0, the overlap coefficient of arc o_a is 1.76 and the overlap coefficient of spark o_s is 0.27, which means the contribution of arc to surface roughness is much bigger than that of spark. This equation proves that peak current and the time percentage of arc are the most important factors of surface roughness.

7.2.3 On-line Performance Predictor of EDM Process

Now, the empirical models for material removal rate and surface roughness have been established respectively. Table 7-4 and Figure 7-5 show the errors of the process performance between the empirical models and the experiments used for training the NN. It can be seen that the material removal rate and the surface roughness from the

ATTENTION: The Singapore Copyright Act applies to the use of this document. Nanyang Technological University Library

empirical models agree well with the experiment results, the errors are within an acceptable range that is smaller than 20%. Table 7-5 and Figure 7-6 show the errors of process performance between empirical models and the experiments used to validate the NN model. It can be seen that the errors are still within an acceptable range. In addition, to ensure the reliability of the empirical models, the screening experiment used for testing the NN is also used to test the empirical models. Table 7-6 and Figure 7-7 show the errors of the process performance between testing experiments and empirical models are still within an acceptable range, which means the empirical models can correctly predict EDM process performance. Thus the reliabilities of these two empirical models are confirmed and an on-line performance predictor can be realized as shown in Figure 7-8.

Table 7-4 Errors of process performance between experiments and empirical models

Trial condition	Material removal rate (mg/min)			Surface roughness, R_a (μm)		
	Experiment	Model	Error (%)	Experiment	Model	Error (%)
1	0.920	0.990	7.56	0.5641	0.5662	0.37
2	2.210	2.426	9.78	0.7940	0.7883	0.71
3	3.380	3.509	3.81	0.8574	0.8338	2.75
4	1.050	1.226	16.79	0.5650	0.5565	1.50
5	3.605	3.638	0.91	0.7934	0.7457	6.01
6	4.385	4.457	1.65	0.8418	0.9073	7.79
7	0.890	0.932	4.66	0.5323	0.4811	9.61
8	3.790	3.803	0.35	0.8526	0.8440	1.01
9	7.040	7.010	0.43	1.0193	0.9771	4.14
10	0.960	1.036	7.91	0.6158	0.6070	1.43
11	1.815	1.950	7.44	0.7121	0.6828	4.11
12	4.385	4.466	1.84	0.8655	0.9114	5.30
13	1.015	1.229	21.06	0.5366	0.5739	6.95
14	2.325	2.325	0.01	0.7083	0.6763	4.52
15	4.295	4.495	4.67	0.8440	0.8018	4.99
16	1.035	1.206	16.52	0.5197	0.5231	0.66
17	4.615	4.702	1.89	0.8888	0.8668	2.47
18	4.290	4.419	3.02	0.8573	0.8181	4.57

ATTENTION: The Singapore Copyright Act applies to the use of this document. Nanyang Technological University Library

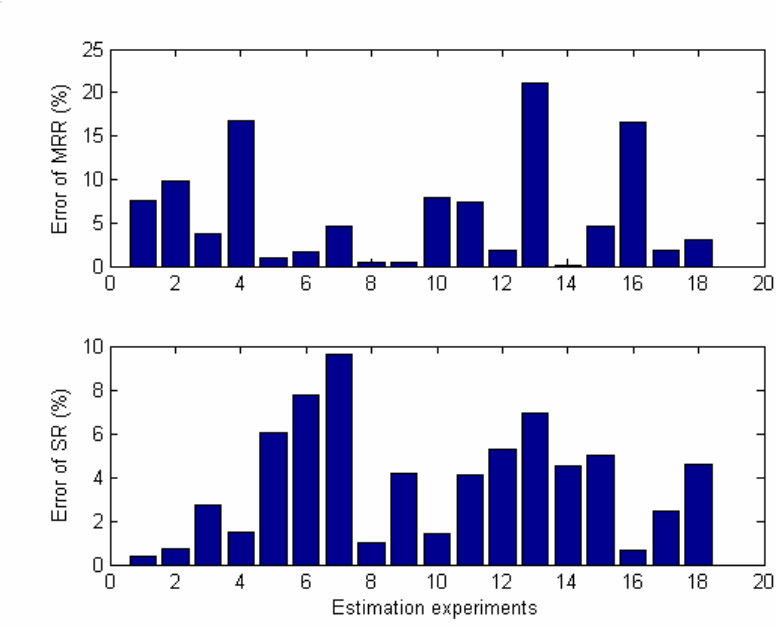

Figure 7-5 Errors of process performance between experiments and empirical models

Table 7-5 Errors of process performance between experiments and empirical models

Trial condition	Material removal rate (mg/min)			Surface roughness, R_a (μm)		
	Experiment	Model	Error (%)	Experiment	Model	Error (%)
1	0.91	1.019	12.01	0.5443	0.5661	4.00
2	2.18	2.427	11.34	0.7551	0.7788	3.14
3	3.42	3.480	1.74	0.8493	0.8397	1.13
4	0.99	1.245	25.70	0.5349	0.5555	3.86
5	3.64	3.643	0.07	0.8151	0.7435	8.79
6	4.32	4.444	2.86	0.8736	0.9104	4.21
7	0.90	0.951	5.61	0.5439	0.4826	11.28
8	3.80	3.832	0.84	0.8287	0.8449	1.96
9	7.085	7.109	0.34	1.0371	0.9711	6.37
10	0.975	1.089	11.70	0.6235	0.6224	0.18
11	1.83	1.957	6.96	0.7368	0.6847	7.07
12	4.32	4.604	6.57	0.8986	0.9168	2.02
13	1.0	1.193	19.28	0.5076	0.5696	12.21
14	2.28	2.434	6.74	0.7211	0.6824	5.36
15	4.23	4.399	4.00	0.8299	0.7962	4.06
16	1.07	1.174	9.69	0.4948	0.5173	4.54
17	4.71	4.796	1.83	0.9168	0.8726	4.82
18	4.30	4.532	5.40	0.8388	0.8281	1.27

ATTENTION: The Singapore Copyright Act applies to the use of this document. Nanyang Technological University Library

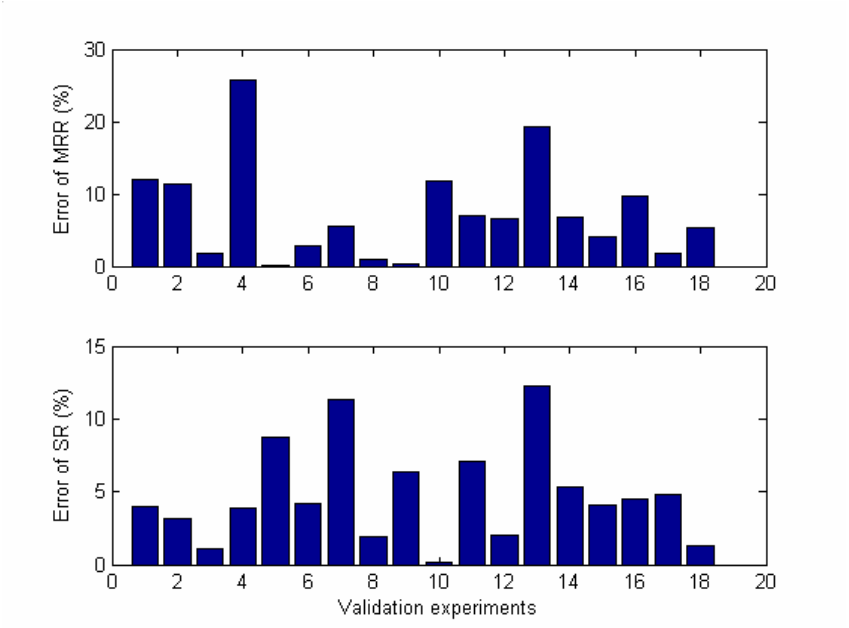

Figure 7-6 Errors of process performance between experiments and empirical models

Table 7-6 Errors of process performance between experiments and empirical models

	Setting		Material removal rate (mg/min)			Surface roughness, R_a (μm)		
			Experiment	Model	Error (%)	Experiment	Model	Error (%)
1	Voltage	80V	4.560	4.589	0.64	0.7927	0.8277	4.42
2		120V	5.945	5.372	9.64	0.9106	0.9047	0.65
3		160V	6.650	6.377	4.10	0.9558	0.9962	4.23
4		200V	7.450	7.075	5.03	1.0054	1.0453	3.96
5	Current	1A	0.515	0.594	15.30	0.3966	0.4048	2.06
6		2A	1.830	1.947	6.38	0.5666	0.5945	4.92
7		3A	4.415	4.207	4.71	0.8228	0.8120	1.32
8		4A	7.450	7.075	5.03	1.0054	1.0453	3.96
9		6A	12.660	12.242	3.30	1.4146	1.4442	2.09
10	On-time	1.6μs	3.095	2.923	5.55	0.7107	0.7134	0.46
11		3.2μs	4.165	3.709	10.95	0.7966	0.8175	2.62
12		6.4μs	5.645	5.329	5.59	0.9113	0.9498	4.22
13		12.8μs	7.450	7.075	5.03	1.0054	1.0453	3.96
14		25.6μs	8.540	8.785	2.86	1.1037	1.1174	1.24
15	Interval	1.6μs	3.685	3.500	5.05	1.1496	1.1641	1.26
16		3.2μs	7.450	7.075	5.03	1.0054	1.0453	3.96
17		6.4μs	7.185	6.582	8.39	0.9113	0.8785	3.60
18		12.8μs	5.850	5.601	4.26	0.8190	0.7932	3.15
19		25.6μs	5.035	4.707	6.51	0.6688	0.7492	12.02

ATTENTION: The Singapore Copyright Act applies to the use of this document. Nanyang Technological University Library

(Continue of table 7-6)

20	Gap size	0.01mm	6.920	6.790	1.89	1.0306	1.0841	5.19
21		0.02mm	7.450	7.075	5.03	1.0054	1.0453	3.96
22		0.05mm	7.530	7.340	2.52	0.9883	1.0009	1.28
23		0.10mm	6.890	6.503	5.62	0.9122	0.9335	2.33
24		0.20mm	5.955	5.519	7.32	0.7850	0.8304	6.25

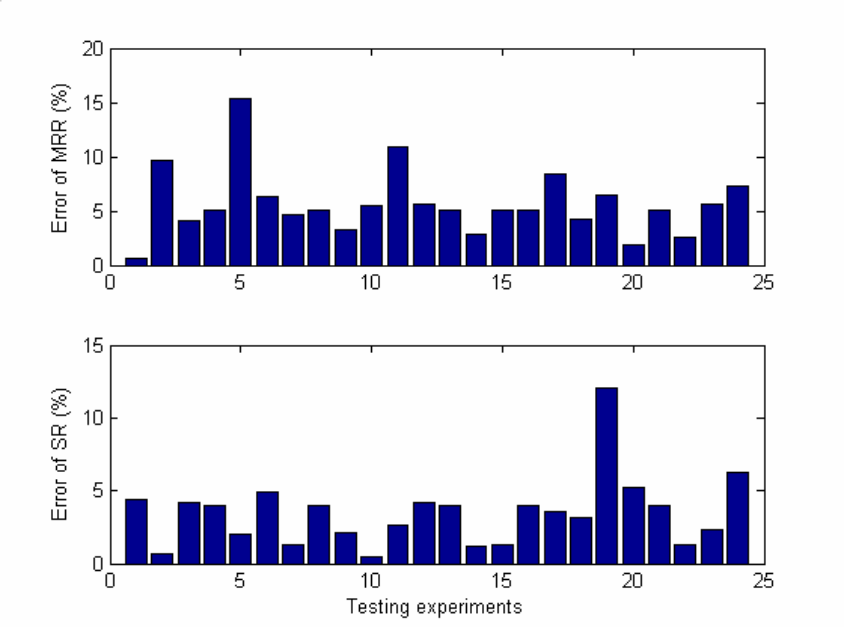

Figure 7-7 Errors of process performance between experiments and empirical models

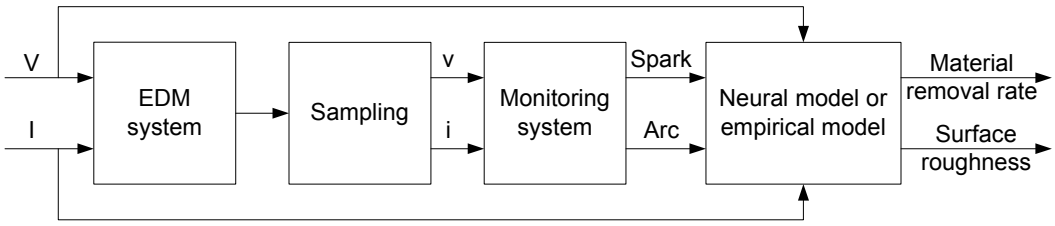

Figure 7-8 On-line performance predictor of EDM process

ATTENTION: The Singapore Copyright Act applies to the use of this document. Nanyang Technological University Library

7.3 Summary

In this chapter, neural network model and empirical models have been developed to predict process performance. The results from neural network model agree well with that from validation experiments. However, because the neural network model was insufficiently trained, the process performance predicted using this model are far from that of testing experiments for those working parameters settings that are not contained in the training data, which means the prediction ability of the model is poor. In order to improve the prediction accuracy of this model, more experiments should be carried out.

Compared with the neural network model, the empirical models give a much better accuracy no matter which working parameters settings are used. The process performance from empirical models agrees quite well with that from experiments. The errors between them are due to the following reasons: (1) the monitoring results have some differences with the real discharge conditions because only limited data are collected and processed. In addition, the realization of the algorithm of monitoring method also has some errors; (2) the measured process performance have some differences with real process performance; (3) the errors from the models themselves. Through overcoming these problems, better empirical models can be achieved. In addition, the empirical models have explicit physical meanings. They prove that voltage, current and discharge conditions actually determine the process performance. They also prove that arc will decrease machining efficiency and cause damage to the surface of workpiece, thus should be avoided effectively during machining. Finally a performance predictor is developed, which is readily to be used in practical applications.

ATTENTION: The Singapore Copyright Act applies to the use of this document. Nanyang Technological University Library

Chapter Eight

Conclusions and Recommendations

8.1 Conclusions

In this research, several studies to address unsolved problems about EDM in investigations were conducted in four areas: the mechanism study of the discharging process, the monitoring of the discharge conditions, the study on the influences of controllable working parameters on discharge conditions and EDM performance, and the study on establishing models for predicting EDM performance.

Among these areas, mechanism and monitoring studies are the bases of the other studies, which were well achieved by employing input electrical impedance as the studied signature. This signature is an inherent characteristic of electrical systems and its changes honestly reflect the changes of the studied electrical system. Through studying the input electrical impedance of EDM process, the mechanism of discharging process were well understood and a reliable monitoring system was developed, quantitative monitoring results of discharge conditions were obtained.

ATTENTION: The Singapore Copyright Act applies to the use of this document. Nanyang Technological University Library

Sequentially, the influences of working parameters on discharge conditions and process performance and the establishment of models for predicting EDM performance were completed after the quantitative monitoring results are available.

Discharge mechanism was well understood through studying input electrical impedance: In this research, the discharge gap was treated as a black box and further simplified as time-varying capacitor and resistor in parallel. Through studying the relationship between the input and the output of this black box, the signature of input electrical impedance, the discharging mechanisms of spark and arc were well interpreted. Based on the imaginary part of the input electrical impedance, a discharging process was divided into five phases. In each phase, input electrical impedance gave a better explanation of the discharge mechanism than voltage and current. The reliability of the obtained discharge mechanism was ensured after investigating the influences of working parameters on the input electrical impedance. In addition, this study proved that input electrical impedance could effectively identify these working parameters, which is almost impossible using other signatures.

An on-line monitoring system of discharge conditions was developed: This research developed an effective monitoring system for the discharge conditions. Based on the understanding of the discharge mechanism, several features were extracted from the waveforms of the input electrical impedance and a fuzzy classifier was developed to differentiate sparks and arcs. This monitoring system could process discharge pulses individually after segmenting the discharge train into separate pulses, thus obtained quantified monitoring results. The correctness of the monitoring results was guaranteed through conducting verification experiments. It is proved that this

ATTENTION: The Singapore Copyright Act applies to the use of this document. Nanyang Technological University Library

monitoring system can honestly reflect the discharge conditions as input electrical impedance is an inherent characteristic of discharging process.

The crucial factors of the performance of EDM process were identified: In this research, the crucial factors affecting the performance of EDM process were identified after investigating the influences of working parameters on discharge conditions and EDM performance. It proved that the input power (open voltage and peak current) and the discharge conditions (mainly the time percentages of spark and arc) are the crucial factors of the performance of EDM process. It also proved that the material removal rate is influenced greatly by the peak current and the time percentage of spark, while peak current and time percentage of arc affect the surface roughness significantly. If the input power is same, the material removal rate and the surface roughness are mainly determined by the time percentage of spark and arc, respectively.

ANN and empirical models for predicting EDM performance were established: In this research, ANN and empirical models were developed to predict EDM performance. Compared with the empirical models, the prediction accuracy of the ANN model is some worse when the working parameter settings were not contained in the data for training this model. The empirical models have better prediction accuracy than the ANN model in spite of the working parameters settings used. If sufficient training data are available, both ANN and empirical models can predict the EDM performance successfully. In addition, the empirical models proved that arcs will decrease the machining efficiency and cause damage to the surface of workpiece, thus, should be avoided effectively during machining. An on-line performance predictor for EDM process was realized, which can be readily put into real applications.

ATTENTION: The Singapore Copyright Act applies to the use of this document. Nanyang Technological University Library

8.2 Recommendations

In this research, an effective monitoring system and suitable process models have been developed. However, several simplifications and neglects have been made convenience for conducting this research. In addition, the control system has not been realized. Hence, some further efforts to perfect the whole study and put the monitoring system into real control application should be continued.

Improve the performance of the monitoring system: Though the validity of the proposed monitoring system has been confirmed, there are still some efforts that can be done to improve the performance of this monitoring system. The first one is using more features to assist the classification of sparks and arcs, such as the phase of electrical impedance. In addition, as the algorithms of segmenting the discharge train and developing the fuzzy classifier have important influences on the monitoring results, some efforts should be spend to make these algorithms more robust. Furthermore, the power supply of the EDM machine used in this research is a commonly used pulse generator, if different power supply is employed, such as R-C circuit, the discharge mechanism should be reinvestigated and the monitoring method need to be modified.

Develop a cost-effective on-line monitoring system: In this proposed monitoring system, voltage and current probes, high-speed sampling system and computer with necessary software are needed. However, they are very expensive and not suitable for mass production in industry. Thus, to lower cost, corresponding hardware and software should be designed to complete the data collection and processing functions. Some pre-works have been done and are shown in Figure 8-1 and 8-2. Figure 8-1 shows the

ATTENTION: The Singapore Copyright Act applies to the use of this document. Nanyang Technological University Library

hardware modules of the on-line monitoring system and Figure 8-2 shows the software interface of this monitoring system programmed using Visual C++.

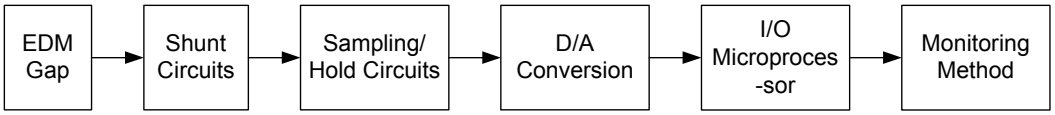

Figure 8-1 Flowchart of the on-line monitoring system

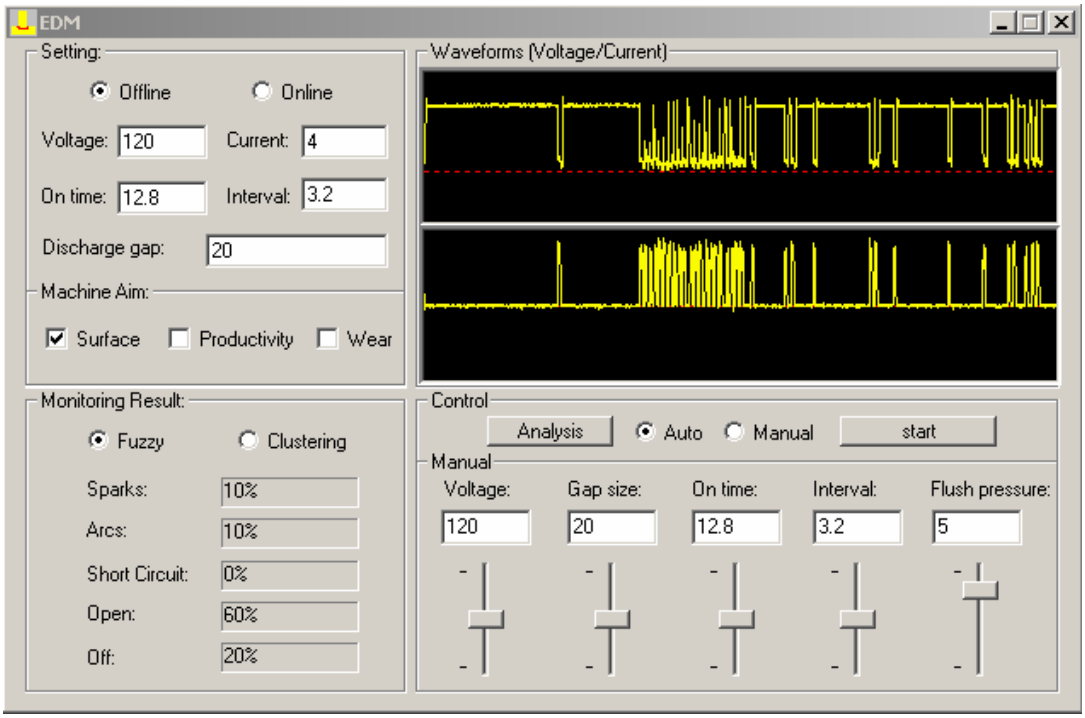

Figure 8-2 Interface of the software of the monitoring and control system

Verify the research results for different material pairs: In this research, the crucial factors of the performance of EDM process have been determined. However, this study is done only for the selected copper-steel material pair. Hence, it is necessary to verify that whether the input power and the discharge conditions still are the crucial factors for difference electrodes or workpieces and can fully interpret the process performance.

ATTENTION: The Singapore Copyright Act applies to the use of this document. Nanyang Technological University Library

In addition, some effort should be spent to determine the crucial factors for the process performance of EDM when negative electrode polarity is used.

Perfect the models by taking the polarity, material properties into account: In this research, neural network and empirical models have been established to predict the performance of EDM process. However, the electrode polarity and material properties have been neglected in developing these models. After doing more comprehensive studies for different electrodes, workpieces and electrode polarities, the electrode polarity and some material properties of the electrode and workpiece can be taken into account to build more perfect models. The material properties should been taken into consideration including the melting and boiling point, heat capacity, thermal conductivity, latent heat of fusion and vapor, etc.

Develop an adaptive control system: As EDM process is complicated and high nonlinear, fuzzy controller is suitable for controlling purpose. A lot of efforts should be continued for developing the fuzzy control system and some works have been done here. An on-line monitoring and control system with the ability of controlling EDM performance was developed in Figure 8-3. In this system, pulse interval and gap size will be mostly controlled, while peak current and pulse on-time will be adjusted only when necessary. The control objective is to obtain the expected discharge conditions for required EDM performance. The control strategy can be summarized as: when predicted material removal rate is much smaller than the expected value, increases peak current or pulse on-time, otherwise decreases pulse interval or gap size. If the predicted surface roughness is much high than the expected value, decreases peak current or pulse on-time, otherwise increases pulse interval or gap size.

ATTENTION: The Singapore Copyright Act applies to the use of this document. Nanyang Technological University Library

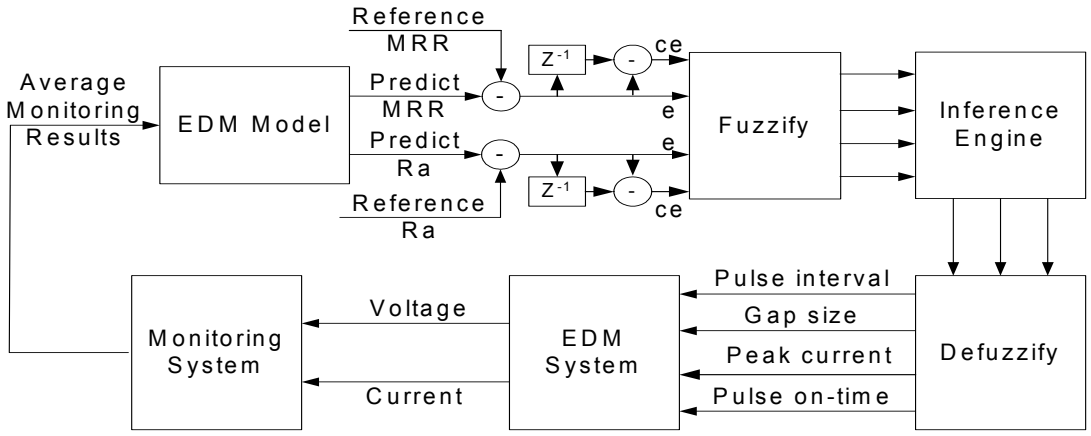

Figure 8-3 On-line monitoring and control system of EDM

The control system above will be influence greatly by the accuracy of the EDM performance models. An alternative way of the control system is shown in Figure 8-4. The inputs of this control system are the time percentages of opens, sparks, arcs and short-circuits. The control strategy can be summarized briefly as: when the time percentage of sparks and arcs are both small and the time percentage of opens is very big, decreases gap size; When the time percentage of sparks is small and the time percentage of arcs is big, decrease pulse on-time or increases pulse interval and gap size; In addition, if the time percentage of short-circuits is big, increase gap size and decrease peak current, otherwise increases pulse interval or decrease pulse on-time.

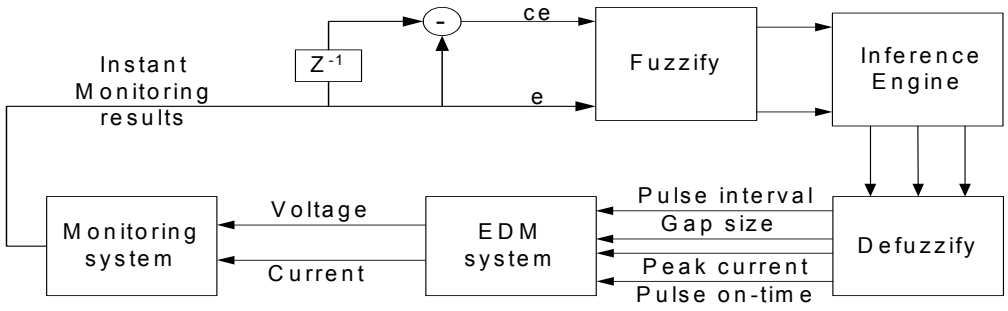

Figure 8-4 On-line monitoring and control system of EDM

ATTENTION: The Singapore Copyright Act applies to the use of this document. Nanyang Technological University Library

REFERENCE

1. Anonymous, History and development, in: The techniques and practice of spark erosion machining, Sparcatron Limited, Gloucester, UK, p. 6, 1965.
2. E.C. Jameson, Description and development of electrical discharge machining (EDM), in: Electrical Discharge Machining, Society of Manufacturing Engineers, Dearbern, Michigan, p. 12, 2001.
3. G. Boothroyd, A.K. Winston, Non-conventional machining process, in: Fundamentals of Machining and Machine tools, Marcel Dekker, Inc, New York, p. 491, 1989.
4. M.L. Jeswani, Roughness and wear characteristics of spark-eroded surface, Wear Vol. 51, p. 227-236, 1978.
5. J.A. McGeough, Electro-discharge machining, in: Advanced Methods of Machining, Chapman & Hall, London, p. 130, 1988.
6. E.I. Shobert, What happens in EDM, in: E. C. Jameson (Ed.), Electrical Discharge Machining: Tooling, Methods and Applications, Society of Manufacturing Engineers, Dearbern, Michigan, 1983.
7. M.S. Ahmed, Texturing of large surface areas by EDM, Proceedings of the SME EDM clinic, September 1987.
8. K.P. Rajurkar, V.V. Navelkar, and J.E. Springer, High-speed pulse train for real-time EDM control, Proceedings of the SME EDM clinic, September 1987.
9. N. Mohri, H. Yamada, K. Furutani, T. Narikiyo, T. Magara, System identification of wire electrical discharge machining, Ann. CIRP, Vol. 47 (1), p. 173-176, 1998.
10. K.P. Rajurkar, Z.Y. Yu, 3D micro-EDM using CAD/CAM, Ann. CIRP, Vol. 49 (1), p. 127-130, 2000.
11. T. Masuzawa, State of the art of micromachining, Ann. CIRP, Vol. 49 (2), p. 473-488, 2000.

ATTENTION: The Singapore Copyright Act applies to the use of this document. Nanyang Technological University Library

12. S.H. Yeo, G.G. Yap, A feasibility study on the micro electro-discharge machining process for photomask fabrication, Int. J. Adv. Manuf. Technol. Vol. 18 (1), p. 7-11. 2001.
13. T. Masuzawa, M. Fujino, K. Kobayashi and T. Suzuki. Wire electro-discharge grinding for micro machining. Annals of the CIRP, Vol. 34 (1), p. 431-434, 1985.
14. Z.X. Jia, J.H. Zhang, X. Ai, Study on a new kind of combined machining technology of ultrasonic machining and electrical discharge machining, Int. J. Mach. Tools Manuf. Vol. 37 (2), p. 193-197, 1997.
15. D.K. Aspinwall, M.L.H. Wise, K.J. Stout, T.H.A. Goh, F.L. Zhao, M.F. El-Menshawy, Electrical discharge texturing, Int. J. Mach. Tools Manuf. Vol. 32 (1/2), p. 183-193, 1992.
16. J. Kozak, K.P. Rajurkar, S.Z. Wang, Material removal in WDWM of PCD blanks, J. Eng. Ind. (Trans. ASME), Vol. 116 (3), p. 363-369, 1994.
17. M. Bayramoglu, A.W. Duffill, Systematic investigation on the use of cylindrical tools for the production of 3D complex shapes on CNC EDM machine, Int. J. Mach. Tools Manuf. Vol. 34 (3), p. 327-339, 1994.
18. A. Arthur, P.M. Dickens, R.C. Cobb, Using rapid prototyping to produce electrical discharge machining electrodes, Rapid Prototyping J. Vol. 2 (1), p. 4-12, 1996.
19. F.T. Weng, M.G. Her, Study of the batch production of micro parts using the EDM process, Int. J. Adv. Manuf. Technol. Vol. 19 (4), p. 266-270, 2002.
20. W. Konig, D.F. Dauw, G. Levy, U. Panten, EDM—future steps towards the machining of ceramics, Ann. CIRP, Vol. 37 (2), p. 623-631, 1988.

ATTENTION: The Singapore Copyright Act applies to the use of this document. Nanyang Technological University Library

21. N. Mohri, Y. Fukuzawa, T. Tani, N. Saito, K. Furutani, Assisting electrode method for machining insulating ceramics, Ann. CIRP, Vol. 45 (1), p. 201-204, 1996.
22. N. Mohri, Y. Fukuzawa, T. Tani, T. Sata, Some considerations to machining characteristics of insulating ceramics—towards practical use in industry, Ann. CIRP, Vol. 51 (1), p. 161-164, 2002.
23. T. Matsuo, E. Oshima, Investigation on the optimum carbide content and machinng condition for wire EDM of zirconia ceramics Ann. CIRP, Vol. 41 (1), p. 231-234, 1992.
24. B.H. Yan, C.C. Wang, W.D. Liu, F.Y. Huang, Machining characteristics of Al_2O_3/6061Al composite using rotary EDM with a disklike electrode, Int. J. Adv. Manuf. Technol. Vol. 16 (5), p. 322-333, 2000
25. A.G. Mamalis, N.M. Vaxevanidis, D.I. Pantelis, On the electrodischarge machining of ceramic plasma-sprayed steel plates, Ann. CIRP, Vol. 41 (1), p. 235-238, 1992.
26. F. Muller, J. Monaghan, Non-conventional machining of particle reinforced metal matrix composite, Int. J. Mach. Tools Manuf. Vol. 40 (9), p. 1351-1366, 2000.
27. M.G. Her, F.T. Weng. Micro-hole machining of copper using the electro-discharge machining process with a tungsten carbide electrode compared with a copper electrode. International journal of advanced manufacturing technology. Vol. 17, p. 715-719, 2001.
28. Yoshiyuki UNO, Akira OKADA and Mitsuru ITOH. The effect of high-speed polarity changing on EDM performance. Proceeding of 11th international symposium for electromachining, ISEM-11, p. 241-249, 1995.

ATTENTION: The Singapore Copyright Act applies to the use of this document. Nanyang Technological University Library

29. Heng XIA, Masanori KUNIEDA. Research on machining characteristics of polarity-changed pulse in EDM. Proceeding of 11th international symposium for electromachining, ISEM-11, p. 181-190, 1995.
30. P.M. Lonardo, A.A. Bruzzone, Effect of flushing and electrode material on die sinking EDM, Ann. CIRP, Vol. 48 (1), p. 123-126, 1999.
31. K. Kagaya, Y. Oishi, K. Yada, Micro-electrodischarge machining using water as a working fluid— I: micro-hole drilling, Precison Eng. Vol. 8 (3), p. 157-162, 1986.
32. Tae-Hyun Jung, Kyu-yeol Park, Won-Kyu Lee. A study on the micro electric discharge grinding characteristics of WC-CO-Relationship between surface integrity and dielectric conditions. Annals of the CIRP, Vol. 48 (1), p134-139, 1999.
33. B. Y. Yan, S. L. Chen. Effects of dielectric with suspended aluminum powder on EDM. Journal of the Chinese society of mechanical engineers, Vol. 14(3), p. 307-312, 1993.
34. B.M. Schumacher, About the role of debris in the gap during electrical discharge machining, Ann. CIRP, Vol. 39 (1), p. 197-199, 1990.
35. M.L. Jeswani, Effect of the addition of graphite power to kerosene used as the dielectric fluid in electrical discharge machining, Wear, Vol. 70, p. 133-139, 1981.
36. Y. F. Tzeng, C. Y. Lee. Effects of Powder characteristics on Electrodischarge machining efficiency. International Journal of advanced manufacturing and technology, Vol. 17, p. 586-592, 2001.
37. Y.H. Guu, H. Hocheng, Effects of workpiece rotation on machinability during electrical discharge machining, J. Mater. Manuf. Processes, Vol. 16 (1), p. 91-101, 2001.

ATTENTION: The Singapore Copyright Act applies to the use of this document. Nanyang Technological University Library

38. M. Kunieda, T. Masuzawa, A fundamental study on a horizontal EDM, Ann. CIRP, Vol. 37 (1), p. 187-190, 1988.

39. T. Sato, T. Mizutani, K. Yonemochi, K. Kawata, The development of an electrodischarge machine for micro hole boring, Precision Eng. Vol. 8 (3), p. 163-168, 1986.

40. J.S. Soni, G. Chakraverti, Machining characteristics of titanium with rotary electro-discharge machining, Wear, Vol. 171, p. 51-58, 1994.

41. S.H. Yeo, L.K. Tan. Effects of ultrasonic vibrations in micro electro-discharge machining of microholes. Journal of Micro mechanical and Micro engineering, Vol. 9, p. 345-352, 1999.

42. D. Kremer, J.L. Lebrun, B. Hosari, A. Moisan. Effects of Ultrasonic vibrations on the performances in EDM. Annals of the CIRP, Vol. 38(1), p. 199-202, 1989.

43. D. Kremer, ENSAM Paris, C. Lhiaubet, LGEP-ESE, Gif-Sur-Yvette, A. Moisan. A study of the effect of synchronizing ultrasonic vibrations with pulses in EDM. Annals of the CIRP, Vol. 40 (1), p. 211-214, 1991.

44. S. Enache, C. Opran, G. Stoica, E. Strajescu, The study of EDM with forced vibration of tool electrode, Ann. CIRP, Vol. 39 (1), p. 167-170, 1990.

45. De Bruyn H. E. slope control: a great improvement in spark erosion. Annals of the CIRP, 1967.

46. K. Kobayashi, T. Oizumi. Electrical discharge machining by special pulse waveform. Journal of the Japan Society of Electrical Machining Engineers, 1975.

47. M. Kunieda, H. Muto, Development of multi-spark EDM, Ann. CIRP, Vol. 49 (1), p. 119-122, 2000.

48. M. Kunieda, S. Furuoya, N. Taniguchi, Improvement of EDM efficiency by supplying oxygen gas into gap, Ann. CIRP, Vol. 40 (1), p. 215-218, 1991.

ATTENTION: The Singapore Copyright Act applies to the use of this document. Nanyang Technological University Library

49. Y. Tsuekawa, N. Okumiya, N. Mohri, I. Takahashi, Surface modification of aluminium by electrical discharge alloying, Mater. Sci. Eng. Vol. 174, p. 193-198, 1994.
50. A.M. Hassan, The effect of ball- and roller-burnishing on the surface roughness and hardness of some non-ferrous metals, J. Mater. Process. Technol. Vol. 72 (3), p. 385-391, 1997.
51. N.H. Loh, S.C. Tam, S. Miyazama, Application of experimental design in ball burnishing, Int. J. Mach. Tools Manuf. Vol. 33 (6), p. 841-852, 1993.
52. B.H. Yan, C.C. Wang, H.M. Chow, Y.C. Lin, Feasibility study of rotary electrical discharge machining with ball burnishing for Al_2O_3/6061Al composite, Int. Mach. Tools Manuf. Vol. 40 (10), p. 1403-1421, 2000.
53. C.L. Lin, J.L. Lin, T.C. Ko, Optimization of the EDM process based on the orthogonal array with fuzzy logic and grey relational analysis method, Int. J. Adv. Manuf. Technol. Vol. 19 (4), p. 271-277, 2002.
54. J. Marafona, C. Wykes, A new method of optimizing material removal rate using EDM with copper-tungsten electrodes, Int. J. Mach. Tools Manuf. Vol. 40 (2), p. 153-164, 2000.
55. J.L. Lin, K.S. Wang, B.H. Yan, Y.S. Tarng, Optimization of the electrical discharge machining based on the Taguchi method with fuzzy logics, J. Mater. Process. Technol. Vol. 102, p. 48-55, 2000.
56. Y.F. Tzeng, F.C. Chen, A simple approach for robust design of high-speed electrical discharge machining technology, Int. J. Mach. Tools Manuf. Vol. 43 (3), p. 217-227, 2003.

ATTENTION: The Singapore Copyright Act applies to the use of this document. Nanyang Technological University Library

57. J.L. Lin, K.S. Wang, B.H. Yan, Y.S. Tarng, An investigation into improving worn electrode reliability in the electrical discharge machining process, Int. J. Adv. Manuf. Technol. Vol. 16, p. 113-119, 2000.

58. S.M. Pandit, K.P. Rajurkar, A stochastic approach to thermal modeling applied to electrical discharge machining, Tans. ASME, J. Heat Transfer Vol. 105, p. 555-562, 1983

59. R. Snoeys, F. van dijck, Physico-mathematical analysis of the EDM process, Proceedings of the North American metal working research conference, Vol. 1, p. 181-200, 1973.

60. T.A. Spedding, Z.Q. Wang, Study on modeling of wire EDM process, J. Mater. Process. Technol. Vol. 69, p. 18-28, 1997.

61. K.M. Tsai, P.J. Wang, Predictions on surface finish in electrical discharge machining based upon neural network models, Int. J. Mach. Tools Manuf. Vol. 41 (10), p. 1385-1403, 2001.

62. K.M. Tsai, P.J. Wang, Semi-empirical model of surface finish on electrical discharge machining, Int. J. Mach. Tools Manuf. Vol. 41 (10), p. 1455-1477, 2001.

63. K. Wang, H.L. Gelgele, Y. Wang, Q. Yuan, M. Fang, A hybrid intelligent method for modeling the EDM process, Int. J. Mach. Tools Manuf. Vol. 43, p. 995-999, 2003.

64. J.H. Zhang, T.C. Lee, W.S. Lau, Study on the electro-discharge machining of a hot pressed aluminum oxide based ceramic, J. Mater. Process. Technol. Vol. 63, p. 908-912, 1997.

65. D.F. Dauw, R. Snoeys, Adaptive control optimization of the electro discharge machining process by real time pulse detection. Advanced manufacturing process. Vol. 1 (1), p. 45-81, 1996.

ATTENTION: The Singapore Copyright Act applies to the use of this document. Nanyang Technological University Library

66. C. Cogun, A technique and its application for evaluation of material removal contribution of pulses in electrical discharge machining, Int. Mach. Tools Manuf. Vol. 30 (1), p. 19-31, 1990.

67. R. Snoeys, D. F. Dauw, J. P. Kruth, Improved adaptive control system for EDM process, Annals of CIRP, Vol. 29 (1), p. 97-101, 1980.

68. S. K. Bhattacharyya, M. F. El-Menshawy. Monitoring the EDM process by radio signals, International p. Res. Vol. 16 (5), 353-363, 1978.

69. S. M. Pandit, T. M. Mueller, Verification of on-line computer control of EDM by data dependent systems, ASME J. Eng. Ind. Vol. 109, p. 109-121, 1987.

70. R. Snoeys, H. Cornelissen, Correlation between electro-discharge machining data and machining settings, Annals of the CIRP, Vol. 24(1), p. 83-88, 1975.

71. D. F. Dauw, R. Snoeys and W. Dekeyser. Advanced pulse discriminating system for EDM process analysis and control, Annals of the CIRP, Vol. 32(1), p. 65-7, 1983.

72. K.P. Rajurkar, S.M. Pandit, and W.H. Wittig, Pulse current signal as a sensor for on-line computer control of EDM, Proc 11th NAMRC, p. 379-385, 1983.

73. K.P. Rajurkar, M.W. Wang, R.P. Lindsay, A new model reference adaptive control of EDM, Ann. CIRP, Vol. 38 (1), p. 183-186, 1989.

74. M. Weck, J.M. Decher, Analysis and adaptive control of EDM sinking process using the ignition delay time and fall time as parameter, Ann. CIRP, Vol. 41 (1), p. 243-246, 1992.

75. W.M. Wang. A new EDM adaptive control plan using self-tuning control algorithm, Proceedings of manufacturing international'88, ASME, Vol. 1, p. 227-233, 1988.

ATTENTION: The Singapore Copyright Act applies to the use of this document. Nanyang Technological University Library

76. S.K. Bhattacharyya, M.F. El-Menshawy, Monitoring the EDM process by radio signals, Int. J. Prod, Res. Vol. 16 (5), p. 353-363, 1978.

77. S.K. Bhattacharyya, M.F. El-Menshawy, Monitoring and controlling the EDM process, J. Eng. Ind. Vol. 102, p.189-194, 1980.

78. K.P. Rajurkar, W.M. Wang, W.S. Zhao. WEDM adaptive control with a multiple input model for identification of workpiece height. Annals of the CIRP Vol. 46 (1), p. 147-150, 1997.

79. K.P. Rajurkar, W.M. Wang. On-line monitor and control for wire breakage in WEDM. Annual of the CIRP, Vol. 40 (1), p. 219-222, 1991.

80. N. Saito, K. Kobayashi. A method for adaptive control in EDM process. Mitsubishi electric corporation, No. 1, 18-chome, Yada-cho, Higashi-ku, Nagoya, Japan.

81. D.F. Dauw, R. Snoeys and W. Dekeyser. Advanced pulse discriminating system for EDM process analysis and control, Annals of the CIRP, Vol. 32 (1), p. 65-75, 1983.

82. M.S. Ahmed. Radio frequency based adaptive control for electrical discharge texturing. EDM digest, Sept./Oct. p. 8-10, 1987.

83. S.F. Yu, B.Y. Lee, W.S. Lin, Waveform monitoring of electrical discharge machining by wavelet transform, Int. J. Adv. Manuf. Technol. Vol. 17 (5), p. 339-343, 2001.

84. W.M. Wang, K.P. Rajurkar, K. Akamatsu, Digital gap monitor and adaptive integral control for auto-jumping in EDM, J. Eng. Ind. Vol. 117, p. 253-258, 1995.

85. K.P. Rajurkar, W.M. Wang, On-line monitoring and control of die-sinking and wire electrodischarge machines, Proceedings of CIRP on PE & MS, p. 803-818, 1991.

ATTENTION: The Singapore Copyright Act applies to the use of this document. Nanyang Technological University Library

86. K.P. Rajurkar, Adaptive control systems for EDM, SME technical paper, EE 89-801, 1989.

87. Y. Ni, J.L. Zhou, L.G. Zheng, A new control system based on grey theory for EDM, Proceeding of 11th international symposium for electromachining, ISEM-11, p. 279-285, 1995.

88. R. Snoeys, W. Dekeyser and C. Tricarico. Knowledge-based system for wire EDM, Annals CIRP, Vol. 37, p. 197-202, 1988.

89. A. Moria, Y. Iami, A. Noda, etc. Fuzzy controller for EDM. Proceeding of 9th international symposium for electromachining, ISEM-9, p. 236-239, 1989.

90. A. Behrens, J. Ginzel, A continuously learning neural network to adapt a fuzzy controller in EDM die-sinking process, Proc. 6th European Congress on Intelligent Techniques & Soft Computing EUFIT, Aachen, p. 1481 – 1485, 1998.

91. M. Boccadoro, D.F. Dauw. About the application of fuzzy controllers in high-performance die-sinking EDM machines. Proceeding of 11th international symposium for electromachining, ISEM-11, p. 333-341, 1995.

92. Y.S. Tarng, C.M. Tseng, L.K. Chung, A fuzzy pulse discriminating system for electrical discharge machining, Int. J. Math. Tools Manuf. Vol. 37 (4), p. 511-522, 1997

93. Y.S. Tarng, J.L. Jang, Genetic synthesis of a fuzzy pulse discriminator in electrical discharge machining, J. Intell. Manuf. Vol. 7, p. 311-318, 1996.

94. M. T. Yan, H. P. Li and J. F. Liang. The application of fuzzy control strategy in servo feed control of wire electrical discharge machining. International Journal of advanced manufacturing technology, Vol.15, p. 780-784, 1995.

ATTENTION: The Singapore Copyright Act applies to the use of this document. Nanyang Technological University Library

95. Y. S. Tarng, S. C. Ma and L. K. Chung. Determination of optimal cutting parameters in wire electrical discharge machining. Int. J. of Mach. Tools and Manuf., Vol. 35 (12), p. 1693-1701, 1995.

96. J. Y. Kao, Y. S. Tarng. A neural-network approach for on-line monitoring of the electrical discharge machining process. Journal of Materials processing Technology, Vol. 69, p. 112-119, 1997.

97. Kuo-ming Tsai, Pei-Jen Wang. Predictions on surface finish in electrical discharge machining based upon neural network models. International Journal of Machine tools and manufacture, Vol. 41, p. 1385-1403, 2001.

98. H.S. Liu, Y.S. Tarng, Monitoring of the electrical discharge machining process by adaptive networks, Int. J. Adv. Manuf. Technol. Vol. 13, p. 264-270, 1997.

99. Ling, Shih-Fu, L.X. Wan, Monitoring a spot welding process via electrical input impedance, SEM IX international congress, Orlando, Florida, USA, June 2000.

100. Jingen Luan. "Model and monitoring of ultrasonic welding of thermoplastic". PhD Thesis, Nanyang Technological University, 2002.

101. Dong Zhang. "Study of mechanism of ultrasonic wire bonding process". PhD Thesis, Nanyang Technological University, 2001.

102. S.F. Ling, L.Y. Fu. Electrical impedance control of spindle motor in micro drilling — Part I: Sensorless measurement of drilling torque. Internal report, CMMS, MPE, Nanyang Technological University, 2003.

103. S.F. Ling, Y. Xie, Detecting mechanical impedance of structure using the sensing capability of a piezo-ceramic inertial actuator, Sensors and Actuators, Vol. 93, p. 243-249, 2001.

104. D. Gabor, Theory of Communications, J. Inst. EE., Part III, Vol. 93, , p. 429-457, Nov. 1946.

ATTENTION: The Singapore Copyright Act applies to the use of this document. Nanyang Technological University Library

105. Stefan L. Hahn, Hilbert Transform in signal processing, Artech House, 1996.

106. A.V. Oppenheim, R.W. Schafer, Discrete-Time Signal Processing, Prentice-Hall, Englewood Cli7s, NJ, 1989, p. 775.

107. H. L. Henderikus. A study on micromachining— Assembly. Thesis of University of Tokyo, 1994

108. Guenter Wollenberg. Simulation of EDM installations. International Journal of Machine tools and manufacture, Vol. 35, No. 12, p. 153-162, 1995

109. S.G Mallat, A Theory for Multiresolution Signal Decomposition: The Wavelet Representation, IEEE Transactions on Pattern Analysis and Machine Intelligence, Vol. 11, p. 674-693, 1989.

110. S. Mallat, Multi-resolution approximations and wavelet orthonormal base of $L^2(R)$. Trans. Amer Math. Soc, Vol. 315, p. 69 ~ 87, 1989.

111. L.A. Zaden, Fuzzy sets, Information and control, Vol. 8, p. 338~353, 1965.

112. J.C. Bezdek, Editorial: Fuzzy Models—What Are They, and Why?, *IEEE* Transactions on Fuzzy Systems, Vol. 1(1), February 1993.

113. E.H. Mamdani, Applications of fuzzy algorithms for simple dynamic plant, Proceedings of IEEE, Vol. 121, p. 1585-1588, 1974.

114. T. Takagi, and M. Sugeno, Fuzzy identification of Systems and its Applications to Modeling and Control, IEEE Transactions on Systems, Man, and Cybernetics, 15(1), January-February 1985.

115. U.P. Singh, P.P. Miller, W. Urquhart, The influence of electrical discharge machining parameters on machining characteristics, in: Proceedings of the 25th International Machine Tool Design and Research Conference, p. 337-345, 1985.

116. D.C. Montgomery, Design and analysis of experiments, Wiley Singapore, 1991.

ATTENTION: The Singapore Copyright Act applies to the use of this document. Nanyang Technological University Library

117. R.A. Fisher, Statistical methods for research worker, Oliver & Boyd, London, 1925.

118. G. Taguchi, Introduction to quality engineering, Asian productivity organization, Tokyo, 1990.

119. Hornik, K.M. Stinchcombe and H. White, Multilayer feedforward networks are universal approximators, Neural Networks, Vol. 2, p. 359~366, 1989.

120. M.T. Hagan, H.B. Demuth and M.H. Beale, Neural network design, Boston, MA: PWS publishing, 1996.

121. R.C. Eberhart, R.W. Dobbins, "Implementations" chapter 2-5 in Neural Network PC Tools, 1990.

122. D. Rumelhart, G.E. Hinton and R.J. Williams, Learning representations by back propagation errors, Nature 1986.

123. Geometrical product specifications (GPS) — Surface texture: Profile method — terms, definitions and structure texture parameters, International organization for standardization, Geneva, 1997. ISO 4287:1997.